

TANGIBLE VISUALISATION

Multi-property 3D/4D printing for the design exploration of percutaneous surgical drains.

MAX SYME

2019



TANGIBLE VISUALISATION

Multi-property 3D/4D printing for the design exploration of percutaneous surgical drains.

A ninety point thesis submitted to the Victoria University of Wellington
in partial fulfilment of the requirements for the degree of
Masters of Design Innovation in Industrial Design

MAX SYME

Victoria University of Wellington
School of Design, 2019

Cover: *Figure 1.* Tangible interaction with the Ellipse stimulus-responsive surgical drain.

ABSTRACT

This thesis proposes a method of Tangible Visualisation, which results in ideas rendered visible and capable of being interacted with for communication, development, and reflection. Physically manifesting a concept adds value to the design process as information known and unknown can now be perceived in a highly resolved lifelike prototype. Multi-property 3D printing is the process of depositing material to create a complex digital model with varying rigid and flexible qualities and using the Stratasys J750 PolyJet 3D printer allowed for the production of micro-millimetre details at a finished product level resolution.

A surgical drain is a tube that removes infected fluids, such as blood, pus or other liquids, from a wound inside the human body after surgery. Initially, they were designed for irrigation, not drainage, which is a contributing factor to their on average 50% complication rate. Common issues include kinking, tube obstruction, clogging, and dislodgment.

Clinicians may be conceptually aware of changes to make medical devices better; however, for the most part, they do not have the expertise to translate their thoughts into reality. The role of the designer is to render ideas into physical prototypes for interpretation. In this study, multi-property 3D printing was deemed the most appropriate additive manufacturing process

for the production of dynamic clinical ideas from the conducted literature and precedent reviews. Research-for-design provided background information for the project. Research-through-design, with a practice-based iterative design approach, explored the capabilities of multi-property 3D printing as a prototyping and visualisation method.

The classification of physical outcomes is either pragmatic concepts designed for current manufacturing technologies and today's market or speculative ideas that investigated 4D printing and dynamic anatomical structures, where 3D printing may be the manufacturing method. Exploring multiple designs during this research allowed a thorough evaluation of multi-property 3D printing and the development of various surgical drain related concepts, which included, irrigation drains, external skin-fixation devices, stimulus-responsive drains and venous valve structures.

The unique additive manufacturing process proved to be an effective prototyping method while the tangible outputs allowed for the visualisation of complex ideas, being assets in the design process. The results of this study identified that incorporating multi-property 3D printing early in the development phase of a concept allows for the understanding of the constraints but also the opportunities of sophisticated ideas.





ACKNOWLEDGEMENTS

To my supervisors, Bernard Guy and Simon Fraser, thank you for your continuous guidance and support towards my studies. The knowledge you have passed on will be invaluable, going into my future endeavours.

Thank you to the members of the greater project, specifically, Anthony Phillips, Alicia Hellens, and Isabelle Hawkins, for your contributions and feedback. It was a pleasure working with all of you. Additionally, to Phil Jaret for your immense technical support and MBIE for the research grant, which greatly assisted with the study.

To my family, Sandra, Brandon, Jacinta and Olly, thank you for the unconditional support and encouragement, which helped me persevere throughout my studies.

Lastly to my friends and fellow design cohort, thanks for the abundant support and motivation, in particular, Chakriya, William, Tony, Maddy and Christy. I wish you all the best for your future endeavours.



PREFACE

“It is a revolutionary technology (3D printing) that will make medical care better and faster, and more personalised... many things that we thought of as impossible are now becoming possible... I think we are moving towards a world where if you can imagine it, you will be able to print it – so we need to start imagining.”

(Trounson, 2017)

- Jason Chuen

CONTENTS

INTRODUCTION	1. BACKGROUND RESEARCH	2. METHODOLOGY	3. DESIGN EXPERIMENTATION	4. DESIGN RESOLUTION	5. DISCUSSION & CONCLUSION
Abstract	1.1 Literature Review	2.1 Overall Approach to research	3.1 Commerical 3D printing investigation	4.1 Contemporary pigtail drain	5.1 Discussion
Acknowledgements	<i>Tangible Visualisation</i>	<i>Aims & Objectives</i>	3.2 Lab testing	4.2 Irrigation drains	5.2 Conclusion
Preface	<i>Medical & Future applications of surgical drains</i>	<i>Background Research methods</i>	3.3 Pragmatic experiments	4.3 Skin Fixation Device	5.3 References
Contents	<i>Research Origins</i>	<i>Design Experimentation methods</i>	<i>Irrigation drains</i>	4.4 Stimulus-responsive drain	5.4 Appendix
List of figures	<i>Additive Manufacturing</i>	2.2 Digital software tools	<i>Skin fixation device</i>	4.5 Internal Structures	
Introduction	<i>Multi-Material 3D/4D printing</i>	2.3 Stratasys J750 technical overview	3.4 Speculative experiments	4.6 Venous Valves	
How the drain works	1.2 Surgical Catheter related products	<i>Multi-property 3D printing cleaning method</i>	<i>Venous valves</i>	4.7 Concluding Clinical evaluation	
Terminology	1.3 Multi-property 3DP/4DP precedents		<i>Stimulus-responsive drains</i>		
	1.4 Background Research summary		3.5 Experimentation summary		

LIST OF FIGURES

Figure 1.	Tangible interaction with the Ellipse stimulus-responsive surgical drain.	Cover
Figure 2.	Interaction with a multi-property 3D printed Tangible Visualisation.	page. 1
Figure 3.	Overview image of the Cook Medical Multi-purpose Drainage Catheter Fr:14.	page. 3
Figure 4.	Detail images of the Cook Medical Multi-purpose Drainage Catheter Fr:14.	page. 4
Figure 5.	Diagram illustrating the procedure of a percutaneous surgical drain.	page. 5
Figure 6.	The step-by-step process for the insertion of a percutaneous pigtail catheter.	page. 6
Figure 7.	Demonstrating Tangible Visualisation with a multi-property 3D printed venous valve.	page. 11
Figure 8.	ConforMIS custom patient-specific 3D printed knee replacement. Reprinted from C. M. Editors, (2015) Retrieved from https://www.cincinnatimagazine.com/top-doctors-archive/future-now-christ-hospital-creates-3d-printed-knee-implants/ . Permission for use granted by Aaron Conway.	page. 13
Figure 9.	Patient-specific 3D printed surgical guide, fabricated in metal. Reprinted from UWTSO (CBM), (2018) Retrieved from http://www.cbmwales.co.uk/our-services/medical-services/ . Permission for use granted by Ffion O’Malley.	page. 13
Figure 10.	Belgian additive manufacturing company Materialise’s anatomical model, changing the way the pathology of diseases can be visualised. Reprinted from Slagmolen, (2017) Retrieved from https://www.materialise.com/en/blog/5-tips-when-printing-anatomical-models . Copyright Materialise, 2019 all rights reserved.	page. 13
Figure 11.	Diagram illustrating the relationship between the greater project and this research.	page. 15

Figure 12.	Overview of the various additive manufacturing processes. Reprinted from Redwood, (2019) Retrieved from https://www.3dhubs.com/knowledge-base/additive-manufacturing-technologies-overview . Permission for use granted by Ana Almeida- 3D Hubs.	page. 17
Figure 13.	MIT Self-Assembly Lab’s self-folding 4D printed multi-property single strand transitioning into a cube. Reprinted from Tibbits (2014). Retrieved from https://onlinelibrary.wiley.com/doi/abs/10.1002/ad.1710 . Permission for use granted by John Wiley and Sons.	page. 19
Figure 14.	Diagram comparing the four different dimensions.	page. 19
Figure 15.	Pigtail catheters, Universa® Loop Drainage Catheter Introductory Set (Left), Percutaneous Neonatal Pigtail Nephrostomy Set (Right). Reprinted from Cook Medical, (2018) Retrieved from https://www.cookmedical.com/ . Permission for use granted by Cook Medical, Bloomington, Indiana.	page. 21
Figure 16.	Malecot catheters, Malecot Nephrostomy Catheter/Stent Set Polyurethane (Left), Silicone Malecot Catheter (Right). Reprinted from Cook Medical, (2018) Retrieved from https://www.cookmedical.com/ . Permission for use granted by Cook Medical, Bloomington, Indiana.	page. 21
Figure 17.	Balloon catheters, Kaye Nephrostomy Tamponade Balloon (Left), Coda® Balloon Catheter (Right). Reprinted from Cook Medical, (2018) Retrieved from https://www.cookmedical.com/ . Permission for use granted by Cook Medical, Bloomington, Indiana.	page. 22
Figure 18.	Expandable stents, Formula 418® Renal Balloon-Expandable Stent (Left), Zilver® Biliary Self-Expanding Stent (Right). Reprinted from Cook Medical, (2018) Retrieved from https://www.cookmedical.com/ . Permission for use granted by Cook Medical, Bloomington, Indiana.	page. 22
Figure 19.	Irrigation catheters, SialoCath™ Salivary Duct Catheter (Left), Whistle Tip Ureteral Catheter (Right). Reprinted from Cook Medical, (2018) Retrieved from https://www.cookmedical.com/ . Permission for use granted by Cook Medical, Bloomington, Indiana.	page. 22
Figure 20.	Molnar Retention Disc. Reprinted from Cook Medical, (2018) Retrieved from https://www.cookmedical.com/ . Permission for use granted by Cook Medical, Bloomington, Indiana.	page. 22

Figure 21.	Mushtari, multi-property 3D printed capillaries. Reprinted from Oxman (2014). Retrieved from http://neri.media.mit.edu/projects/details/mushtari . Permission pending.	page. 23
Figure 22.	Royal Philips and Stratasys 3D printed anatomical model. Reprinted from Phillips (2017). Retrieved from https://www.usa.philips.com/a-w/about/news/archive/standard/news/press/2017/20171127-philips-teams-with-3d-printing-industry-leaders-3d-systems-and-stratasys.html . Courtesy of Philips.	page. 24
Figure 23.	Hydrophytes, multi-property 3D/4D printed aquatic plants. Reprinted from Hone (2018). Retrieved from https://www.nicolehone.com/hydrophytes . Permission granted by Nicole Hone.	page. 24
Figure 24.	A kinked surgical drain, which is a common issue that impacts drainage.	page. 25
Figure 25.	Overview of the aims, objectives and methods used to achieve the research question.	page. 31
Figure 26.	Diagram illustrating the iterative design process.	page. 33
Figure 27.	Diagram illustrating the step-by-step process from ideation to CAD modelling to 3D print.	page. 35
Figure 28.	Solidworks interface.	page. 35
Figure 29.	Meshmixer interface (top).	page. 36
Figure 30.	Netfabb interface (middle).	page. 36
Figure 31.	GrabCad Print interface (bottom).	page. 36
Figure 32.	3D prints on the Stratasys J750 build tray.	page. 37
Figure 33.	The Stratasys J750.	page. 38
Figure 34.	The various blends of shore hardnesses produced with Agilius and Vero on the Stratasys J750. Shore hardness is a term used to signify the hardness of a material. The colour of higher shore value materials is more opaque.	page. 38
Figure 35.	Multi-property 3D print encased in support material.	page. 39

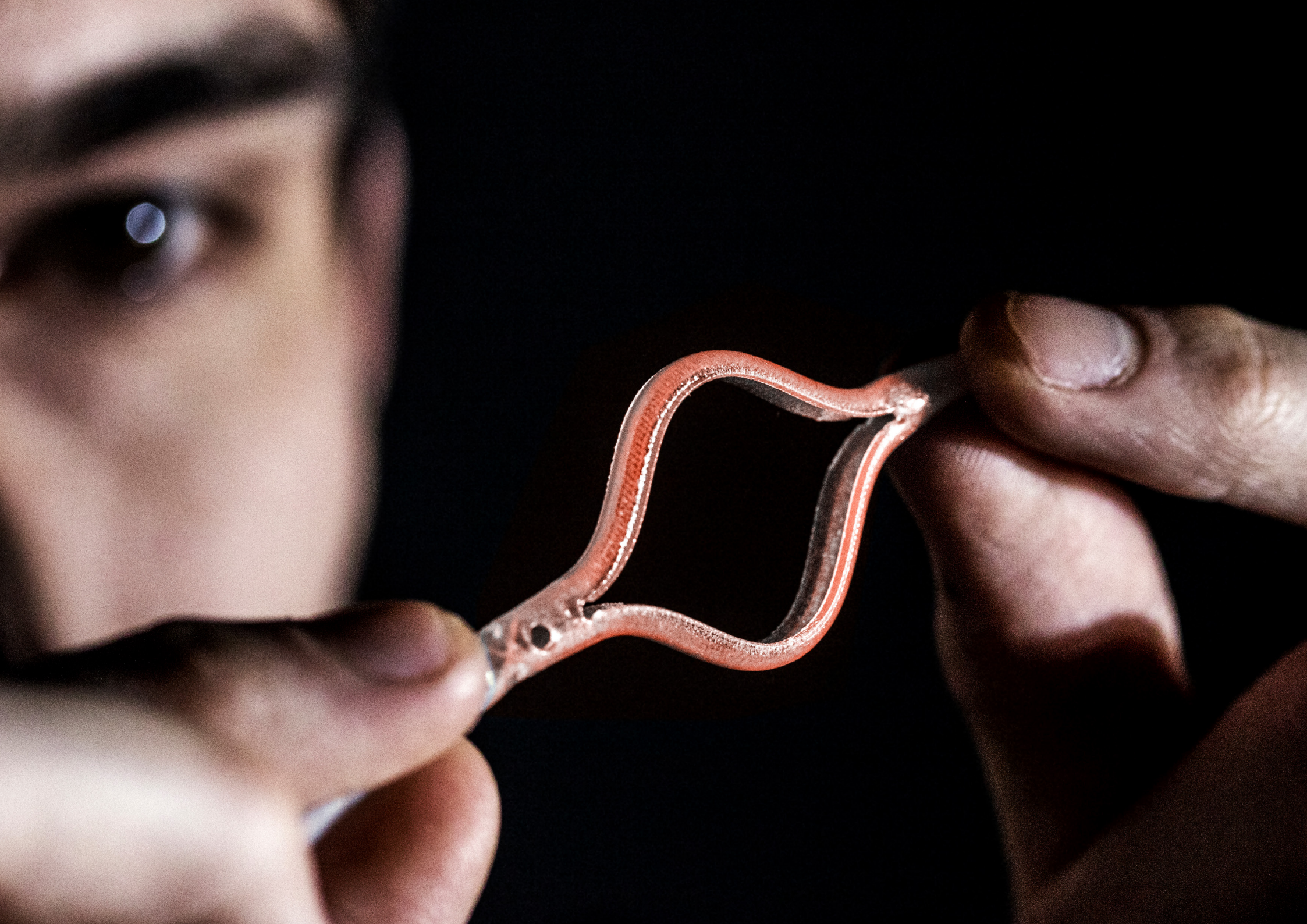
Figure 36.	Removal of an internal stent.	page. 40
Figure 37.	Delicately breaking up support material.	page. 40
Figure 38.	Magnified view of the Polyimide (MJF) material from i.Materialise.	page. 43
Figure 39.	The three different straight drain designs in the Polyimide (MJF) material from i.Materialise.	page. 44
Figure 40.	Shapeways 3D print materials documentation.	page. 45
Figure 41.	i.Materialise 3D print materials documentation.	page. 46
Figure 42.	Sculpteo 3D print materials documentation.	page. 47
Figure 43.	Commercial 3D printing analysis diagram.	page. 48
Figure 44.	3D printed Lab Test prototypes produced on the 3Dsystems ProJet MJP 3600.	page. 49
Figure 45.	Test-rig setup.	page. 50
Figure 46.	Test-rig before the introduction of 3D printing.	page. 51
Figure 47.	Test-rig after the introduction of 3D printing.	page. 51
Figure 48.	Assembly of the Luer test-rig fitting.	page. 51
Figure 49.	Computational fluid dynamic analysis on LGC003 (top) and LGC004 (bottom) Lab testing designs.	page. 53
Figure 50.	Pragmatic designs, Irrigation drain (left), Skin fixation (right).	page. 55
Figure 51.	Early concept of the self-cleaning pigtail irrigation drain.	page. 57
Figure 52.	Irrigation drain ideation sketches.	page. 59
Figure 53.	Expert advice feedback indicating potential changes.	page. 60
Figure 54.	Tight external spiral irrigation concept documentation.	page. 61
Figure 55.	Sparse external spiral irrigation concept documentation.	page. 62
Figure 56.	Internal irrigation concept documentation.	page. 63

<i>Figure 57.</i> Pigtail irrigation concept documentation.	<i>page. 64</i>	<i>Figure 75.</i> View of the base. The mesh is constructed with .6mm diameter thick rods.	<i>page. 76</i>	<i>Figure 92.</i> Movement sequence of the pneumatic valve structure, simulating muscles contracting to pump fluid towards the heart.	<i>page. 89</i>	<i>Figure 109.</i> The iterative form development of the Anchor stimulus-responsive drains.	<i>page. 101</i>
<i>Figure 58.</i> Detail image of a 3D printed Tight external spiral irrigation concept.	<i>page. 65</i>	<i>Figure 76.</i> Detail view of the mesh segment of the skin fixation device.	<i>page. 77</i>	<i>Figure 93.</i> Pneumatic valve structure.	<i>page. 90</i>	<i>Figure 110.</i> Overview of the developed Anchor drain.	<i>page. 102</i>
<i>Figure 59.</i> Overview of a current skin fixation device.	<i>page. 67</i>	<i>Figure 77.</i> Speculative designs, Stimulus-responsive drain (left), Venous valve structure (right).	<i>page. 79</i>	<i>Figure 94.</i> Dynamic 3D printed valves channelling fluids.	<i>page. 91</i>	<i>Figure 111.</i> Movement sequence of the Anchor drain.	<i>page. 102</i>
<i>Figure 60.</i> Skin fixation ideation sketches.	<i>page. 69</i>	<i>Figure 78.</i> Tangible interaction with a 3D printed venous valve.	<i>page. 81</i>	<i>Figure 95.</i> Stimulus-responsive Helix drain under compression.	<i>page. 93</i>	<i>Figure 112.</i> The iterative form development of the Helix stimulus-responsive drains.	<i>page. 103</i>
<i>Figure 61.</i> Analysis of current skin fixation devices.	<i>page. 70</i>	<i>Figure 79.</i> Diagram illustrating the function of a bicuspid venous valve.	<i>page. 82</i>	<i>Figure 96.</i> Stimulus-responsive drains ideation sketches.	<i>page. 95</i>	<i>Figure 113.</i> Overview of the developed Helix drain.	<i>page. 104</i>
<i>Figure 62.</i> Form study of the various skin fixation devices explored.	<i>page. 71</i>	<i>Figure 80.</i> Venous valve ideation sketches.	<i>page. 83</i>	<i>Figure 97.</i> The various stimulus-responsive drain concepts.	<i>page. 96</i>	<i>Figure 114.</i> Movement sequence of the Helix drain.	<i>page. 104</i>
<i>Figure 63.</i> Analysis into the path of the drain from several skin fixation iterations.	<i>page. 72</i>	<i>Figure 81.</i> The iterative form development of the venous valve.	<i>page. 84</i>	<i>Figure 98.</i> Exploring fins like structures protruding from the Vero rods, however, they were too weak and broke off when cleaning support.	<i>page. 97</i>	<i>Figure 115.</i> The iterative form development of the Ellipse stimulus-responsive drains.	<i>page. 105</i>
<i>Figure 64.</i> Early low fidelity prototypes of the skin fixation device were generated with FDM 3D printing (Fused-Deposition-Modelling).	<i>page. 73</i>	<i>Figure 82.</i> Valve leaflets bowing open due to being too thin and spaced apart.	<i>page. 85</i>	<i>Figure 99.</i> Miniscule sized drain to test the capabilities of the J750.	<i>page. 97</i>	<i>Figure 116.</i> Overview of the developed Ellipse drain.	<i>page. 106</i>
<i>Figure 65.</i> Support material proved to be an issue with FDM printing.	<i>page. 73</i>	<i>Figure 83.</i> Valve leaflet that fell out of the tube during the removal of support material.	<i>page. 85</i>	<i>Figure 100.</i> An investigation into Vero Voronoi forms to increase the strength of the bands.	<i>page. 97</i>	<i>Figure 117.</i> Movement sequence of the Ellipse drain.	<i>page. 106</i>
<i>Figure 66.</i> Detail view of a mesh form printed with FDM 3D printing.	<i>page. 73</i>	<i>Figure 84.</i> Exploring valve leaflets at a smaller scale to assess the J750's capabilities, the tubes inside diameter is 5mm.	<i>page. 85</i>	<i>Figure 101.</i> Thin strands of Vero were printed within the fins to provide more strength; however, some fins still broke off during cleaning.	<i>page. 97</i>	<i>Figure 118.</i> Overview of various stimulus-responsive drain prototypes.	<i>page. 107</i>
<i>Figure 67.</i> Labelling of FDM prototypes.	<i>page. 73</i>	<i>Figure 85.</i> Detail image highlighting the Voronoi structure within the venous valves.	<i>page. 85</i>	<i>Figure 102.</i> Printing a thin strand of Vero piercing through all the fins provides enough strength to survive cleaning.	<i>page. 98</i>	<i>Figure 119.</i> Iterative development in a documentation logbook, ideas generated from physically interacting with a multi-property 3D print.	<i>page. 109</i>
<i>Figure 68.</i> The project advanced to high-fidelity prototyping with the J750 when it was acquired.	<i>page. 74</i>	<i>Figure 86.</i> Vero ribs on the exterior surface of the tube to help the form return to its original state after being compressed.	<i>page. 86</i>	<i>Figure 103.</i> Exploration into internal skeletal forms for added strength, restricting the bands from being easily crushed by tissue or other body organs.	<i>page. 98</i>	<i>Figure 120.</i> Diagram illustrating the accumulation of knowledge after each iterative cycle, represented by the dots.	<i>page. 113</i>
<i>Figure 69.</i> Drains popping out of the slit was a frequent issue.	<i>page. 74</i>	<i>Figure 87.</i> Vero helix structure within the tube to help the form return to its original state after being compressed.	<i>page. 86</i>	<i>Figure 104.</i> Thin strands of support started printing within the fins when the size of the bands increased. The support would not dissolve in the DT3 cleaning bath.	<i>page. 98</i>	<i>Figure 121.</i> Overview of the 3D printed Contemporary pigtail drain.	<i>page. 115</i>
<i>Figure 70.</i> Sketching on prototypes signified changes. The red lines indicate the excess material to remove on the next iteration.	<i>page. 74</i>	<i>Figure 88.</i> Gills on the pneumatic valve to release air, in an attempt to prevent the material from splitting due to over inflation.	<i>page. 86</i>	<i>Figure 105.</i> An investigation into internal lattice structures within the bands of a Helix drain.	<i>page. 98</i>	<i>Figure 122.</i> Detail images of the 3D printed Contemporary pigtail drain.	<i>page. 116</i>
<i>Figure 71.</i> A curved path increased the friction on the drain, significantly improving the security.	<i>page. 74</i>	<i>Figure 89.</i> Detail image highlighting the Voronoi structure and tangible interaction of the venous valves.	<i>page. 86</i>	<i>Figure 106.</i> The iterative form development of the Pigtail stimulus-responsive drains.	<i>page. 99</i>	<i>Figure 123.</i> Overview of the various irrigation drains, Tight External Spiral (top left), Sparse External Sprial (top right), Internal Irrigation (bottom left), Irrigation Pigtail (bottom right).	<i>page. 117</i>
<i>Figure 72.</i> Refining the skin fixation form, the drain still pops out of the path.	<i>page. 75</i>	<i>Figure 90.</i> Movement sequence of the valve structure with a 50/50 solution of water and detergent flowing through the prototype.	<i>page. 87</i>	<i>Figure 107.</i> Overview of the developed Pigtail drain.	<i>page. 100</i>	<i>Figure 124.</i> Detail images of the various irrigation drains, Tight External Spiral (left), Sparse External Sprial (middle left), Internal Irrigation (middle right), Irrigation Pigtail (right).	<i>page. 118</i>
<i>Figure 73.</i> The base does not bend that well, it would not move well with the body.	<i>page. 75</i>	<i>Figure 91.</i> Left: Dormant valve, Right: Closed valve.	<i>page. 88</i>	<i>Figure 108.</i> Movement sequence of the Pigtail drain.	<i>page. 100</i>	<i>Figure 125.</i> Context image of the Tight External Spiral irrigation drain within the human body.	<i>page. 119</i>

Figure 126. Context image of the Sparse External Spiral irrigation drain within the human body.	page. 119
Figure 127. Context image of the Internal irrigation drain within the human body.	page. 120
Figure 128. Context image of the Irrigation pigtail drain within the human body.	page. 120
Figure 129. Context image of the skin fixation drain attached to the back of a patient.	page. 121
Figure 130. Step-by step process of attaching the skin fixation device over an indwelling surgical drain.	page. 122
Figure 131. Packaging concept for the skin fixation device.	page. 123
Figure 132. Packaging concept for the skin fixation device.	page. 124
Figure 133. Interaction with the Ellipse stimulus-responsive drain.	page. 125
Figure 134. Detail images of the Ellipse stimulus-responsive drain.	page. 126
Figure 135. Context image of the Ellipse drain within the kidney.	page. 127
Figure 136. Context image of the Ellipse drain transitioning from the dormant state (top) for percutaneous entry into the active state (bottom) once it reaches the abscess area.	page. 128
Figure 137. Internal helix structure supporting the tip of the drain.	page. 129
Figure 138. Internal helix structure weaved around the drainage holes.	page. 130
Figure 139. Interaction with a Y-path venous valve prototype.	page. 131
Figure 140. Movement sequence of fluids passing through a valve leaflet.	page. 132
Figure 141. Fluid flowing through the Y-tube venous valve prototype.	page. 133
Figure 142. One valve in the dormant state (left) while one valve is in the dormant state (right).	page. 134
Figure 143. Ellipse drain in support material printed with the gloss setting.	page. 141

Figure 144. Tight External Spiral irrigation drain splitting during the removal of the internal stent.	page. 143
Figure 145. Tangible Visualisation.	page. 145
Figure 146. Lab testing drains, Series of small drains exploring various sizes and shapes of drain holes.	page. 153
Figure 147. Lab testing drains, Series of large drains exploring various sizes and shapes of drain holes.	page. 154
Figure 148. Lab testing drains, Series of large drains exploring various orientations of multiple drain holes.	page. 155
Figure 149. Lab testing drains, Series of large drains exploring various orientations of multiple drain holes.	page. 156





INTRODUCTION

This thesis proposes that an understanding and communication can occur in a specialist field by using 3D printing technologies to tangibly visualise ideas.

This thesis explores a method of Tangible Visualisation, where the physical representation of an idea adds value to the design. The process results in designs rendered visible, capable of being touched and experienced for development, reflection, and communication (Figure 2). Typically visualisation in the medical field is displayed in 2D on computer screens, such as computed tomography (CT) scans. Viewing data in 2D limits the communication to primarily the visual receptors, potentially withholding one’s overall understanding of a complicated issue.

Multi-property 3D printing allows for the manifestation of physical concepts at a level normally associated with finished products or ideas thought unmakeable. Recent advancements in PolyJet additive manufacturing by Stratasys enables high-resolution, flexible 3D printing in full colour, technology with the potential to provide a greater understanding of sophisticated designs. Physical prototypes also introduce information that was not previously available, such as material qualities or the build composition. These concepts provide an understanding of complex ideas through interaction, which is the ideology of Tangible Visualisation.

In 2016 the New Zealand Ministry of Business, Innovation, and Employment (MBIE) funded a project addressing issues with the design of percutaneous surgical drains, medical catheters used to drain abscesses within the human body. Although serving an important purpose, initially they were designed for irrigation, not drainage, which is a contributing factor to their on average 50%

complication rate (Heider, Meyer, Galanko & Behrns, 1999). The high failure percentage provides the rationale for novel surgical drain solutions to address common issues. 3D printed physical prototypes may be used to help clinical experts visualise and understand these concepts.

Five chapters structure this research. The background research chapter provides the literature and precedent review addressing existing knowledge within the medical field and the 3D printing industry. The methodology chapter establishes the aims and objectives, and the methods employed to complete them. Then the design experimentation and design resolution chapters investigate how implementing multi-property 3D printing can change the function, fabrication and communication of medical devices. Design concepts are classified as either pragmatic or speculative. In the context of this research, pragmatic ideas are nearfield solutions that would allow for traditional mass-manufacturing production. Speculative concepts utilise the unique production and material qualities of the Stratasys J750 multi-property 3D printer to investigate more experimental ambiguous designs, such as dynamic anatomical structures. Lastly, the discussion and conclusion chapter synthesises the research addressing the opportunities and limitations acquired from the study; this chapter qualifies 3D printings ability to communicate and understand sophisticated ideas. Clinical personal will evaluate the acceptance of ideas through tangible 3D printed models. Communicating novel ideas to industry professionals are one of the prominent challenges within the study.

Figure 2. Interaction with a Multi-property 3D printed Tangible Visualisation.

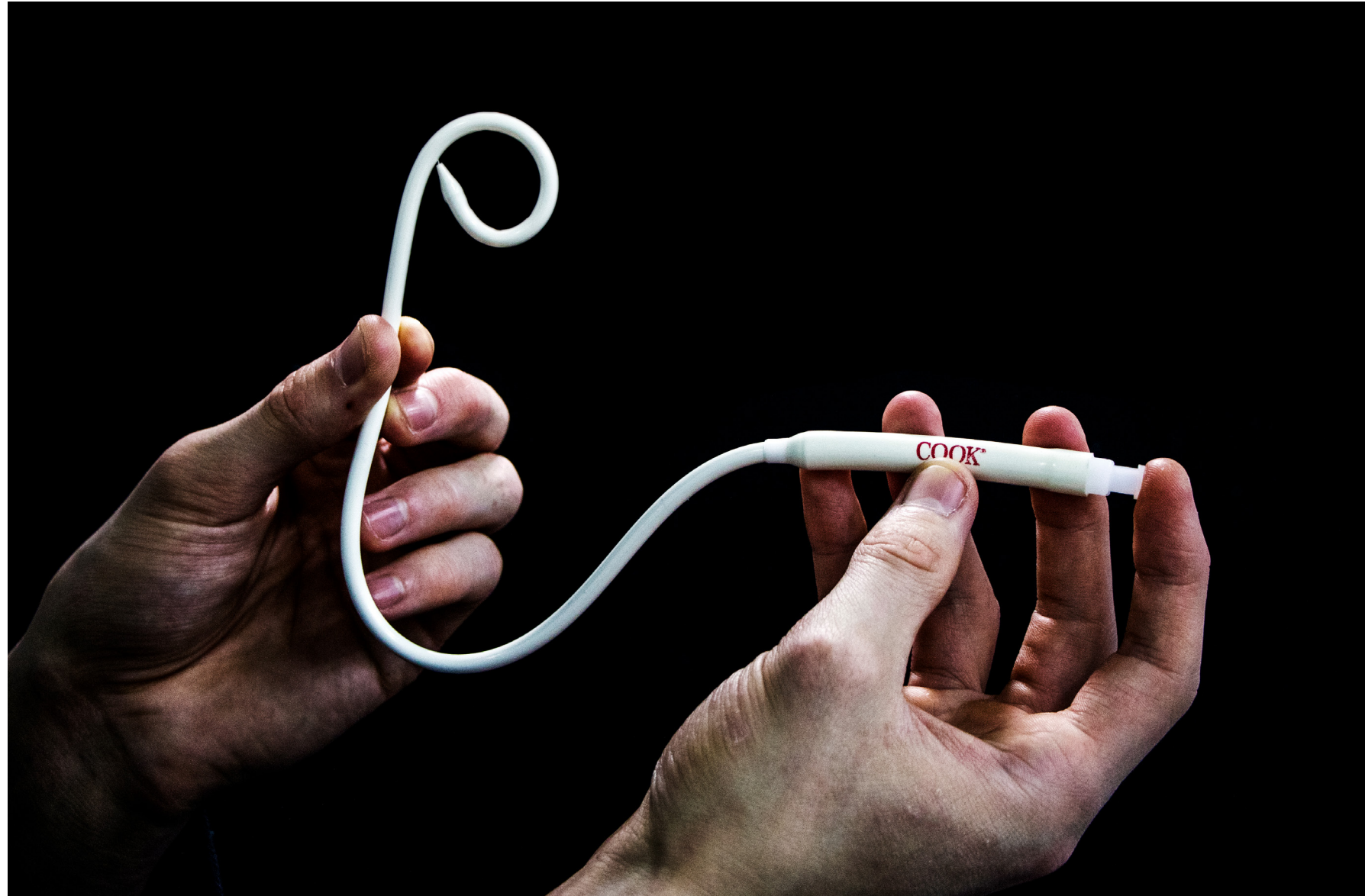


Figure 3. Overview image of the Cook Medical Multi-purpose Drainage Catheter Fr:14.

HOW THE DRAIN WORKS

A radiologist uses imaging guidance to manipulate a percutaneous surgical drain (Figures 3—4) through the skin and into the abscess, to remove or drain infected fluids. Removal of unwanted fluids such as blood, pus, and other body fluid, allows a gradual collapse and apposition of tissue. The typical drainage process, or classification of catheters, is active and passive. Active drains utilise suction to create a low continuous, low intermittent, or high suction drainage. Passive drains act by the mechanism of capillary action, gravity or the fluctuation of intra-cavity pressure. (Makama & Ameh, 2008) It often has a string, which is pulled to curl the tip into a pigtail form for internal retention. A series of drainage holes are located at the tip to collect and remove infected fluids. The French scale or French gauge, (Fr) is used to measure catheters, which is three times the size of the outer diameter in millimetres.

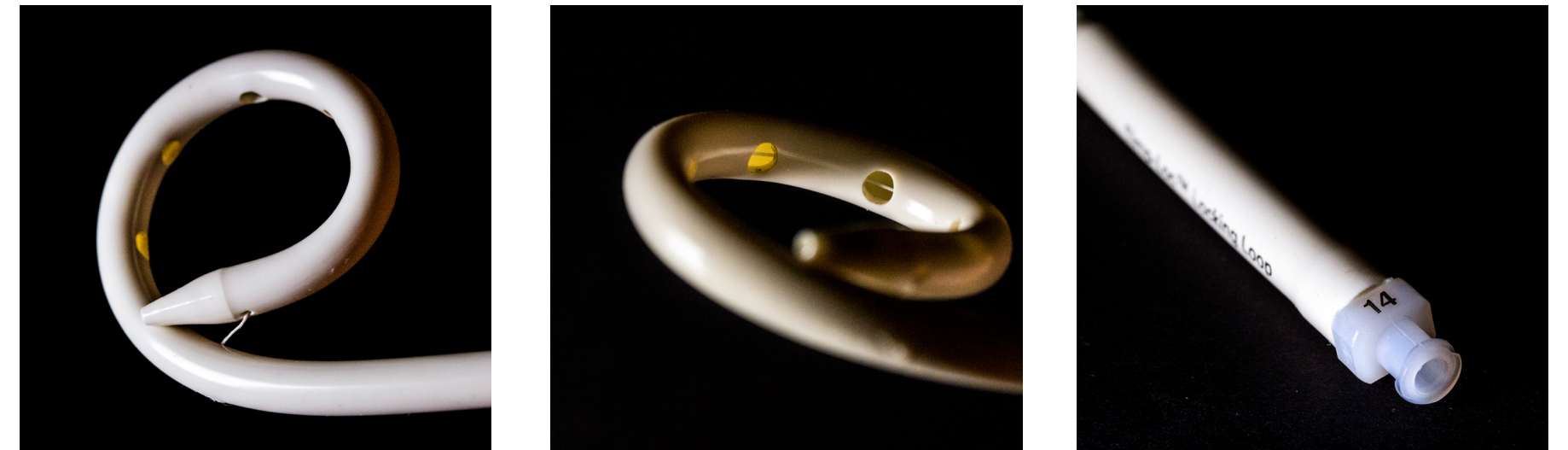


Figure 4. Detail images of the Cook Medical Multi-purpose Drainage Catheter Fr:14.

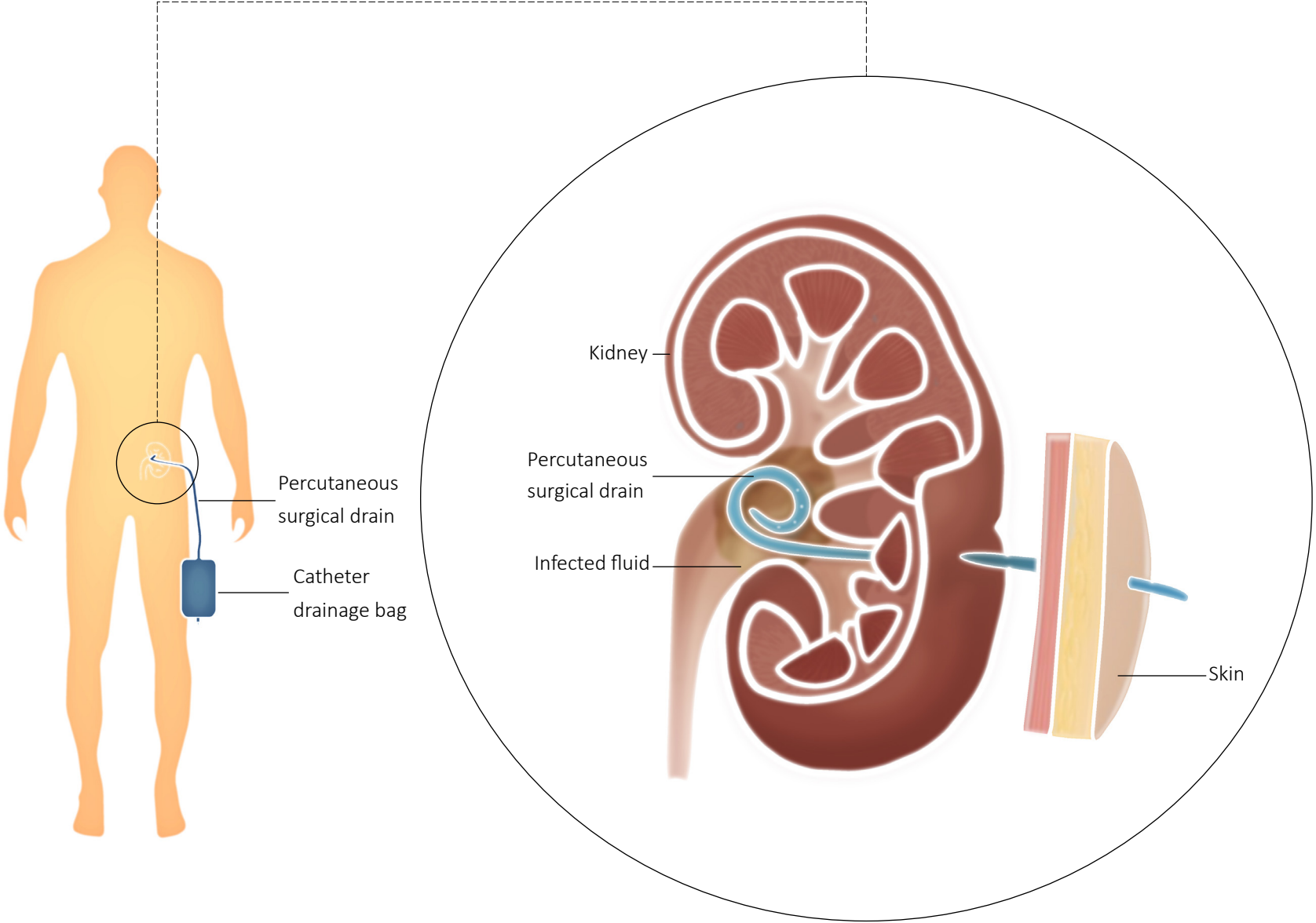


Figure 5. Diagram illustrating the procedure of a percutaneous surgical drain.

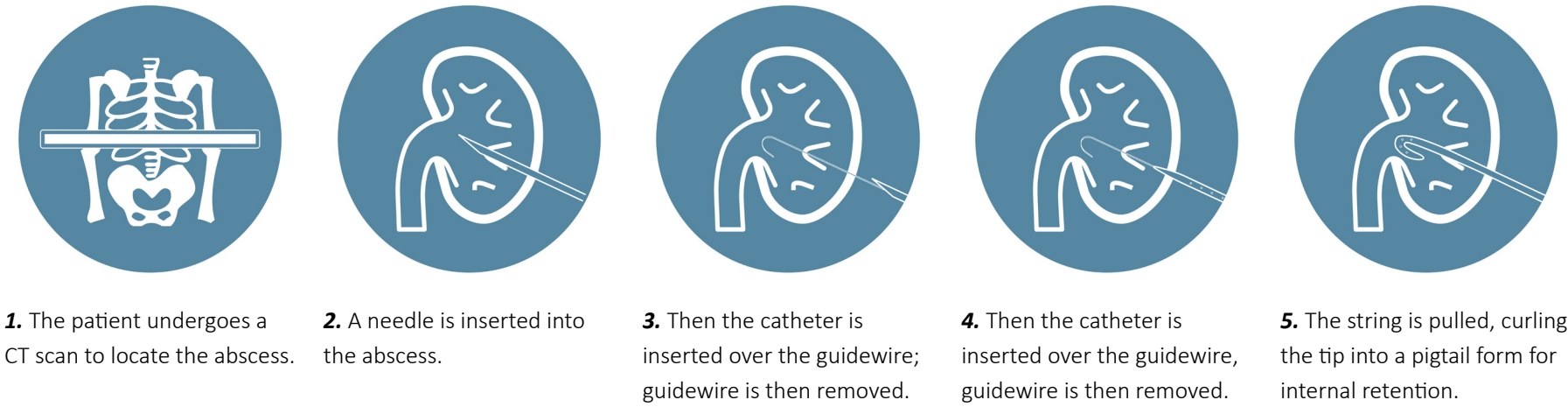


Figure 6. The step-by-step process for the insertion of a percutaneous pigtail catheter.



TERMINOLOGY

SURGICAL DRAIN: a tube used to remove infected fluids, such as blood, pus, or other bodily fluids from a wound in the human body.

PERCUTANEOUS: made, done, or effected through the skin.

CATHETER: a thin tube inserted into the body to treat diseases or drain fluids.

LUMEN: the inside space of a tubular structure, such as an artery or catheter.

MINIMALLY INVASIVE: surgical procedures involving less pain, shorter hospital stays and fewer complications.

CAD MODELLING: Computer Aided Design, the use of computer systems to aid in the creation, modification, and analysis of digital designs.

MICRON (µm): a unit of length equal to one millionth of a metre, used in many technological and scientific fields.

STRATASYS J750: A Polyjet multi-material 3D printer capable of printing details down to 14 microns in a variety of colours and rigid or flexible qualities. The J750 uses the additive manufacturing process of material jetting, which dispenses tiny droplets of photosensitive materials that solidify under ultraviolet light, layer by layer.

HIGH-DEFINITION MULTI-PROPERTY 3D PRINTING: 3D printing where multiple materials are deposited to create complex digital models capable of varying rigidity and flexible qualities, also referred to as multi-material by Stratasys.

VERO & AGILIUS: the materials used in the Stratasys J750 for multi-property 3D printing. Vero is a rigid acrylic-like material, Agilius is a flexible photopolymer.

1.1 LITERATURE REVIEW

This section aims to ascertain trends and opportunities within the medical field and additive manufacturing industry by reviewing current literature and establishing precedents.

Topics:

- Contextualise the term ‘Tangible Visualisation.’
- Analyse how multi-property 3D printing can be used to manifest physical outputs to help communicate and understand ideas.
- Provide an insight into the current performance of surgical drains.
- Analyse the benefits 3D printing is already having in the medical field while exploring trends and possibilities between the two industries.
- Acquire knowledge of the current state of additive manufacturing.
- Learn multi-property 3D/4D printing and the possibilities this process provides.

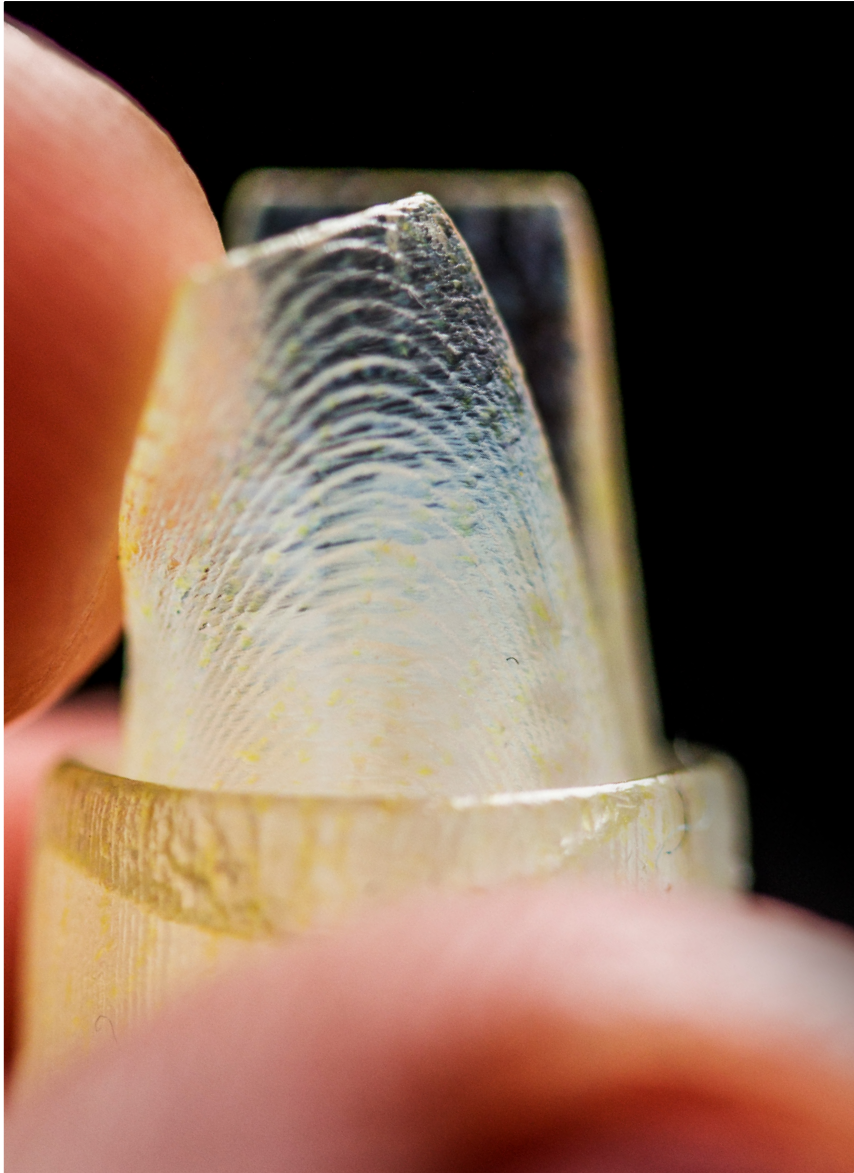


Figure 7. Demonstrating Tangible Visualisation with a multi-property 3D printed venous valve.

TANGIBLE VISUALISATION

Tangible can be defined as having actual physical existence with the capability of being touched and experienced (“Tangible,” n.d.). Visualising can be defined as forming a mental image of a concept and then rendering it visible for design development, reflection, and communication of ideas (Dix, 2013; “Visualising,” n.d.). In the context of this study, Tangible Visualisation stands for the physical existence of an idea, rendered visible, capable of being touched and experienced for communication and understanding (Figure 7).

A study by Wu (2010) explains how visualising digital information should escape the constraints of screens and instead manifest in the real world, allowing for physical interactions. Tangible interactions provide the ability to perceive information that before was unavailable such as the material properties or overall composition of an object. Further studies show how haptic feedback can mediate other sense perceptions, even visual. Physically interacting with an object allows users to understand the texture, hardness, temperature, and weight of materials (Peck & Childers, 2003a; Peck & Childers 2003b).

Medical image data acquired from computed tomography (CT) and magnetic resonance imaging (MRI) until recently was only able to be visualised in 2D (Ghosh & Mitchell, 2006). 3D printing eludes this limitation with the ability to produce elaborate tangible models of patient’s anatomy from scanned data, allowing for an increased understanding of the complexity of unique procedures (Rengier et al., 2010, pp. 336-337). 3D printed models from CT data gives an insight into the anatomical context of surgical procedures, acting as an educational tool for not only the medical

team but also the patient and their family. (Mitsouras et al., 2015, p.1983) Research by Mogali et al. (2018) shows that multi-property 3D printing is a beneficial educational tool for understanding complex anatomical structures. Medical students found the ability to distinguish anatomical structures through colour-coding and pliability of the material helpful in interpreting the anatomy. Typically medical students work with static images or virtual models, the tangible provided haptic feedback, which can enhance learning by offloading cognition during problem-solving (Fredieu et al., 2015).

Several studies established a limitation of 3D printing for the generation of physical visualisations of anatomical data, which is the accuracy of thin structures, such as fascia (Fredieu et al., 2015; Martelli et al., 2016; Li et al., 2017). Some structures might be too minuscule to produce, resulting in a loss of data and miscommunication of structural features when 3D printed.

The next section examines surgical drains and 3D printing in greater detail; establishing trends while analysing how additive manufacturing can be used to produce tangible visualisations for medical design.



Figure 8. ConforMIS custom patient-specific 3D printed knee replacement. Reprinted from C. M. Editors, (2015) Retrieved from <https://www.cincinnati.com/top-doctors-archive/future-now-christ-hospital-creates-3d-printed-knee-implants/>. Permission for use granted by Aaron Conway.

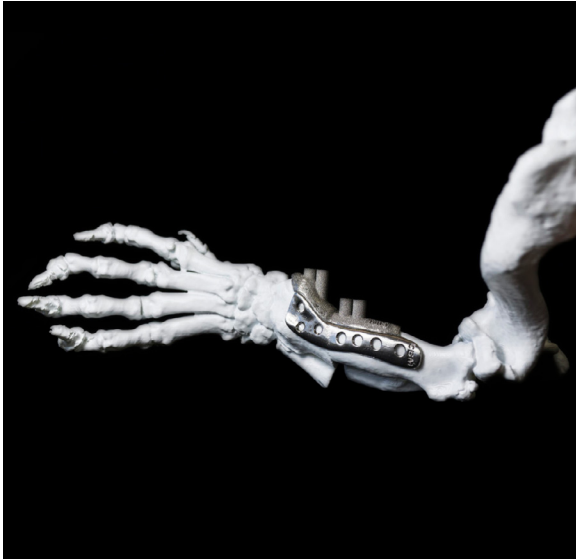


Figure 9. Patient-specific 3D printed surgical guide, fabricated in metal. Reprinted from UWTSD (CBM), (2018) Retrieved from <http://www.cbmwales.co.uk/our-services/medical-services/>. Permission for use granted by Ffion O'Malley.

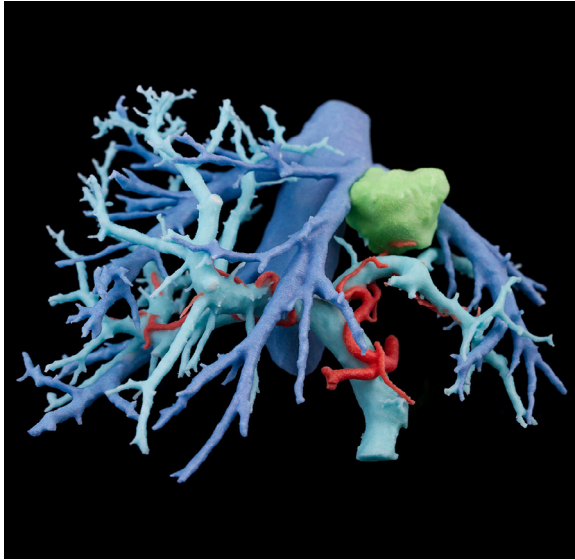


Figure 10. Belgian additive manufacturing company Materialise's anatomical model, changing the way the pathology of diseases can be visualised. Reprinted from Slagmolen, (2017) Retrieved from <https://www.materialise.com/en/blog/5-tips-when-printing-anatomical-models>. Copyright Materialise, 2019 all rights reserved.

MEDICAL & FUTURE APPLICATIONS OF SURGICAL DRAINS

Surgical drains are tubes used to remove pus, blood, and other fluids from an internal body cavity after surgery or in an infection. Common complications with surgical drains established during patient studies included leakages, kinking, tube obstruction, tube dislodgment, inadvertent removal, infection, and occlusion while more severe complications are hemobilia, fever, sepsis bleeding and rarely death (Mueller, Van Sonnenberg, & Ferrucci, 1982; Durai & Ng, 2010).

Percutaneous drainage procedures are not currently as successful as they are expected to be, and can lead to extended hospital stays equating to increased costs for patient care (Heider, Meyer, Galanko, & Behrns, 1999). Approximately one-third of patients experience a complication with surgical drains as expressed in Mueller, Van Sonnenberg, & Ferrucci (1982) and Cinat, Wilson, & Din (2002) studies, which were 28% and 31% respectively. The most frequent complications to be addressed throughout the iterative design phase are internal and external dislodgment of the drain, tube obstruction, and leakages.

The recent advancements in 3D printing technologies and materials are rapidly expanding and are expected to revolutionise medical applications of 3D printing (Ventola, 2014, p. 704). Surgeons and radiologists have established that there is enormous potential for 3D printing within the medical design field (Mitsouras et al., 2015, p.1973). It is being used to produce orthopaedics, customised prosthetics (Figure 8), implants, surgical guides (Figure 9), anatomical models (Figure 10), tissue and organ fabrication, and many more (Ventola, 2014; Tack et al., 2016).

One of the prominent advantages 3D printing has over other manufacturing processes is the ability to produce custom medical products and equipment specific for each patient at lower costs (Banks, 2013, p. 23). Makama, & Ameh, (2008) claims that an ideal drain does not currently exist, radiologists choose the most appropriate catheter for the situation, and hopes for a one size fits all design in the future with advancements in technology (p. 247). While a one size fits all drain might not be the answer due to the vast number of variables such as patient anatomy, types of drainage procedures, and the viscosity of fluids, a more suitable solution could be customised drains designed for each patient. Another advantage with 3D printing is the ability to accurately produce models down to micron level resolutions, allowing for the production of high-resolution microscopic features that other manufacturing processes are not capable of producing (Sachs et al., 1997, p.121).

However, the introduction of 3D printing into the medical field has also brought with it new regulatory changes from the FDA (Food and Drug Administration). 3D printed medical devices are broken into three classes (Class I, II, III) depending on the risk and the level of control needed. Class I being low-risk, while Class III is high-risk, such as implants. Material powder and printing parameters such as build orientation and laser power need to be addressed to ensure a high-quality print that meets the established FDA guidelines. Post-processing, such as cleaning, finishing, and sterilisation, while biocompatible materials also need to be addressed (Morrison et al., 2015, pp. 594-599). Another limitation with medical based 3D printing is that it was initially an engineering method rather than medicinal. Medical and engineering additive manufacturing research is independent, which has partially limited the development of this technology in the medical field (Yan et al., 2018).

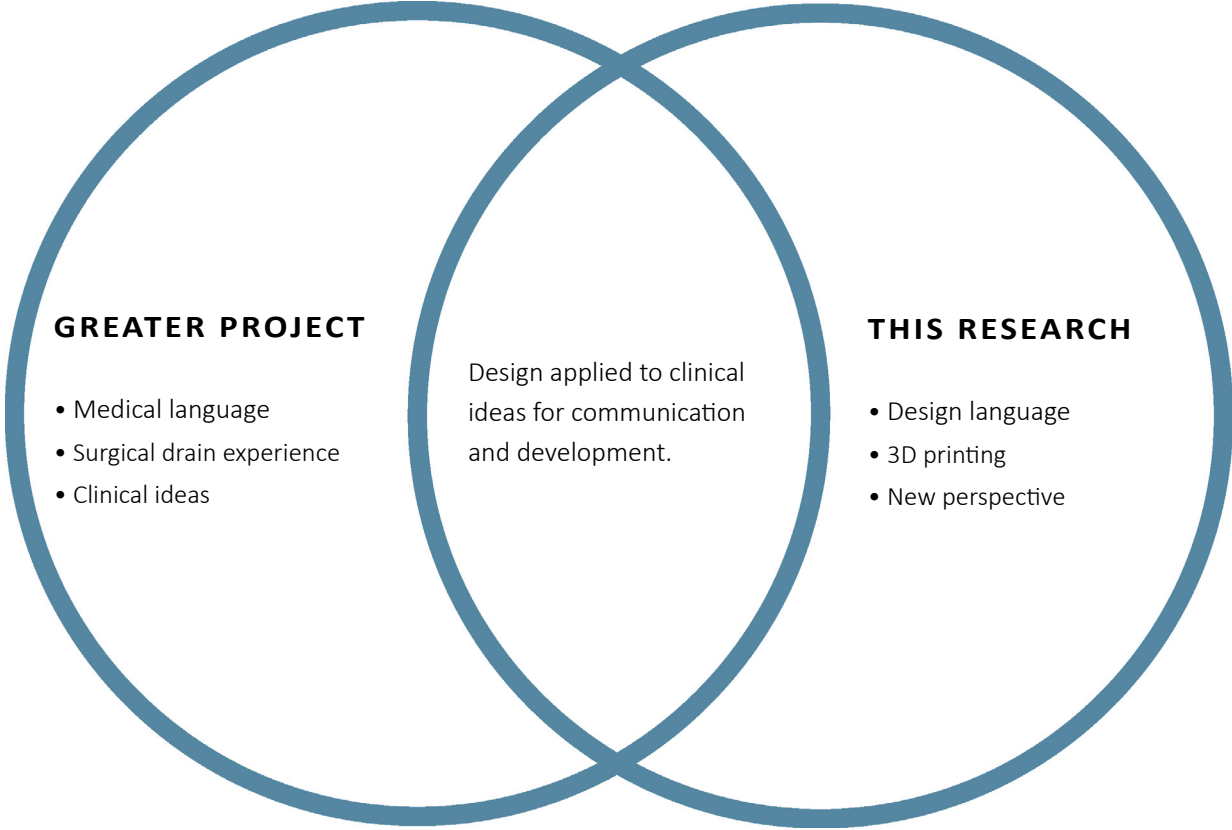


Figure 11. Diagram illustrating the relationship between the greater project and this research.

RESEARCH ORIGINS

THE GREATER PROJECT

This research is part of a greater project founded in 2016 that is aiming to redesign percutaneous surgical drains. The introduction of an industrial design student into the project is to explore methods to prototype and visualise clinical ideas. Within the project are industry professionals from the fields of industrial design, biological sciences and surgery. These professionals lend expert advice from their specialist fields.

***MBIE (MINISTRY OF BUSINESS,
INNOVATION AND EMPLOYMENT)***

MBIE is a government lead business-facing agency. Their purpose is to grow New Zealand for all, as they contribute to improving the well-being of New Zealanders. MBIE has provided the funding for this project.

PRIOR RESEARCH

Isabelle Hawkins conducted prior research for this project in 2017/2018. This research explored a range of innovative ideas that helped direct some of the design focusses.

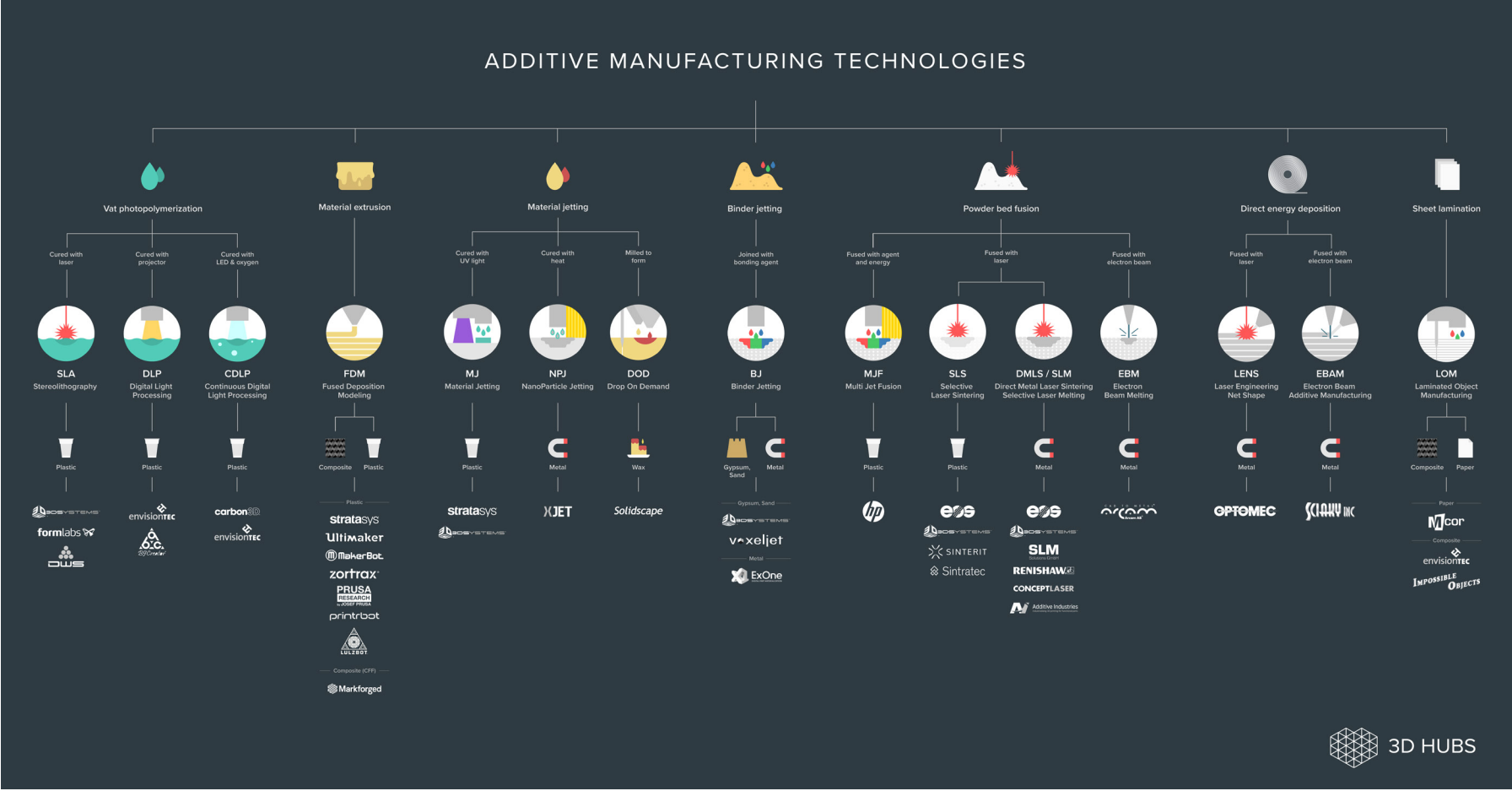


Figure 12. Overview of the various additive manufacturing processes. Reprinted from Redwood, (2019) Retrieved from <https://www.3dhubs.com/knowledge-base/additive-manufacturing-technologies-overview>. Permission for use granted by Ana Almeida- 3D Hubs.

ADDITIVE MANUFACTURING

The additive manufacturing (AM) process joins materials layer by layer to construct objects from 3D data, it can also be referred to as rapid prototyping (RP) or more commonly three-dimensional (3D) printing (Wohlers Associate, 2010).

There have been substantial technological advancements with additive manufacturing technologies since its introduction in the late 1980s. It has many different applications including, the fabrication of prototypes, functional evaluation, health care products, custom products such as prosthetics, production of moulds and many more (Ventola, 2014; Chua & Leong, 2014; Khoo et al., 2015). It can decrease the time and cost spent during the iterative prototyping phase of a project due to its quick and cheap production costs as opposed to other manufacturing processes such as tooling or injection moulding for individual part production (Wohlers Associate, 2010). The processes capability to generate diverse and complex structures with micro-millimetre accuracy allows for the production of outputs that is not possible with other manufacturing processes (O'Donnell et al., 2014; Xiong et al., 2015).

There are various 3D printing processes, each utilising different production methods, materials, and purposes (Figure 12). One additive manufacturing process is material jetting, which deposits droplets of photosensitive material that is cured by ultraviolet light. The Stratasys J750 is a material jetting multi-property 3D printer produced by Stratasys that utilises their PolyJet technology. It can generate a single part from several blended resins with a range of different mechanical properties, colours, and opacities (Stratasys, 2015). This process can print up to 14 microns (µm) with access to Vero, a rigid material, and Agilus, which is a flexible photopolymer with superior

tear resistance making it ideal for rapid prototyping and design validation (Stratasys, 2018). Dr Adnan Siddiqui claims that Agilus30 allows for the production of more robust and realistic models with the ability to 3D print smaller vessels simulating patient procedures (Stratasys, 2017). The material qualities of Agilus are demonstrated by Waran, Narayanan, Karuppiyah, Owen, & Aziz (2013) as they were able to produce more realistic neurosurgical models that almost mimic human tissue.

The Stratasys J750, along with Agilus, allows for the production of more realistic life-like models with greater physiology through the deposition of flexible and rigid materials. Although, Agilus isn't a bio-based material restricting it from being used in the body for practical use. Models printed on the J750 allow for physical visualisation and analysis of novel ideas that wouldn't be possible through other means, making it a uniquely suitable method for this research.

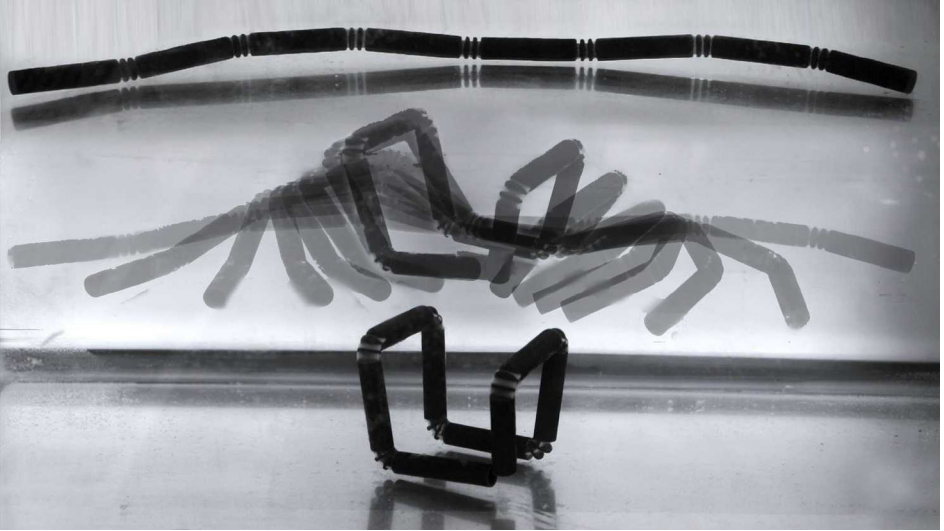


Figure 13. MIT Self-Assembly Lab's self-folding 4D printed multi-property single strand transitioning into a cube. Reprinted from Tibbitts (2014). Retrieved from <https://onlinelibrary.wiley.com/doi/abs/10.1002/ad.1710>. Permission for use granted by John Wiley and Sons.

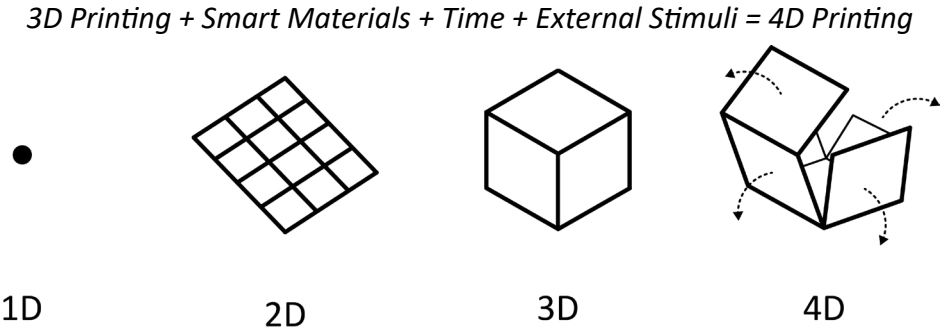


Figure 14. Diagram comparing the four different dimensions.

MULTI-MATERIAL 3D/4D PRINTING

Multi-property 3D printing can print smart materials constructed from shape memory polymers (SMP's) that contain stimulus-responsive qualities (Gul et al. 2018, pp. 243-254). Smart materials are active materials that can undergo observable change when exposed to an external stimulus, such as thermal, chemical, mechanical, optical, moisture, pH, pneumatic, and electric or magnetic field (Gul et al. 2018, pp. 254). SMP's can recover their permanent state from one or more programmed temporary states when exposed to an external stimulus (Yu et al., 2015).

4D printing (Figure 13) is the phenomenon of utilising 3D printed Smart materials with the potential to alter its shape or properties over time when exposed to an external stimulus (Gul et al. 2018, p. 254). A similar term is Soft Robotics, which involves the construction of robots from highly compliant materials comparable to a living organism (Trivedi, Rahn, Kier, & Walker, 2008, p. 99). Soft Robotics involves actuators, artificial muscles, electroactive polymers, soft electronics, and several other components to mimic natural organism's traits using Smart materials (Gul et al. 2018, pp. 243-254).

Wu et al. (2016) describe 4D printing as 3D printing active materials that change shape over time, depending on the environmental temperature (p. 7). The thermal stimulus can thermomechanically program SMP's by heating the material above its glass-transition temperature (Tg). Glass-transition is the gradual and reversible transformation from a hard glassy state into a viscous rubbery state as the temperature increases (Ge, Qi & Dunn, 2013; Ge et al., 2016). SMP's can be thermomechanical programmed to change shape when the temperature increases. Thermomechanical programming an SMP involves exposing it to a temperature higher than the materials Tg transitioning it into a rubbery state allowing for manipulation and strain to

be applied, once the desired shaped form is achieved the SMP gets cooled to 0°C transitioning it back into a glassy state. Exposing the thermomechanical programmed SMP to a temperature over its Tg will revert it to its original 3D printed state (Bodaghi, Damanpack, & Liao, 2016).

Other research shows how incorporating varying SMP's with different Tg's in a single build allows for controllability over the shape recovery process as the lower Tg material will activate its shape retention properties before materials with a higher Tg (Khoo et al., 2015; Yu et al., 2015; Ge et al., 2016). Bodaghi, Damanpack, & Liao (2016) have demonstrated how 4D printing can produce adaptive self-expandable/shrinking structures exhibiting dynamic stimulus-responsive movements.

However, unsatisfactory material properties have restricted the development of 4D printing research. The mechanical properties are currently insufficient to reproduce functioning biological movements (Momeni, Mehdi Hassani, Liu & Ni, 2017). Repetitively altering and applying strain to a 4D print can weaken the structural integrity of the material, making it susceptible to breaking.

1.2 SURGICAL CATHETER RELATED PRODUCTS

Cook Medical, founded in 1963 provides medical products in 41 diverse specialities to over 135 different countries, and are one of the leading suppliers of catheter related products. A precedent review will explore commonly used designs along with more novel outputs to establish existing ideas and potential gaps.

Figures 15-20. Surgical catheter related products. Reprinted from Cook Medical, (2018) Retrieved from <https://www.cookmedical.com/>. Permission for use granted by Cook Medical, Bloomington, Indiana.

PIGTAIL

The pigtail features a tightly curled tip enhancing internal retention within the abscess. The drain is straightened for insertion into the body over a guidewire. After removing the guidewire, pulling the string curls the tip. Radiologists noted that the string can tangle around the drain, making it hard to remove.

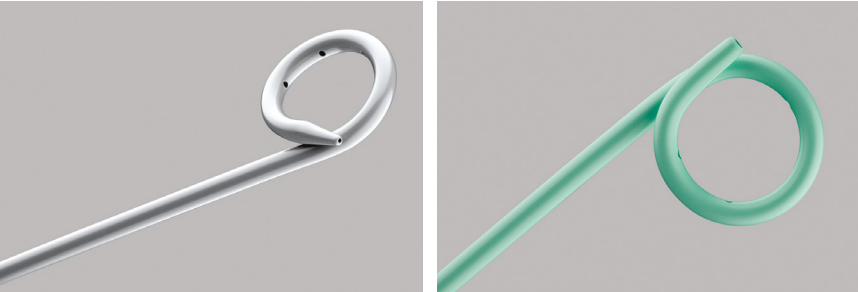


Figure 15. Pigtail catheters, Universa® Loop Drainage Catheter Introductory Set (Left), Percutaneous Neonatal Pigtail Nephrostomy Set (Right).

MALECOT

The malecot provides drainage after open renal or bladder surgeries. The opening of the wings enhance retention and increase the size of the primary point of drainage. Removing the straightener wire from the lumen activates the retention wings.

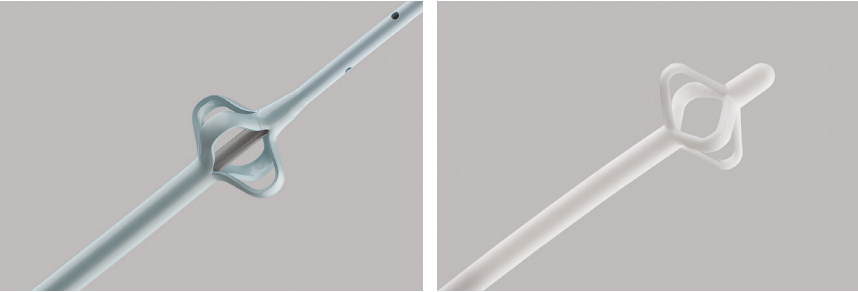


Figure 16. Malecot catheters, Malecot Nephrostomy Catheter/Stent Set Polyurethane (Left), Silicone Malecot Catheter (Right).

BALLOON

Balloon catheters feature an inflatable component at the tip to enlarge narrow passages. The inflatable pocket allows for temporary occlusion of large vessels and expansion of vascular prosthetics.

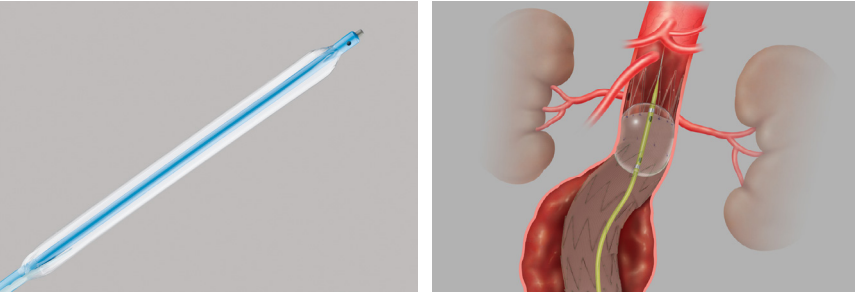


Figure 17. Balloon catheters, Kaye Nephrostomy Tamponade Balloon (Left), Coda® Balloon Catheter (Right).

EXPANDABLE STENT

Similar in function to the balloon drains, the balloon-expandable stents are noninvasive medical tools. Inserted into a clogged or collapsed artery, inflating the balloon expands the stent, locking it in place and unblocking or opening the artery.

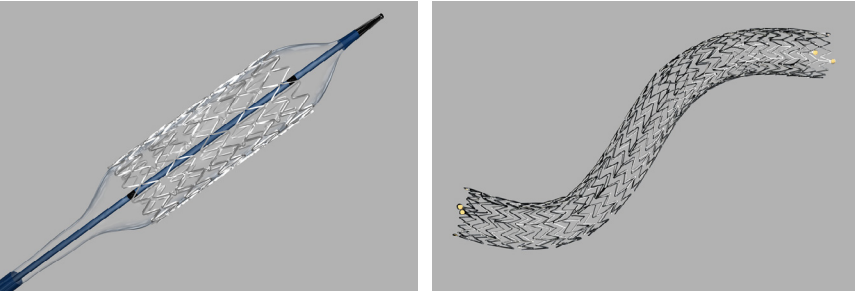


Figure 18. Expandable stents, Formula 418® Renal Balloon-Expandable Stent (Left), Zilver® Biliary Self-Expanding Stent (Right).

IRRIGATION

One purpose of irrigation drains is to deliver saline, and other solutions, into the surrounding area of the drain, making it easier to drain higher viscosity fluids. There does not seem to be a drain on Cook Medical that irrigates both the internal and external area of the catheter.

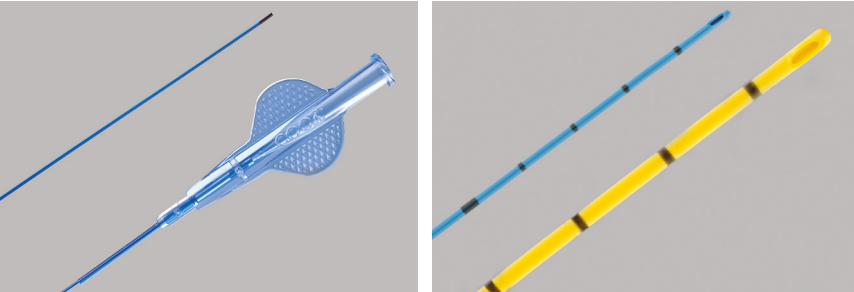


Figure 19. Irrigation catheters, SialoCath™ Salivary Duct Catheter (Left), Whistle Tip Ureteral Catheter (Right).

EXTERNAL RETENTION

The external retention disc is used to stabilise indwelling catheters. It aids against accidental pulls that might dislodge the drain. The Molnar retention disc is the only one of its kind on Cook Medical, which suggests a potential gap in the market for a redesign of external skin retention devices.

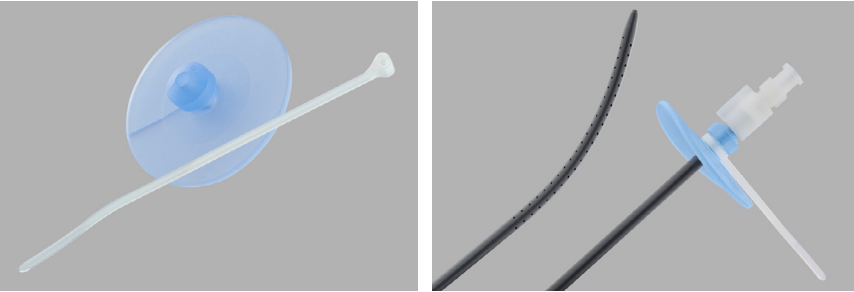


Figure 20. Molnar Retention Disc.

1.3 MULTI-PROPERTY 3D/4D PRINTING PRECEDENTS

As a tool for designers, multi-property 3D printing is still in its initial development. A precedent review examines how others have utilised this technology and to discover the possibilities. The investigation will be broad, looking at how its been used in the medical design field, for the creation of speculative products, and used to elicit human interactions.

MUSHTARI

Mushtari, Jupiter's Wanderer, is part of the Wanderers series of futuristic wearable capillaries (Figure 21). Inspired by the form and function of the human gastrointestinal tract, Mushtari theorises the idea of a wearable organ system that consumes and digests biomass, absorbs nutrients and expels waste (Oxman, 2014). The Wanderers is part of Stratasys's collection 'The Sixth Element: Exploring the Natural Beauty of 3D Printing'. The collection explores the relationship between multi-property 3D printing and Synthetic Biology. The ability to produce sophisticated models in a range of colours and opacities demonstrates multi-property 3D printings capabilities as a visualisation method. However, this precedent does not make use of flexible qualities, lacking the dynamic characteristics to communicate organic movement.



Figure 21. Mushtari, multi-property 3D printed capillaries. Reprinted from Oxman (2014). Retrieved from <http://neri.media.mit.edu/projects/details/mushtari>. Permission pending.

PHILIPS ANATOMICAL MODEL

Royal Philips partnered with 3D Systems and Stratasys to help progress patient care and improve clinicians experience (Figure 22). Anatomical models based on patient data were 3D printed on the Stratasys J750, presenting information that was previously unavailable. The prototypes enhanced how clinicians visualised sophisticated anatomy and diseases, such as cancerous tumours, which profoundly heighten the care they can provide patients (Phillips, 2017). Physical models allow medical personnel to interact and view disease states in the procedure from any angle, as opposed to visualising it on a screen restricted to specific viewpoints. The use of colour communicates the physiological composition, and how each complex structure is intertwined. It helps differentiate minuscule features, while highlighting areas of importance, such as disease states.



Figure 22. Royal Philips and Stratasys 3D printed anatomical model. Reprinted from Phillips (2017). Retrieved from <https://www.usa.philips.com/a-w/about/news/archive/standard/news/press/2017/20171127-philips-teams-with-3d-printing-industry-leaders-3d-systems-and-stratasys.html>. Courtesy of Philips.

HYDROPHYTES

Hydrophytes is a series of multi-property 3D/4D printed futuristic aquatic plants (Figure 23). It explores the ability of multi-property additive manufacturing to produce immersive experiences for museums, theme parks, and the film industry. The set of models investigate the idea of dynamic computer-generated objects (CGO). CGO focuses on blending the qualities of the digital and analogue worlds, forming lively physical objects offering immediate responses to actors in a film scenario (Stevens & Guy, 2015). Sealed chambers allow for independent activation through pneumatic inflation, bringing the 4D prints to life. The balance between controlled digital design with unrestrictive organic interaction results in compelling natural performances (Hone, 2018). The dynamic interactions aid in communicating the physiological capabilities of the materials.



Figure 23. Hydrophytes, multi-property 3D/4D printed aquatic plants. Reprinted from Hone (2018). Retrieved from <https://www.nicolehoney.com/hydrophytes>. Permission granted by Nicole Hone.



1.4 BACKGROUND RESEARCH SUMMARY

There is an established need for new percutaneous surgical drains that address common complications, some of which are,

Kinking: when the catheter forms a sharp twist or curve, preventing fluid from draining (Figure 24).

Dislodgement: when the catheter is forced out of position in the abscess, usually by unexpectedly being pulled on.

Blockages: thick viscous fluids clog drainage holes preventing less viscous fluids from draining.

Inadvertent removal: accidentally pulling on the drain dislodges it from the external skin fixation.

The precedent review of surgical catheter-related products revealed potential gaps in the market. While there are irrigation drains, there does not seem to be a catheter dedicated to both irrigating and draining, which could address blockages by reducing thick fluids allowing it to drain more efficiently. There appears to be a lack of skin fixation devices, which could address inadvertent

removal by externally securing an indwelling catheter. Incorporating rigid internal structures in certain areas of a drain could provide enough support to restrict it from kinking. Lastly, including stimulus-responsive materials into the tip of a drain could provide autonomous internal retention to prevent dislodgment while eliminating the need for a pigtail string. The customisation options that additive manufacturing offers, opens up avenues for patient-specific catheters suited for that particular procedure. Instead of producing a one size fits all surgical catheter, they could be tailored depending on the situation, providing the most suitable design for the patient.

From the array of various additive manufacturing processes, multi-property 3D printing with the Stratasys J750 appears the most suitable for translating clinical ideas into physical prototypes for comprehension of sophisticated designs. The high-resolution and ability to blend materials to generate a range of shore hardnesses all in one prototype allows for the production of dynamic models that accurately represent that of a finished product. Also, the availability of smart materials containing SMP's provides the means to explore stimulus-responsive structures. The multi-property 3D printed precedents analysed demonstrates the technologies capabilities to produce prototypes that communicate through interaction and visualisation.

Figure 24. A kinked surgical drain, which is a common issue that impacts drainage.

RESEARCH QUESTION

How can multi-property 3D/4D printing be an effective prototyping and visualisation method for the design and communication of novel percutaneous surgical drain ideas?

2.1 OVERALL APPROACH TO RESEARCH

Research-for-design (RFD) is the first stage, which provides the foundation for the project. Findings from this stage aid in determining design decisions used to produce the end outcomes. The overall information gathered in this stage will then help drive the next research stage (Frankel & Racine, 2010).

Research-through-design (RTD) is the second stage, where knowledge is generated by designing innovative outputs. These outputs are validated through tangible methods, such as touch, flow, and sharing with clinicians to answer the proposed research question (Schneider, 2007; Martin & Hanington, 2012). It is an inquiry into the methods and processes of design practice through research and experimentation (Zimmerman, Stolterman, & Forlizzi, 2010).

A practice-based design approach will explore the potential of multi-property 3D printing on the Stratasys J750, which is an original investigation initiated to attain new knowledge by practice and outcomes produced from that practice (Candy, 2016). This approach allows an idea that is addressing an issue to translate from a theoretical concept into a tangible concept for critical reflection, discussion, and comprehension.

- Issue: RFD
- Ideas- RTD (Aim 1 & Aim 2)
- Critical reflection- RFD
- Resolve concept- RTD

AIM	OBJECTIVE	METHOD
AIM 1 (PRAGMATIC): Investigate the current state of surgical drains and explore how contemporary technologies could address the issues.	1a. Acquire expert advice on the known complications with current surgical drains.	Literature & precedent review, expert clinical advice
	1b. Identify and generate ideas to address the known complications with surgical drains.	Ideation, discussion, renders, sketches
	1c. Develop a series of prototypes to evaluate the pragmatic capability of 3D printing.	3D model, 3D print, evaluate, discussion.
	1d. Digitally evaluate drains using computational fluid dynamics (CFD) to visualise and communicate flow data.	3D model, Computational fluid dynamics
AIM 2 (SPECULATIVE): Produce examples of tangible visualisation to explore the potential of multi-material additive manufacturing focussing on speculative ideas.	2a. Explore dynamic and responsive complex structures based on anatomical features.	3D model, rendering, multi-property 3D printing
	2b. Investigate 4D printing techniques to simulate organic anatomical movements.	3D model, multi-property 3D printing

Figure 25. Overview of the aims, objectives and methods used to achieve the research question.

BACKGROUND RESEARCH METHODS

Literature & Precedent Review

Literature in the medical and additive manufacturing fields will be collected and synthesised, providing the essential background knowledge related to the key themes of the research question (Hanington & Martin, 2012). An analysis of established designs is required to understand the current state of surgical drain products, including gaps in the market. Design precedents will evaluate how others have explored multi-material 3D/4D printing, providing the potential and limitations of the new technology. The precedent review serves as secondary research, which will establish definitional boundaries within the project topic and potential opportunities (Hanington & Martin, 2012).

Expert Advice

Tertiary professors in the fields of industrial design, biological sciences and surgery provided personal experience related to the topic. Insight acquired from industry professionals helped guide design decisions and provide background knowledge. Additionally, a colorectal surgeon provided clinical feedback on the resolved designs. Interaction with physical prototypes prompted feedback on whether or not certain design features would be viable within the industry or meet the required standards for medical devices. A medical-based perspective helped to assess the potential and limitations of 3D printing and the proposed outcomes. Ethic details on page 152.

DESIGN EXPERIMENTATION METHODS

Iterative Design Process:

The iterative design process (Figure 26) is the means of reaching the desired outcome by repetitively analysing an idea through a cycle of methods (Business Dictionary, 2019). Lawson (2005) illustrates the design process in three principal stages that are revisited numerous times in an unstructured cycle forming an iterative design process. The first stage is analysis, which involves defining and ordering the problem or objective. The second stage is synthesis, which is an attempt to progress forward by generating a solution to the problem or objective. The third stage is the appraisal, which is the critical evaluation or reflection of the proposed solutions against the

problems/objectives. The interpretation of the iterative process throughout this research incorporates the methods, reflection, ideation, 3D modelling, 3D printing, and evaluation in an unrestricted cycle (Figure #).

A parallel prototyping approach will be implemented, which involves producing multiple iterations in tandem. This approach leads to higher quality and more diverse work leading to an increase in self-efficacy, which can help foster a positive outlook toward critique (Dow et al., 2010). Utilising a parallel prototyping approach during the early stages of the project allows for a range of ideas to be explored, improving the nature of critiques, leading to more effective design results (Hanington & Martin, 2012).

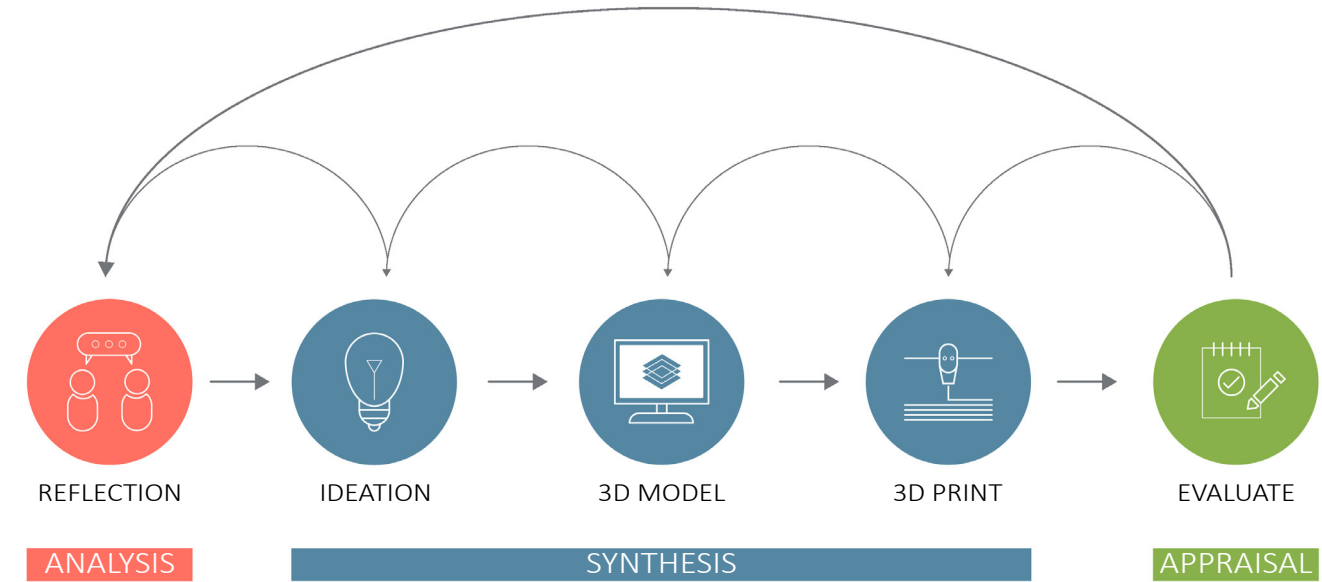


Figure 26. Diagram illustrating the iterative design process.

Reflection

Reflection acts as the analysis phase for defining and ordering of problems. Self-reflection is conducted to assess design outputs to determine what worked, what aspects need refining and potential avenues to explore during the next iterative cycle. Newell (1992) explains how self-reflection and critical thinking are fundamental to self-directed learning.

Ideation

The beginning of the synthesis phase, ideation involves generating solutions to the established problems. Sketches provide quick iterative visualisations to express concepts.

3D Model

Several computer-aided design (CAD) programmes are used throughout this research to translate ideation concepts into digital models. Solidworks is the primary program used, along with Netfabb, Meshmixer, and GrabCad Print. One CAD model can be systematically processed through multiple programmes depending on the design choices.

Prototyping / 3D printing

Digital models are translated into tangible visualisations through 3D printing, allowing for analysis and interpretation. A range of 3D printing techniques are used to explore material finishes and print quality with material jetting being the primary process. The majority of designs produced during this research are printed on the Stratasys J750. GrabCad Print is a programme that allows

for the setup of numerous CAD models to be 3D printed on one tray. Batch printing allows for fast in-house production of multiple prototypes on one tray speeding up the iterative design process. Colour and material properties can be assigned to individual parts of a model in an assembly, allowing for the creation of complex geometries.

Evaluate

Evaluation acts as the appraisal stage for critical reflection of proposed design concepts. Interacting with designs provides haptic feedback and most importantly, an understanding of the physiology of complex blended multi-material 3D/4D prototypes. The knowledge provided by interacting with physical models is the only way to ascertain the characteristics and behavioural properties of intricately fused materials, fundamental to the ideology of tangible visualisation. Expert advice received from clinicians is also included in the evaluation step.

2.2 DIGITAL SOFTWARE TOOLS

The set of CAD software used to translate clinical ideas into digital models for 3D printing. Output files from one program can systematically be processed in another program, depending on the required purpose. The general form of a CAD model is created in Solidworks, run through Meshmixer for the generation of anatomical structures, optimised and repaired in Netfabb, and lastly run through GrabCad Print for 3D printing on the J750.

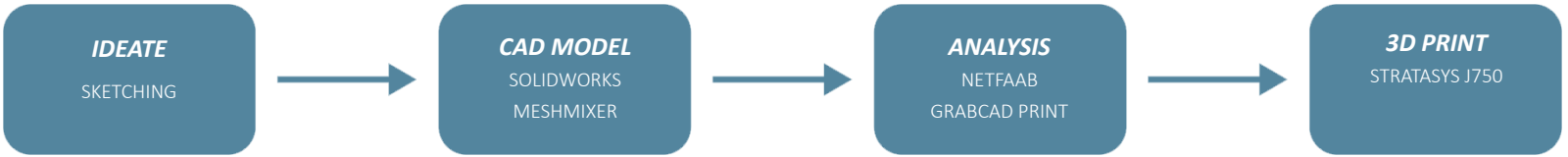


Figure 27. Diagram illustrating the step-by-step process from ideation to CAD modelling to 3D print.

SOLIDWORKS

SolidWorks is a CAD engineering computer program published by Dassault Systèmes. The program utilises solid modelling technology with a parametric feature-based approach (Figure 28). SolidWorks can produce accurate structured models down to several numerical point values, making it well suited for the accuracy of the J750. This accuracy means the control of design intent is maintained when working in parts with microscopic features. During this research, SolidWorks is the primary software used to create accurate base models to then transfer into other programs for the generation of more anatomical structures.

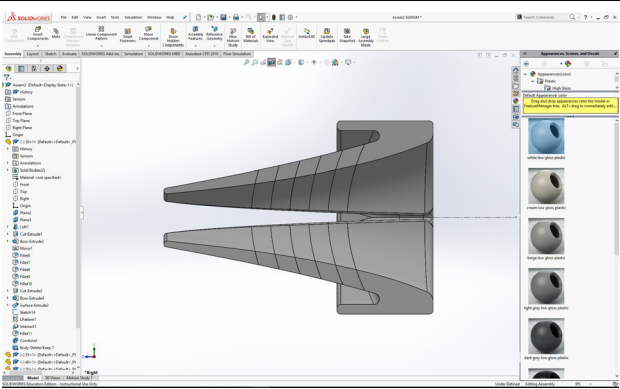
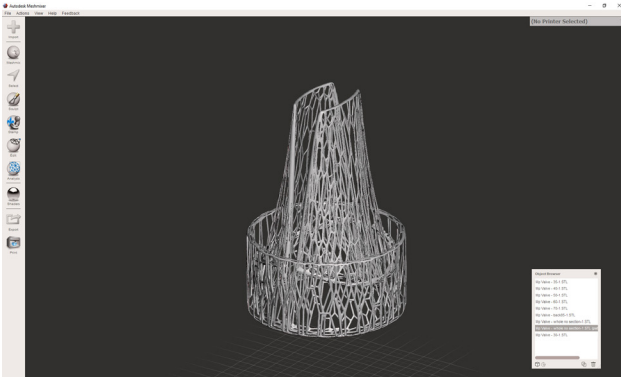


Figure 28. Solidworks interface.

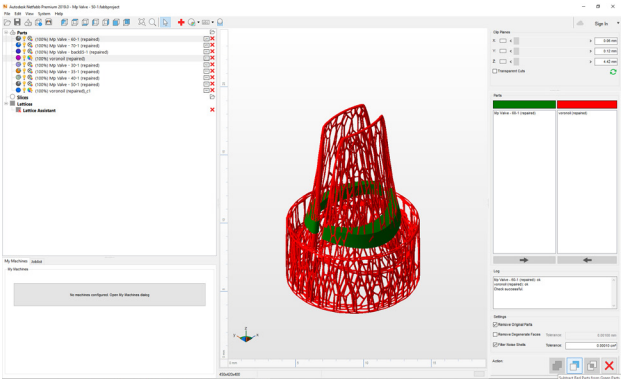
MESHMIXER

Meshmixer is a 3D sculpting-based CAD program ideal for working with triangle meshes published by Autodesk. It is useful for creating, manipulating and analysing standard-tessellation-language (STL) files for 3D printing (Figure 29). Throughout this study, Meshmixer is used to alter STL files from other programmes, primarily SolidWorks. Meshmixer was used to integrate various internal lattice forms and complex Voronoi structures into models to explore how internal microscopic structures may affect the physiological build of multi-property 3D printed models.



NETFABB

Netfabb is an additive manufacturing software produced by Autodesk that allows for mesh repairs and optimisation of files for 3D printing (Figure 30). During this research, Netfabb is used to boolean complex internal structures from a base structure to ensure microscopic details accurately print on the J750. A boolean process either adds, subtracts or creates an intersect from overlapping parts. While exporting files, they are optimised to eliminate holes and split edges, which may detrimentally impact the performance of 3D printed objects.



GRABCAD PRINT

GrabCad Print is the program used to setup STL files for production, assigning of materials and colour properties, and analysing files to ensure an accurate 3D print (Figure 31). This software is tailored for Stratasys machines; it provides an effortlessly smooth 3D printing workflow. Multiple files can be placed in one tray and produced simultaneously. This ability provides an efficient parallel prototyping process due to the ability to generate various ideas at once.

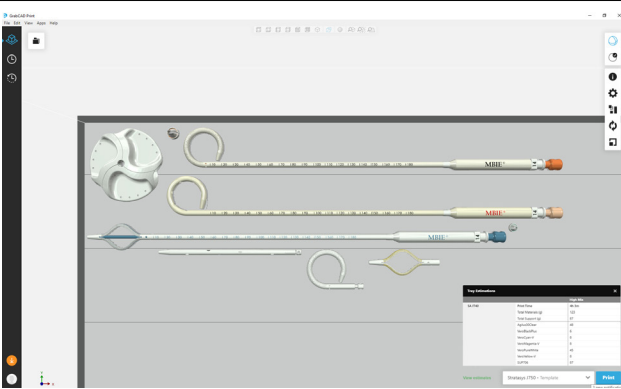


Figure 29. Meshmixer interface (top).

Figure 30. Netfabb interface (middle).

Figure 31. GrabCad Print interface (bottom).

2.3 STRATASYS J750 TECHNICAL OVERVIEW

The Stratasys J750 (Figure 33) is the latest in Polyjet multi-property 3D printing, with vast unexplored potential. It can produce models at a resolution of 14 microns, in over 360,000 different colour combinations and various shore hardnesses (Figure 34). The J750 uses the additive manufacturing process of material jetting, which dispenses tiny droplets of photosensitive materials that solidify under ultraviolet light, layer by layer.

Multi-property functionality blends various Vero materials providing the colour and rigidity with Agilius, a flexible photopolymer with superior tear resistance. The result is a wide array of diverse material properties, producing dynamic prototypes. 3D printed outputs print encased in a soluble support material called SUP706. A sodium hydroxide solution can dissolve small amounts of the support with the bulk of it being removed by gently compressing to break it up. This capability allows for the production of prototypes with the feel and function of finished products. With a build size of 490mm x 390mm x 200mm enables the J750 to produce multiple models during one print run, speeding up the iterative design process (Figure 32).



Figure 33. The Stratasys J750.

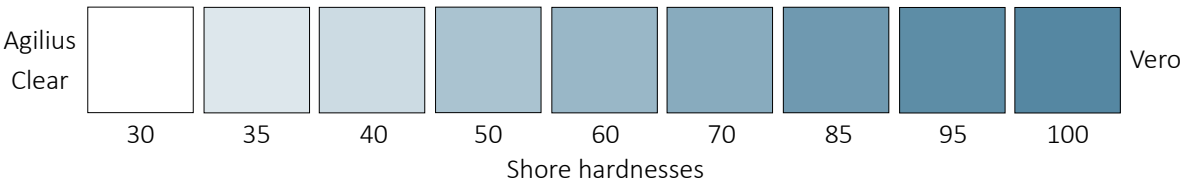
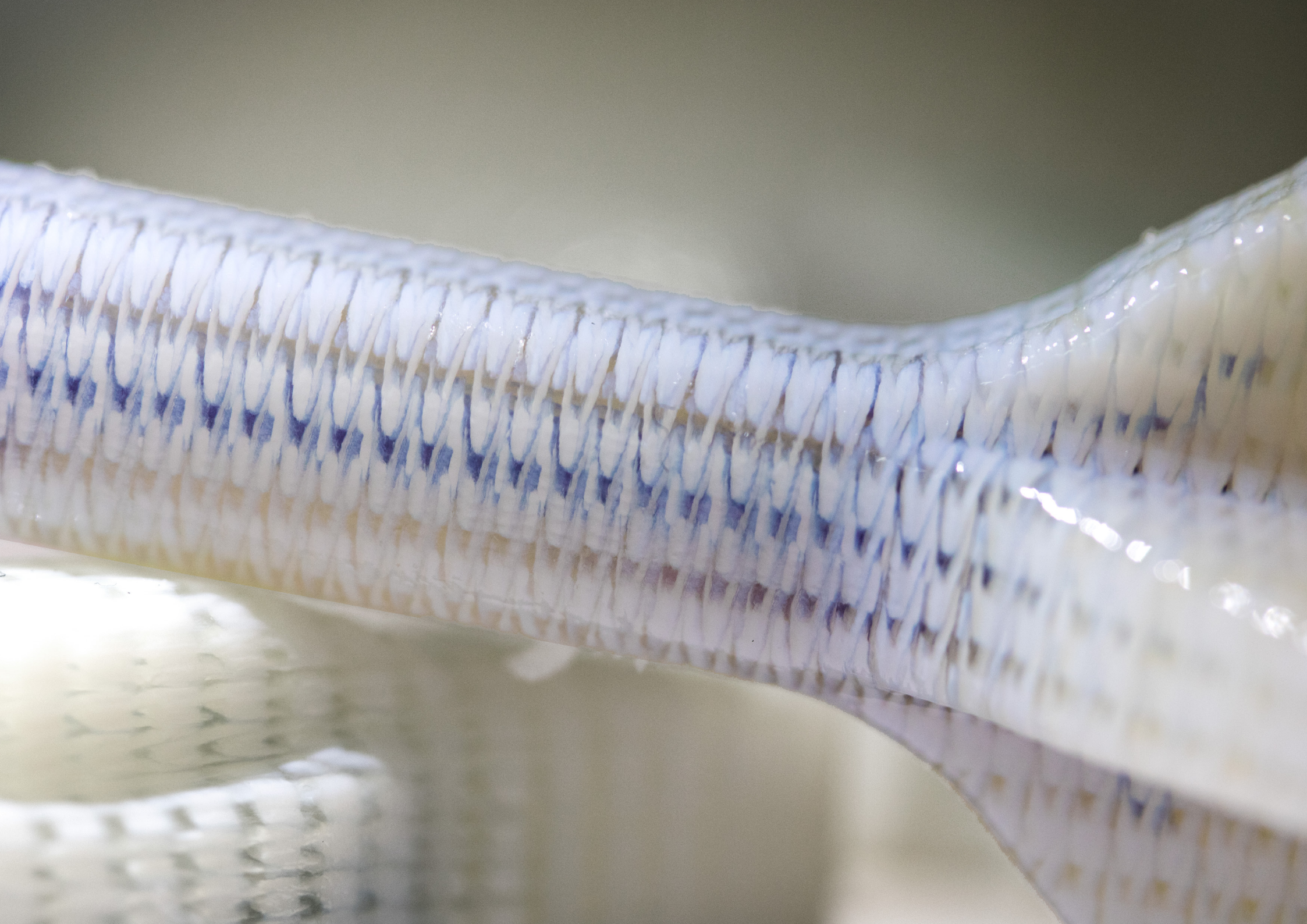


Figure 32. 3D prints on the Stratasys J750 build tray.

Figure 34. The various blends of shore hardnesses produced with Agilius and Vero on the Stratasys J750. Shore hardness is a term to signify the hardness of a material. The colour of higher shore value materials is more opaque.



MULTI-PROPERTY 3D PRINTING CLEANING METHODS

3D printed models on the J750 print encased in a soluble gel-like support material called SUP706 (Figure 35). Considerable time during this research is taken to remove support material to make sure delicate details don't accidentally break. A rigorous cleaning method is employed, so models don't split or get damaged, ensuring high-quality outputs for critical evaluation.

1. The bulk of the support material surrounding the print is carefully removed by gently compressing it, breaking it apart (Figure 37). As many prints are tubular forms, there is a lot of support material within the models that can be difficult to remove. Removable internal stents printed inside models to reduce the amount of support material (Figure 36). Brushes and toothpicks are used to remove excess material from delicate, intricate details.

2. Then, submerging models in a DT3 CleanStation that circulates a solution of 2% sodium hydroxide and 1% sodium metasilicate, dissolves small areas of support material. Prints are left in the cleaning bath for around 30 minutes to two hours. Multiple models can soak in the cleaning bath at one time, speeding up the cleaning process.

3. After the DT3, prints are thoroughly washed in water and left to dry. Enclosed tubes will still contain support material; this is removed by lightly compressing and massaging it out. Occasionally immersing prints in warm water helps to loosen and wash out support material. However, it appears that leaving 3D prints in water for too long weakens the material, making it susceptible to tearing, as it absorbs moisture causing it to expand slightly.



Figure 36. Removal of an internal stent.

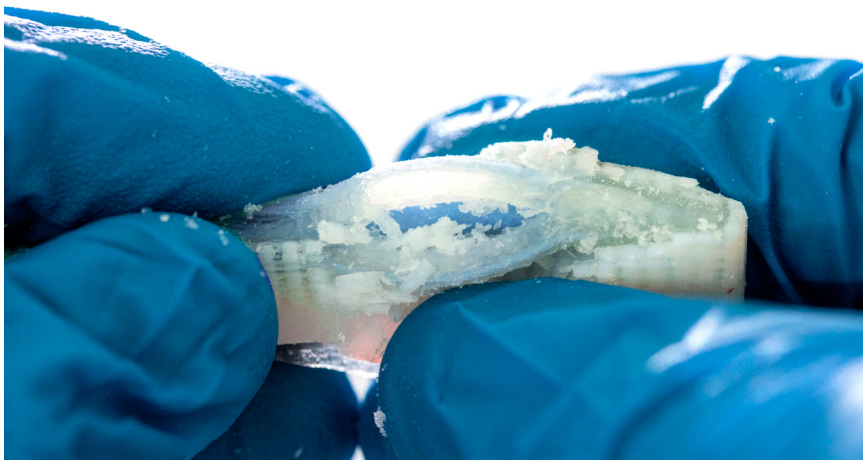


Figure 37. Delicately breaking up support material.

Figure 35. Multi-property 3D print encased in support material.

3.1 COMMERCIAL 3D PRINTING INVESTIGATION

A series of three different straight drains were printed in various materials to ascertain the possible resolution, smoothness, flexion, and capability of 3D printing methods (Figure 39). Three commercial 3D printing services were assessed, Shapeways based in the USA, i.Materialise situated in Belgium, and Sculpteo located in France. This evaluation provides a reference library of the possible resolutions and finishes that additive manufacturing is capable of producing.

Conclusion: The Standard Resin material produced through stereolithography (SLA) from i.Materialise provided the best qualities. The resolution of the tiny drain holes printed exceptionally, the surface was smooth, and all of the support material was able to be removed. However, the 3Dsystems Ultra high detail printer, more detail about this is in the next section, is logistically the best option. It provides the most accurate details, the capability to be post-treated, and is locally available.

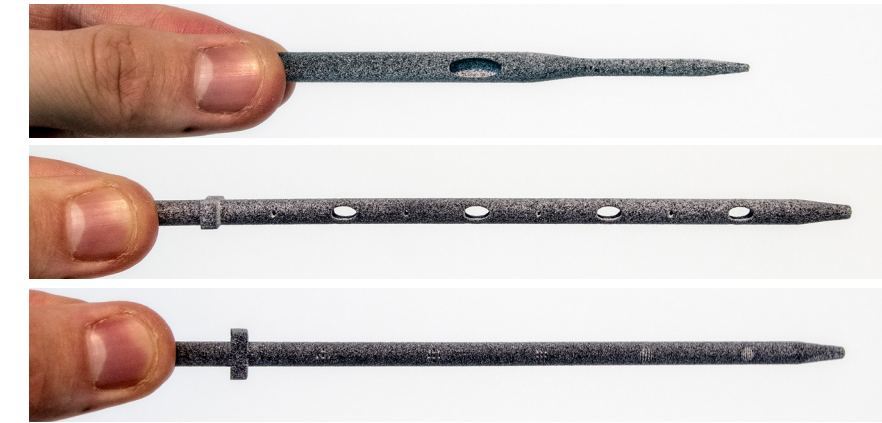


Figure 39. The three different straight drain designs in the Polymide (MJF) material from i.Materialise.

Figure 38. Magnified view of the Polymide (MJF) material from i.Materialise.


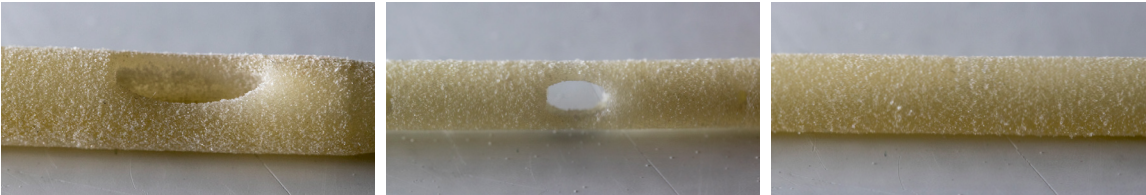
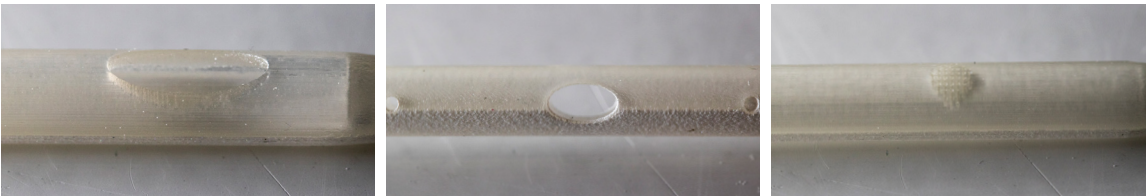
SHAPEWAYS 3D PRINT MATERIAL IMAGES			MATERIAL PROPERTIES	NOTES
			STRONG & FLEXIBLE PLASTIC (NYLON 12 PLASTIC) SLS (Selective Laser Sintering) Layer Thickness (Resolution): 0.12mm Cost (USD): \$3.07- \$3.62	<ul style="list-style-type: none">• Grainy surface texture.• Accurate details on medium-large holes.• Small mesh holes failed.• Double lumen printed well.
			HP NYLON PLASTIC (MULTI-JET FUSION PLASTIC) MJF (Multi-Jet Fusion) Layer Thickness (Resolution): 0.08mm Cost (USD): \$7.14- \$8.25	<ul style="list-style-type: none">• Grainy surface texture.• Accurate details on medium-large holes.• Small mesh holes failed.• Double lumen printed well.
			ELASTO PLASTIC SLS (Selective Laser Sintering) Layer Thickness (Resolution): 0.12mm Cost (USD): \$2.91- \$3.64	<ul style="list-style-type: none">• Grainy surface texture.• Accurate details on medium-large holes.• No mesh holes printed• Decent flexibility.• Starting to tear.
			FROSTED DETAIL PLASTIC (RESIN-BASED ACRYLIC PLASTIC) Material Jetting Layer Thickness (Resolution): 0.0016mm Cost (USD): \$6.00- \$7.42	<ul style="list-style-type: none">• One side is smooth the other is rough• Very accurate details.• Smallest mesh printed.• Double lumen printed well.
			HIGH-DEFINITION ACRYLATE DLP (Digital Light Processing) Layer Thickness (Resolution): 0.05mm Cost (USD): \$10.00- \$10.23	<ul style="list-style-type: none">• Drain printed very deformed, starting to curve.• Accurate details on medium-large drain holes.• Small mesh holes failed.

Figure 40. Shapeways 3D print materials documentation.

i.MATERIALISE 3D PRINT MATERIAL IMAGES			MATERIAL PROPERTIES	NOTES
			POLYIMIDE (SLS) SLS (Selective Laser Sintering) Layer Thickness (Resolution): 0.12mm Cost (USD): \$21.84	<ul style="list-style-type: none">• Grainy surface texture.• Accurate details on medium-large holes.• Small mesh holes failed.• Double lumen printed well.
			POLYIMIDE (MJF) MJF (Multi-Jet Fusion) Layer Thickness (Resolution): 0.08mm Cost (USD): \$21.84	<ul style="list-style-type: none">• Grainy surface texture.• Accurate details on medium-large holes.• Small mesh holes failed.• Double lumen printed well.
			RUBBER-LIKE SLS (Selective Laser Sintering) Layer Thickness (Resolution): 0.12mm Cost (USD): \$14.83- \$17.59	<ul style="list-style-type: none">• Grainy surface texture.• Accurate details on medium-large holes.• Largest mesh holes printed• Good flexibility.
			STANDARD RESIN SLA (Sterolithography) Layer Thickness (Resolution): 0.01mm Cost (USD): \$20.67- \$22.23	<ul style="list-style-type: none">• Very smooth• Very accurate details.• Smallest mesh printed.• Double lumen printed well.• The smoothest and highest quality print.
			HIGH-DEFINITION ACRYLATE SLA (Sterolithography) Layer Thickness (Resolution): 0.05mm Cost (USD): \$52.51	<ul style="list-style-type: none">• Accurate details on medium-large drain holes.• Small mesh holes failed.• Not able to be print the mesh design so hard to analyse small details.

Figure 41. i.Materialise 3D print materials documentation.


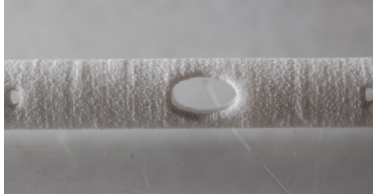


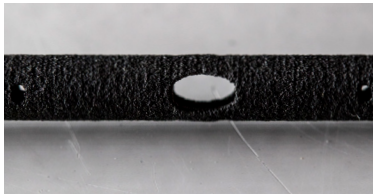

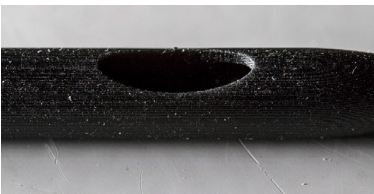
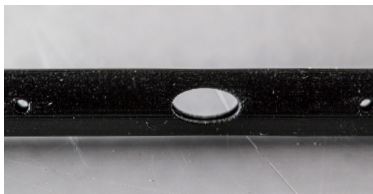
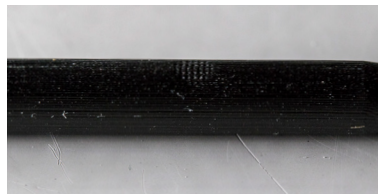
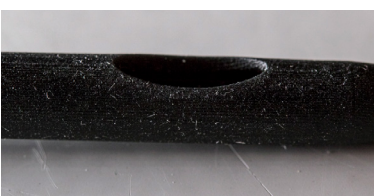
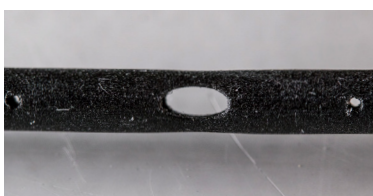
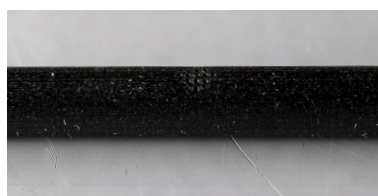
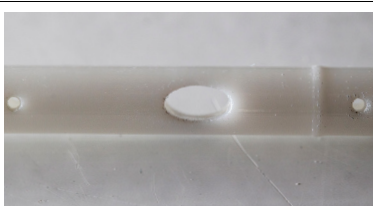
SCULPTEO 3D PRINT MATERIAL IMAGES			MATERIAL PROPERTIES	NOTES
			NYLON PA12 (SLS) SLS (Selective Laser Sintering) Layer Thickness (Resolution): 0.15- .1mm Cost (USD): \$6.86	<ul style="list-style-type: none">• Grainy surface texture.• Accurate details on medium-large holes.• Small mesh holes failed.• Double lumen printed well.• Best Nylon PA12 SLS print.
			NYLON PA12 (MJF) MJF (Multi-Jet Fusion) Layer Thickness (Resolution): 0.08mm Cost (USD): \$6.86	<ul style="list-style-type: none">• Grainy surface texture.• Very accurate details on medium-large holes.• Small mesh holes failed.• Double lumen printed well.
			RIGID POLYURETHANE 70 DLS (Digital Light Synthesis) Layer Thickness (Resolution): 0.1mm Cost (USD): \$56.09	<ul style="list-style-type: none">• Very accurate details.• Small mesh holes printed very well.• The most similar material to current surgical drains.
			FLEXIBLE POLYURETHANE DLS (Digital Light Synthesis) Layer Thickness (Resolution): 0.1mm Cost (USD): \$56.09	<ul style="list-style-type: none">• Very accurate details.• Small mesh holes printed very well.• The most similar material to current surgical drains.• The best flexible material.
			PROTOTYPING ACRYLATE RESIN DLS (Digital Light Synthesis) Layer Thickness (Resolution): 0.1mm Cost (USD): \$21.22	<ul style="list-style-type: none">• Very accurate details.• Small mesh details printed.• Odd ridges printed along the length of the drains.• Very smooth surface.

Figure 42. Sculpteo 3D print materials documentation.

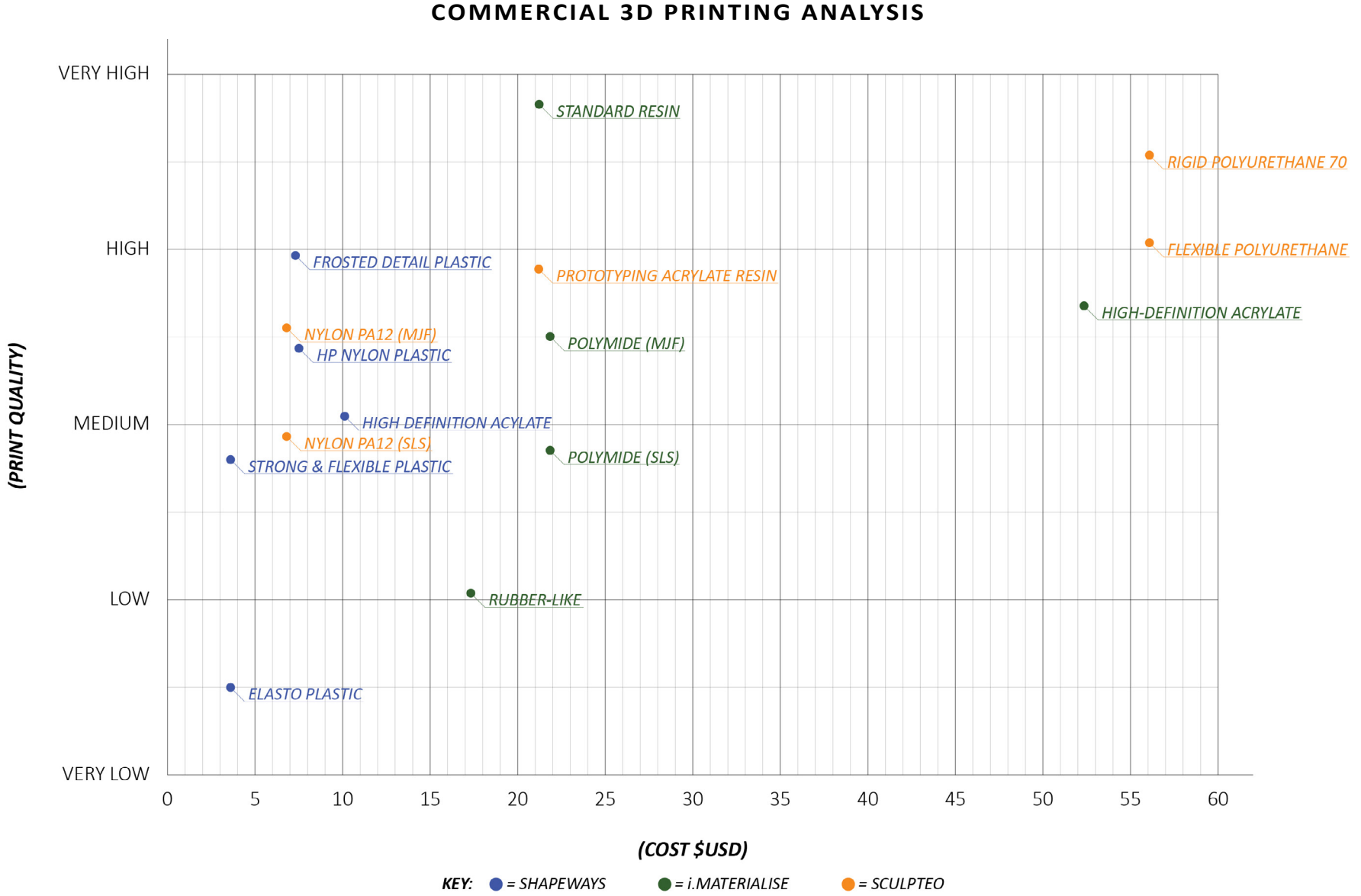


Figure 43. Commercial 3D printing analysis diagram.

3.2 LAB TESTING

An exploration looked into how different drainage hole shapes, sizes, and orientations affect drainage efficiency. Increasing efficiency would reduce the patient's time spent in hospital and time requiring a catheter. A test-rig flows fluids of varying viscosity, applying pressure to simulate the force the body provides (Figure 45). Glass-beads and oil formulations are also mixed with liquids to generate more realistic bodily fluids. The total surface area of drain holes for models in the same batch is kept the same to ensure fair testing.

3Dsystems ProJet MJP 3600 3D printer, utilising multi-jet printing (MJP) technologies, generated models for testing; each iteration gets printed in triplicate to ensure accurate results (Figure 44). Multi-Jet printing is an inkjet

3D printing process that deposits photocurable resin or casting wax layer by layer. It can achieve a layer resolution of 16 microns but is limited to mono-material. In itself, this is also a test of additive manufacturing's capability to consistently produce precise models in bulk for testing. The 3Dsystems printer was chosen due to its high resolution, ensuring tiny details across all models are equivalent, and its ability to effortlessly remove support. The use of a rigid mono-material 3D print was to make sure that models flexing during tests would not be a variable affecting drainage speeds.

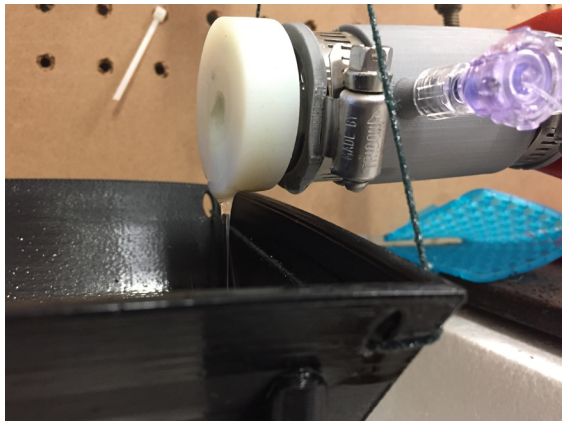
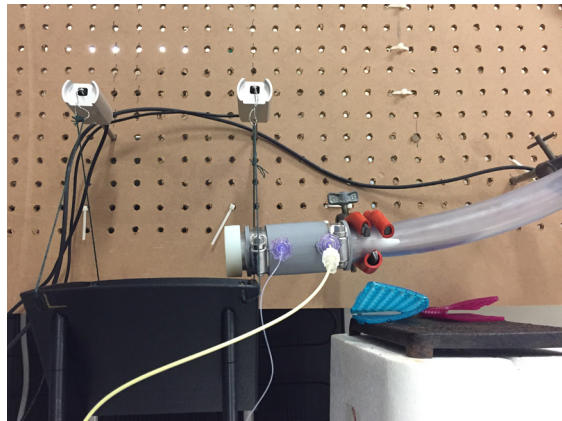


Figure 44. 3D printed Lab Test prototypes produced on the 3Dsystems ProJet MJP 3600.

Figure 45. Test-rig setup.



Figure 46. Test-rig before the introduction of 3D printing.

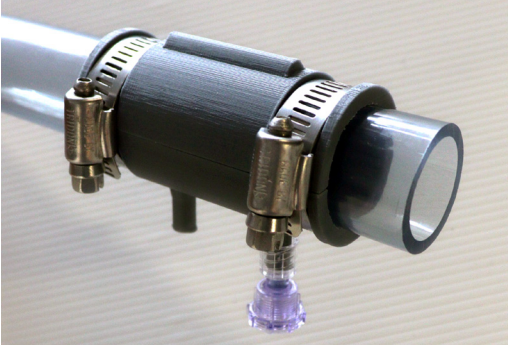


Figure 47. Test-rig after the introduction of 3D printing.

LUER TEST-RIG FITTING

Before the introduction of 3D printing, hot glue and cable ties were used to attach Luer locks onto the test-rig crudely (Figure 46). A redesign of the Luer test-rig fitting was imperative to ensure accurate testing as leakages were prevalent with the previous set-up (Figures 47—48).

This example demonstrates how additive manufacturing can overcome custom, one-off design problems promptly and inexpensively, in ways other manufacturing processes are not capable of executing.

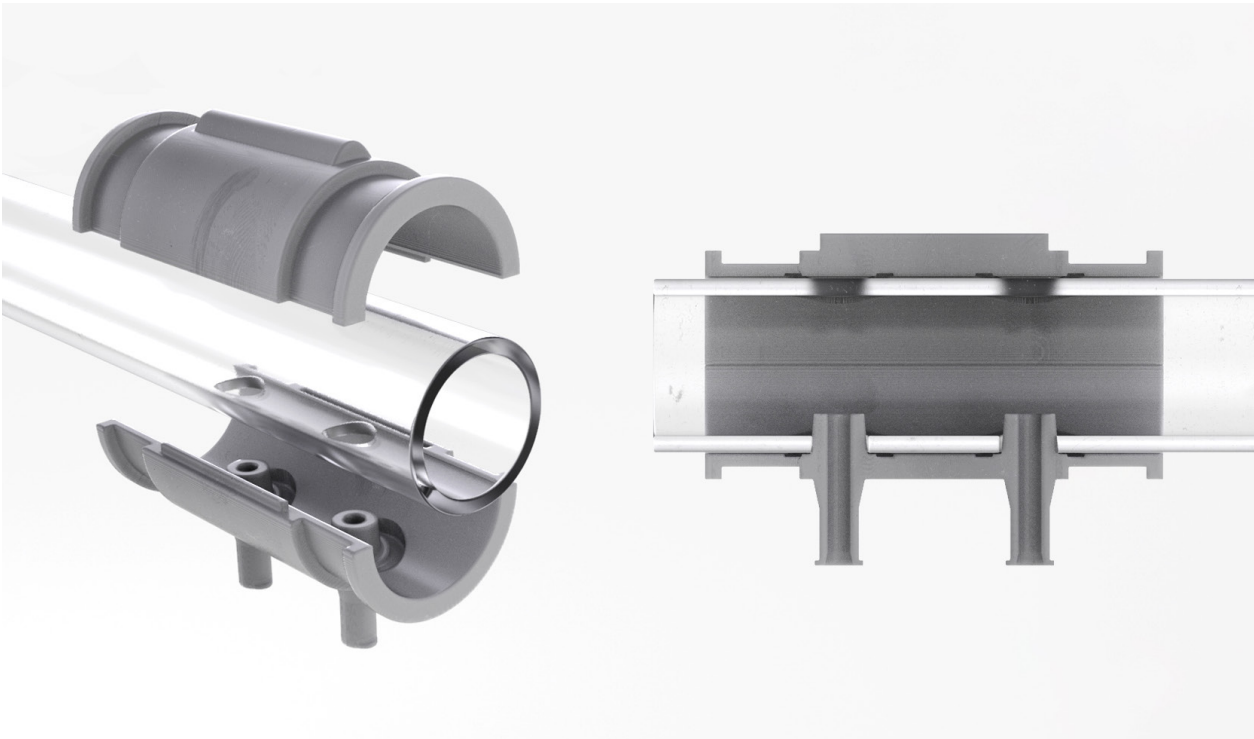


Figure 48. Assembly of the Luer test-rig fitting.

OVERVIEW OF LAB TESTING

Over 50 iterations explored drainage efficiency by varying drain hole shape, sizes, and orientation. An in-depth catalogue, in the appendix (Figures 146—149), recorded every drain by applying a unique code to each design, similar to a number plate, based on their characteristics. Figure 49 demonstrates a section of the comprehensive record, while a concise history on page # exhibits all tested designs.

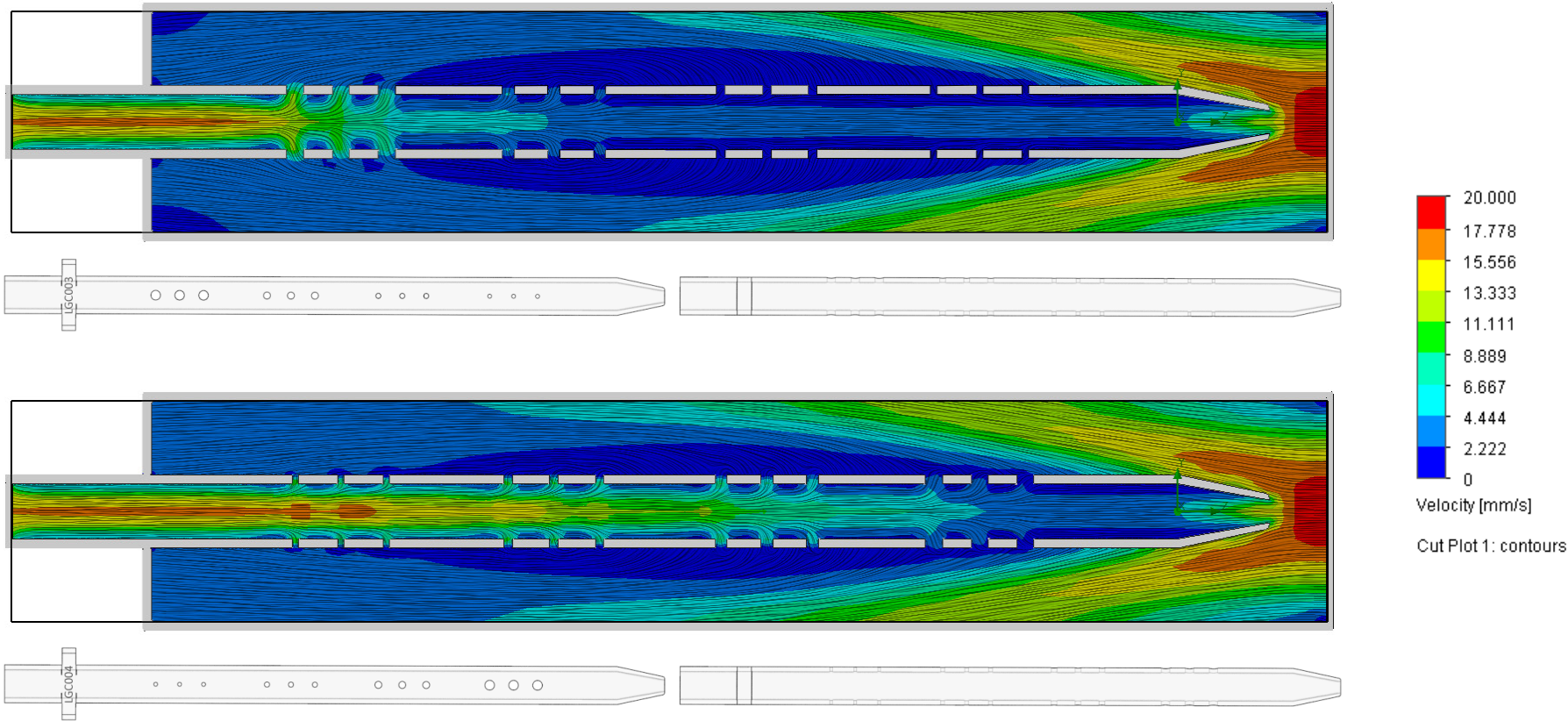
The overall results from the Lab testing approximated that either circle or oval drain holes are the most efficient. Drain holes located at the tip of the catheter appear to increase drainage speeds. Lastly, a combination of lots of little holes, like a sieve, surrounding one large hole may be the optimal orientation. The small holes will drain less viscous fluids while the larger will focus on the thicker matter. If the large drainage holes get blocked by a dense substance, then the surrounding little holes can still drain less viscous fluids.

From a design research perspective, this investigation proved additive manufacturing’s abilities to produce a multitude of iterative models with incremental micron level alterations for testing.

LAB TESTING SUMMARY

A limitation from this study was working with commercial companies with access to the required 3D printer. During this study, two different 3D printing services produced the test-models. Consistent quality is required with all the test-models to ensure that it is not a variable affecting results. The print resolution, orientation, model material, support material, cleaning of support material, and post-processing need to all remain consistent to guarantee a fair experiment. Working with two different commercial companies with different setups was an issue that could have an impact on the findings.

Despite the limitation, additive manufacturing is still the only process capable of producing the required outputs quickly and efficiently. This investigation confirmed not only the effect of various drainage hole shapes, sizes and orientation has on drainage efficiency but also the quality of 3D printing for batch experiments.



LGC003 & LGC004

Large, Gradient, Circle

- 12 drain holes on each side gradienting in size
- Total surface area of drain holes = 30mm²
- Smallest drain hole radius = 0.33mm Area = 0.34mm²
- Small drain hole radius = 0.46mm Area = 0.66mm²
- Large drain hole radius = 0.65mm Area = 1.33mm²
- Largest drain hole radius = 0.922mm Area = 2.67mm²

Figure 49. Computational fluid dynamic analysis on LGC003 (top) and LGC004 (bottom) Lab testing designs.

COMPUTATIONAL FLUID DYNAMICS

Computational-fluid-dynamics (CFD) was employed to analyse test-models against the physical Lab testing, digitally. It assisted in making accurate assumptions about how the drain hole variables would affect velocity — demonstrated by two test-models, LGC003, and LGC004 (Figure 49). The CFD results from LGC004 shows that having larger drain holes closer to the tip of the drain induces a higher velocity earlier, whereas LGC003 shows that having smaller drain holes at the tip produces a slower velocity at the same point that eventually reaches the same speed further down at the location of the larger drain holes. CFD is also useful to visualise potential circulation issues, and how minor changes, such as angling the entry drain hole or applying a radius to the edge could positively, or negatively, impact drainage.

The evidence of CFD’s ability to produce accurate results similar to the physical testing demonstrates how it can be applied in the design process to influence decisions. However, the FDA ISO 14708-5 standard declares that CFD is limited for analysis in the early design stages instead of evaluating total quantities. (Malinauskas et al., 2017)

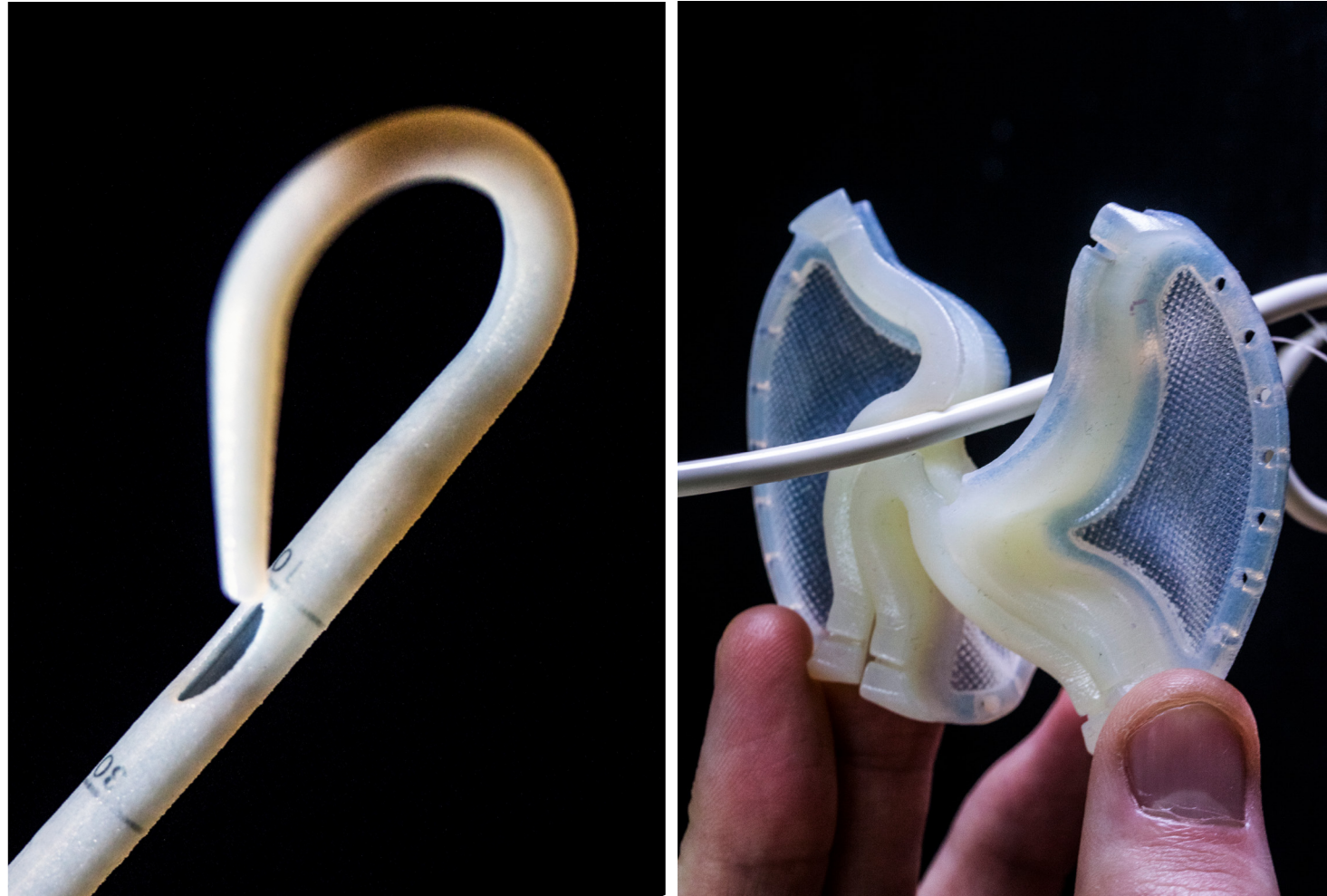


Figure 50. Pragmatic designs, Irrigation drain (left), Skin fixation (right).

3.3 PRAGMATIC EXPERIMENTS

Pragmatic solutions utilise the iterative nature of additive manufacturing to explore multiple solutions to common complications with current surgical drains (Figure 50). The result is the implementation of ideas for today's market and manufacturing processes. An investigation into various additive manufacturing methods examines appropriate materials and processes for rigorous testing, while also assessing the J750's capability to produce models at a similar level to finished products.



Figure 51. Early concept of the self-cleaning pigtail irrigation drain.

IRRIGATION DRAINS

PRAGMATIC DESIGN

Currently, it appears that there is not a catheter that has separate lumens focusing on irrigation and drainage. These irrigation drains feature an additional lumen that concentrates on introducing fluid into the abscess, and the external/internal area of the catheter. Irrigation solutions, such as saline reduce the viscosity of infected fluids, making them easier to drain (Figure 51). Flushing fluid through the irrigation channel can also act as a means for unblocking drainage holes.

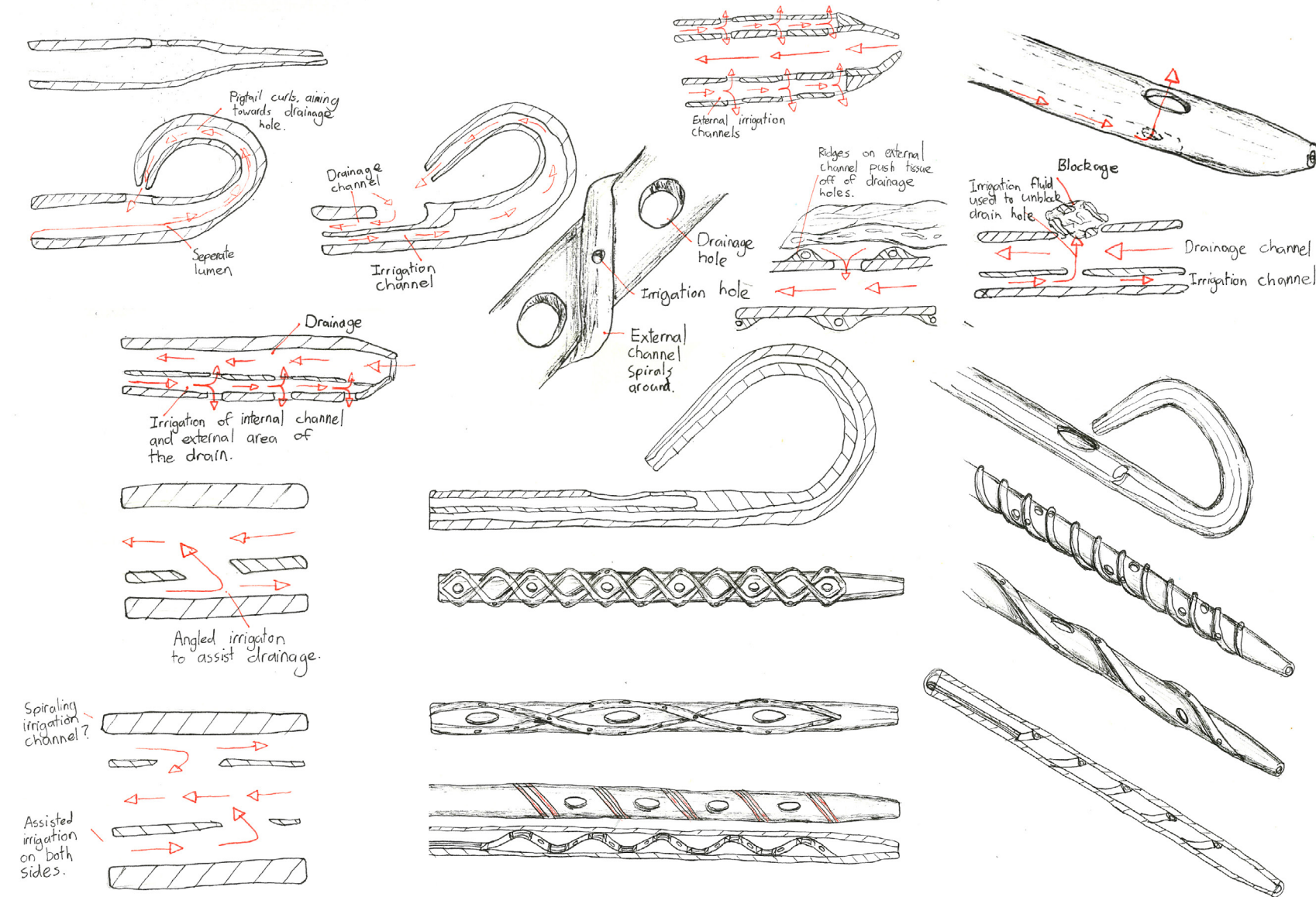


Figure 52. Irrigation drain ideation sketches.

Develop variations that have tighter and more sparse external spirals.

Explore more rigid external channels for pushing tissue off of the drainage holes.

Highlight any internal features on the exterior surface of the drain, so it is visible if radiologists decide to make any manual adjustments, such as creating more drainage holes.

Highlight the internal channel so radiologists can see it if they need to make manual adjustments.

The Archimedes screw function would only work on straight paths.

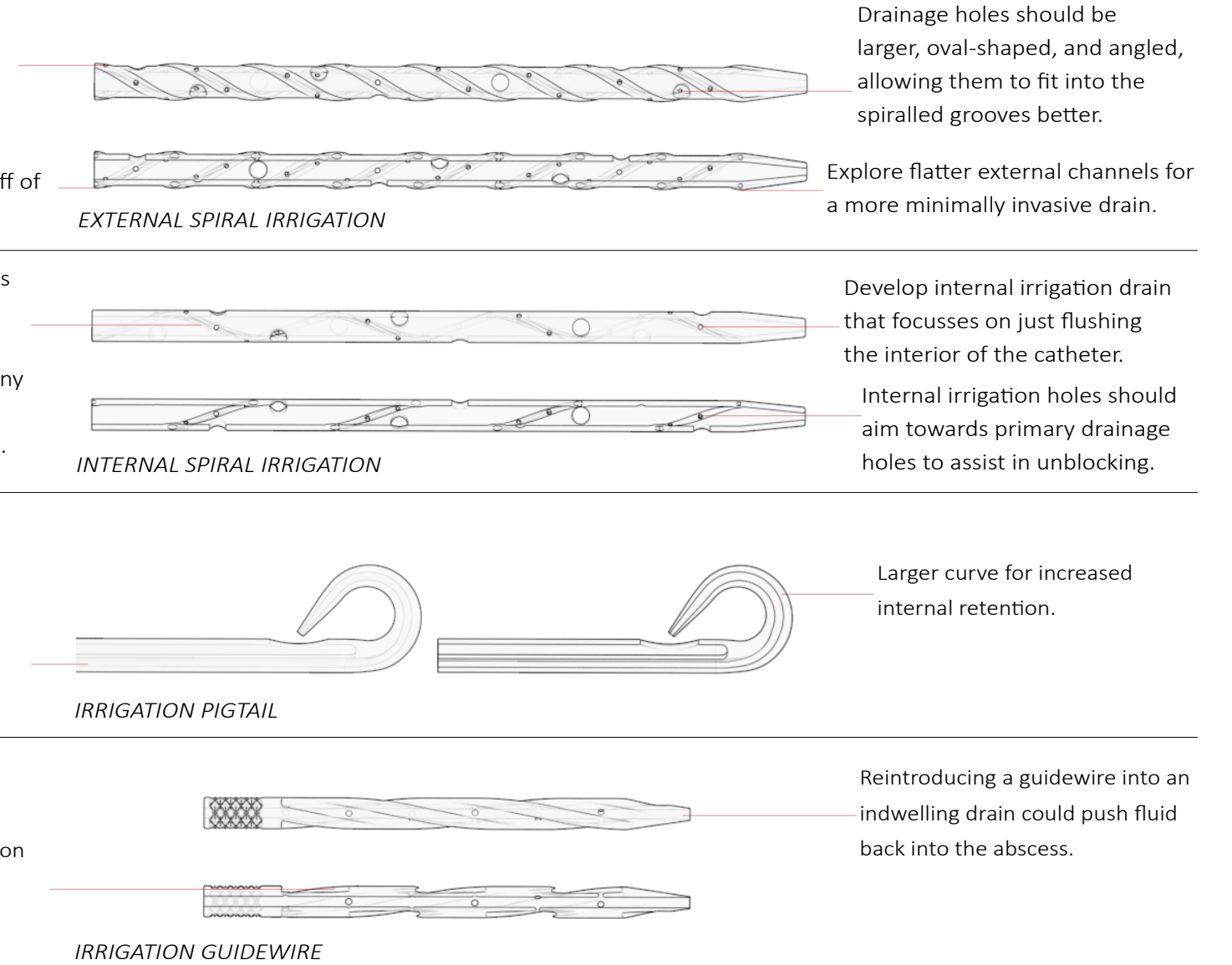
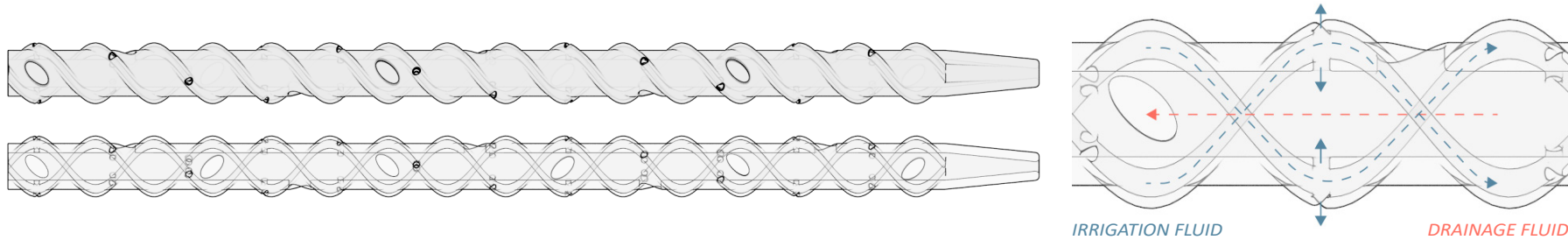
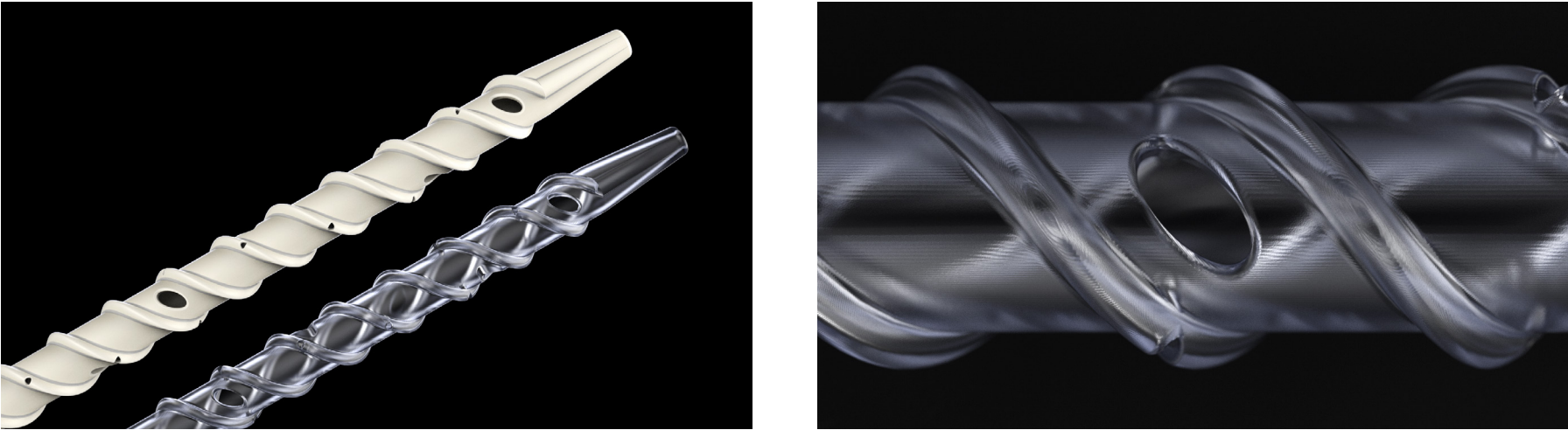


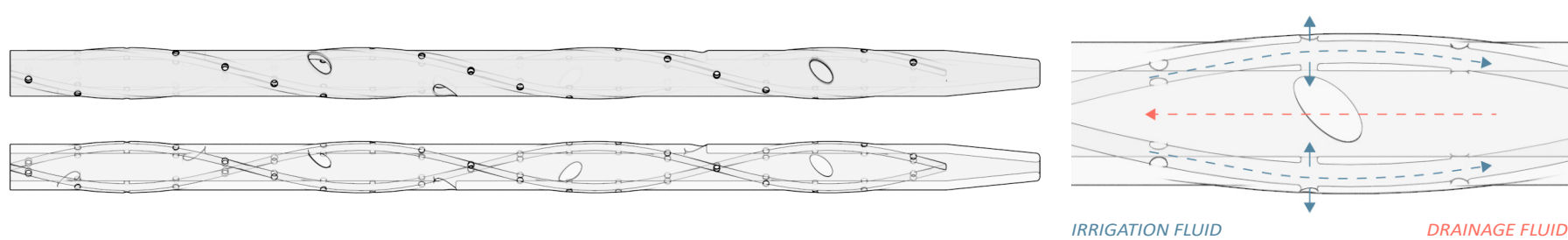
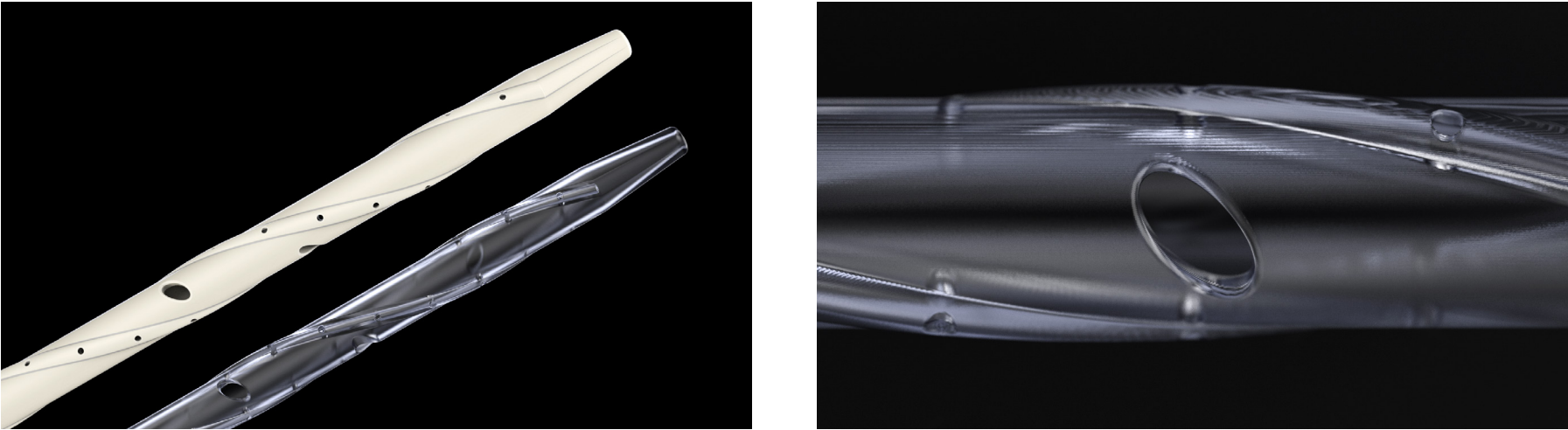
Figure 53. Expert advice feedback indicating potential changes.



TIGHT EXTERNAL SPIRAL IRRIGATION

A triple lumen drain with two smaller lumens spiralling around the external surface of the drain providing irrigation for the interior and exterior area of the catheter. The protruding spirals also push tissue off of the drainage holes to reduce obstructions (Figure 54).

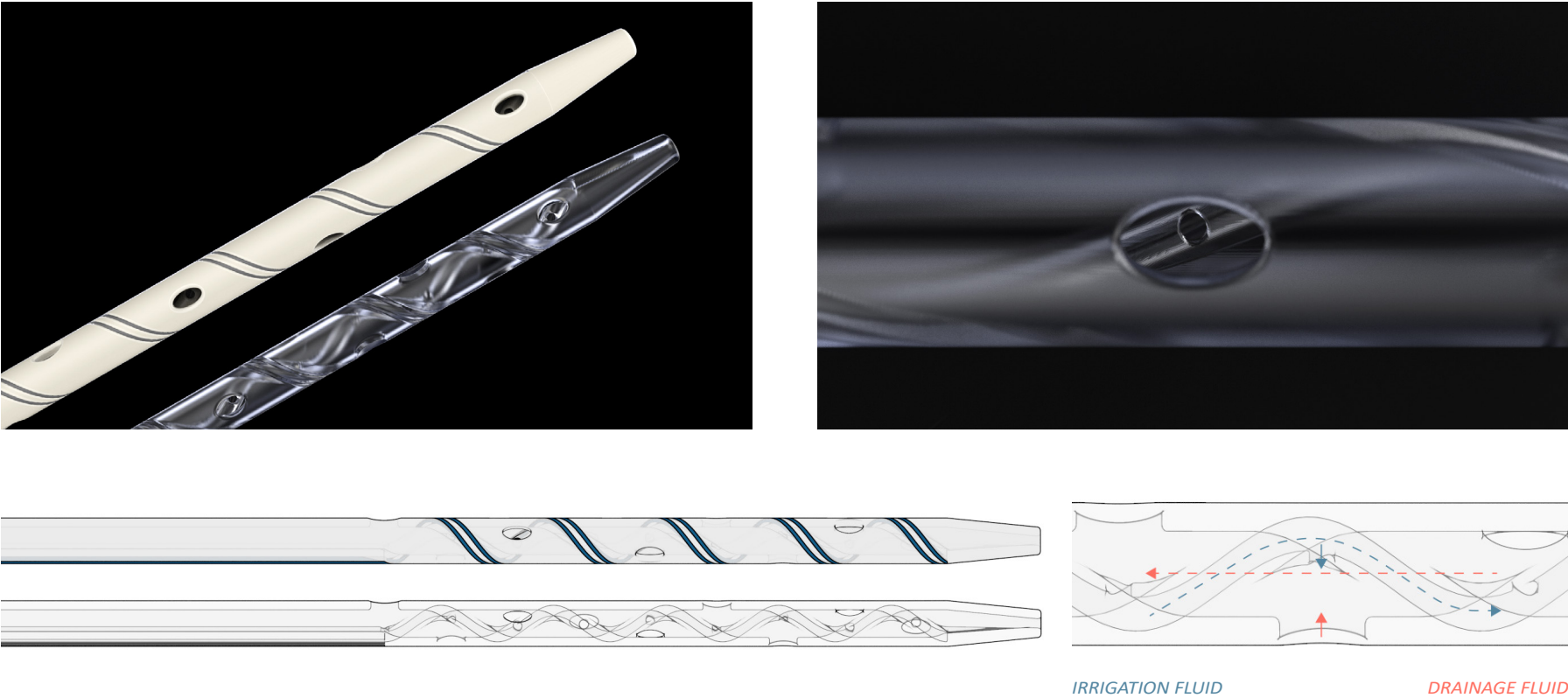
Figure 54. Tight external spiral irrigation concept documentation.



SPARSE EXTERNAL SPIRAL IRRIGATION

A triple lumen drain with smaller channels spiralling around the external surface providing irrigation for the interior and exterior area of the catheter. The flatter outer spiral provides a more minimally invasive drain (Figure 55).

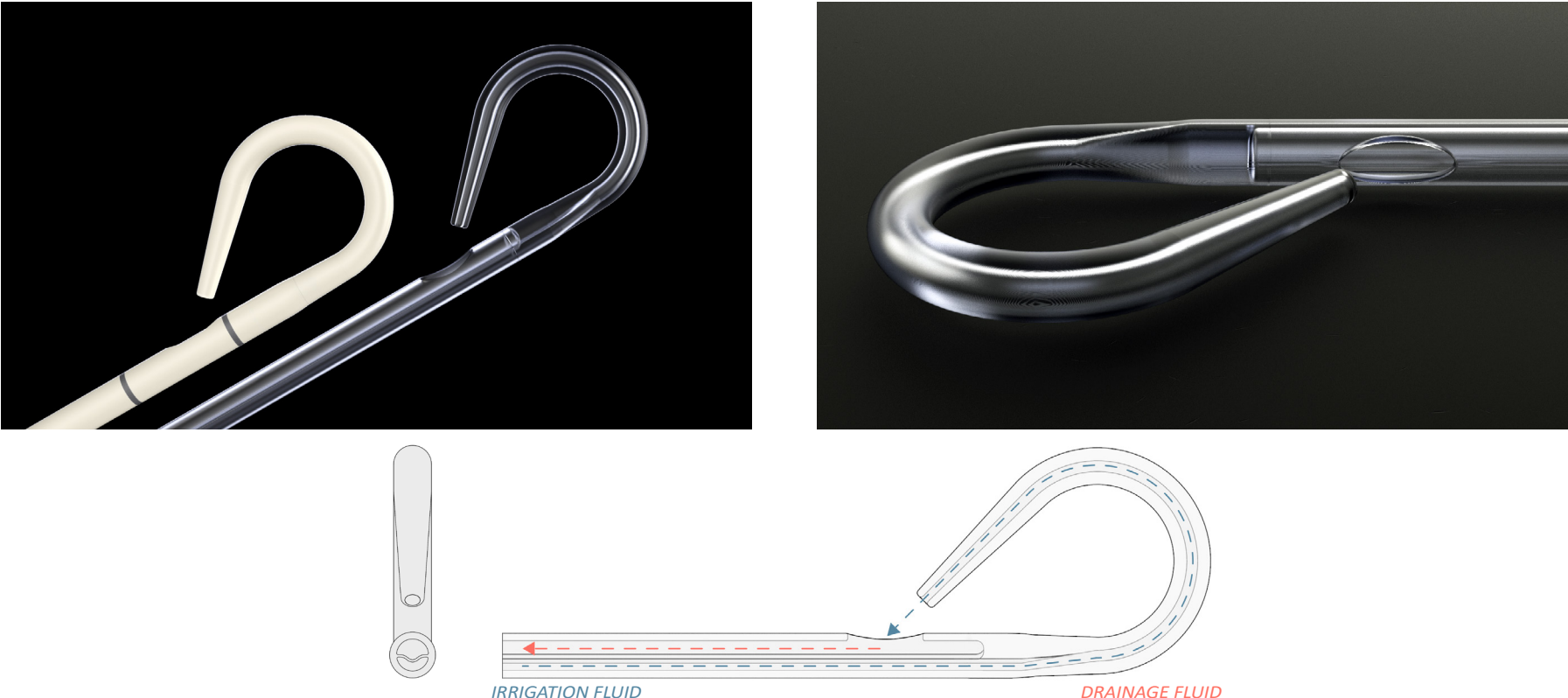
Figure 55. Sparse external spiral irrigation concept documentation.



INTERNAL IRRIGATION

A double lumen drain with a smaller channel spiralling around the internal surface providing irrigation for the interior of the catheter. The irrigation fluid can be used to unblock the drainage holes as they are located opposite each other. Markings on the exterior surface of the drain signify the internal channels to radiologists that may want to make manual adjustments (Figure 56).

Figure 56. Internal irrigation concept documentation.



PIGTAIL IRRIGATION

A double lumen pigtail catheter with a smaller lumen extending through to the tip allowing for guidewire entry and irrigation. Once the tip curls for retention it is positioned towards the primary drainage hole. Irrigation fluid also promotes flow back through the drain (Figure 57).

Figure 57. Pigtail irrigation concept documentation.



IRRIGATION DRAINS EXPERIMENTATION SUMMARY

The irrigation concepts explore introducing external or internal channels to interject fluid into the interior of the catheter or the abscess, reducing the viscosity of infected fluids, making them easier to drain. Having external channels does not impact the size of the primary drainage lumen, while also providing a screw thread form that pushes tissue off of drainage holes (Figure 58). However, the outer ridges produce a less-invasive catheter. Internal channels maintain a minimally invasive profile but impact drainage by occupying space from the primary lumen.

Support material proved to be a significant limitation with the production of functioning irrigation drains. While it is possible to produce channels that are .5mm, or less, in diameter, it is almost impossible to print removable stents occupying the channel without them breaking during removal. Support material, therefore, permeates in the irrigation channels. Manual removal is an option by flushing fluid through the channels and squeezing the tubes to break up support, but only on small-scale models as there is too much support on larger prints. Also repeatedly compressing the material to remove support weakens it making it susceptible to tearing, which is more apparent the higher the shore value.

Figure 58. Detail image of a 3D printed Tight external spiral irrigation concept.

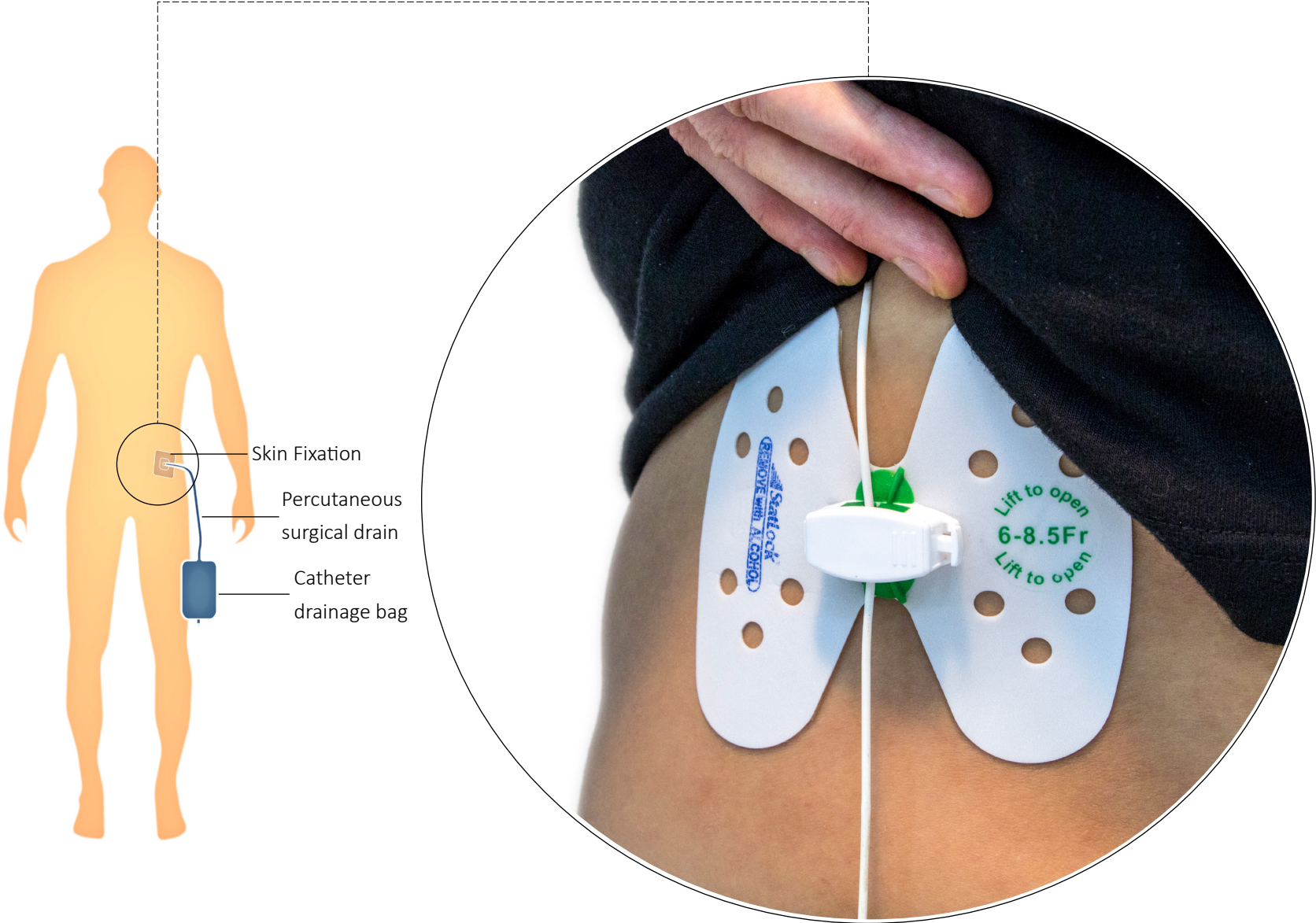


Figure 59. Overview of a current skin fixation device.

SKIN FIXATION DEVICE

PRAGMATIC DESIGN

Drains may be situated in the body for extended lengths of time. The external fixation prevents inadvertently pulling on an indwelling catheter, which can lead to dislodgment and bleeding if the wound reopens. Typically catheters are externally secured by a rigid clip attached to a surgical plaster or sutured to the skin (Figure 59). These can be uncomfortable to rest on due to the bulkiness. A redesign of external skin fixation devices would address, tight security of a drain, patient comfort, and ability for radiologists to replace catheters.

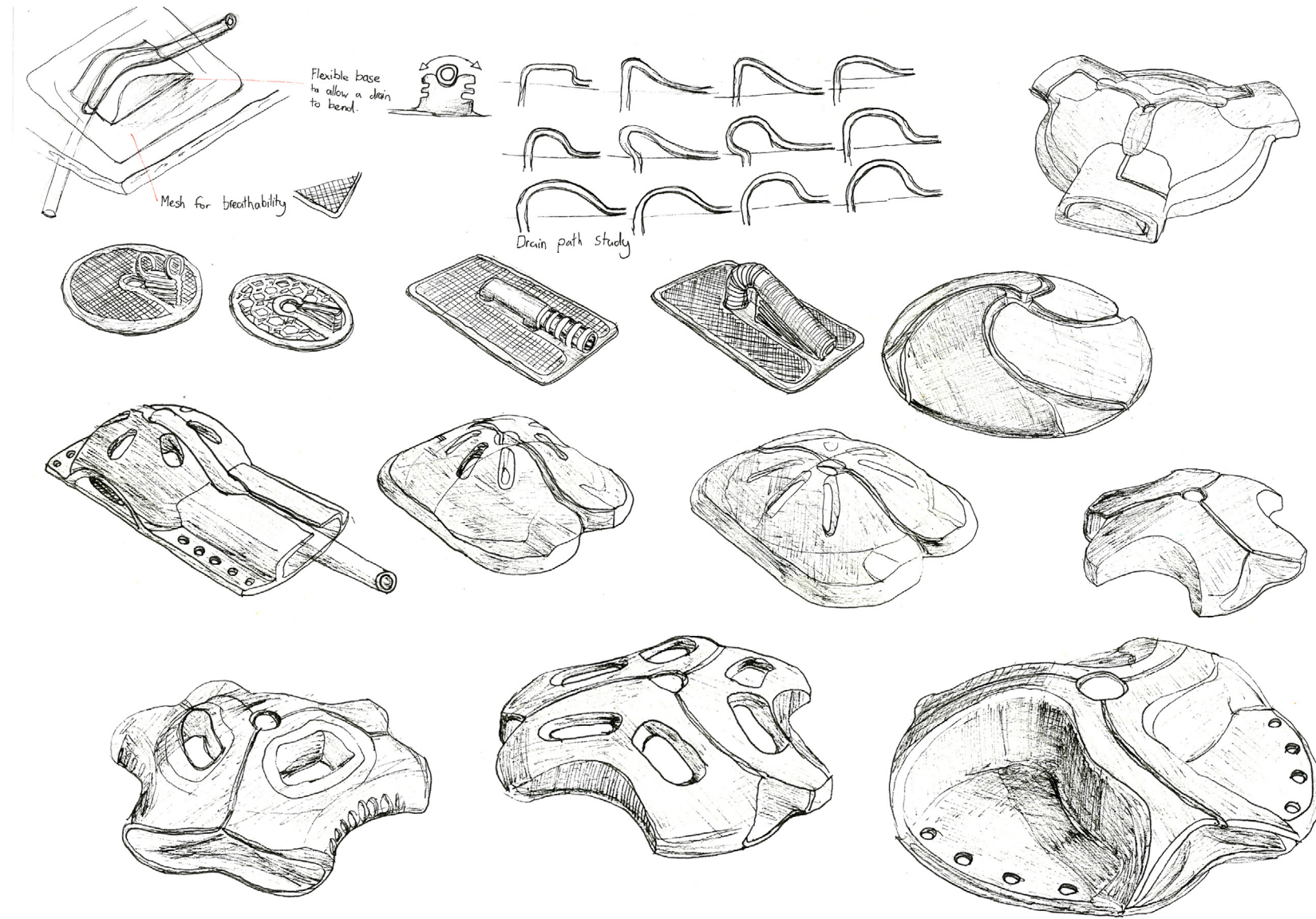


Figure 60. Skin fixation ideation sketches.

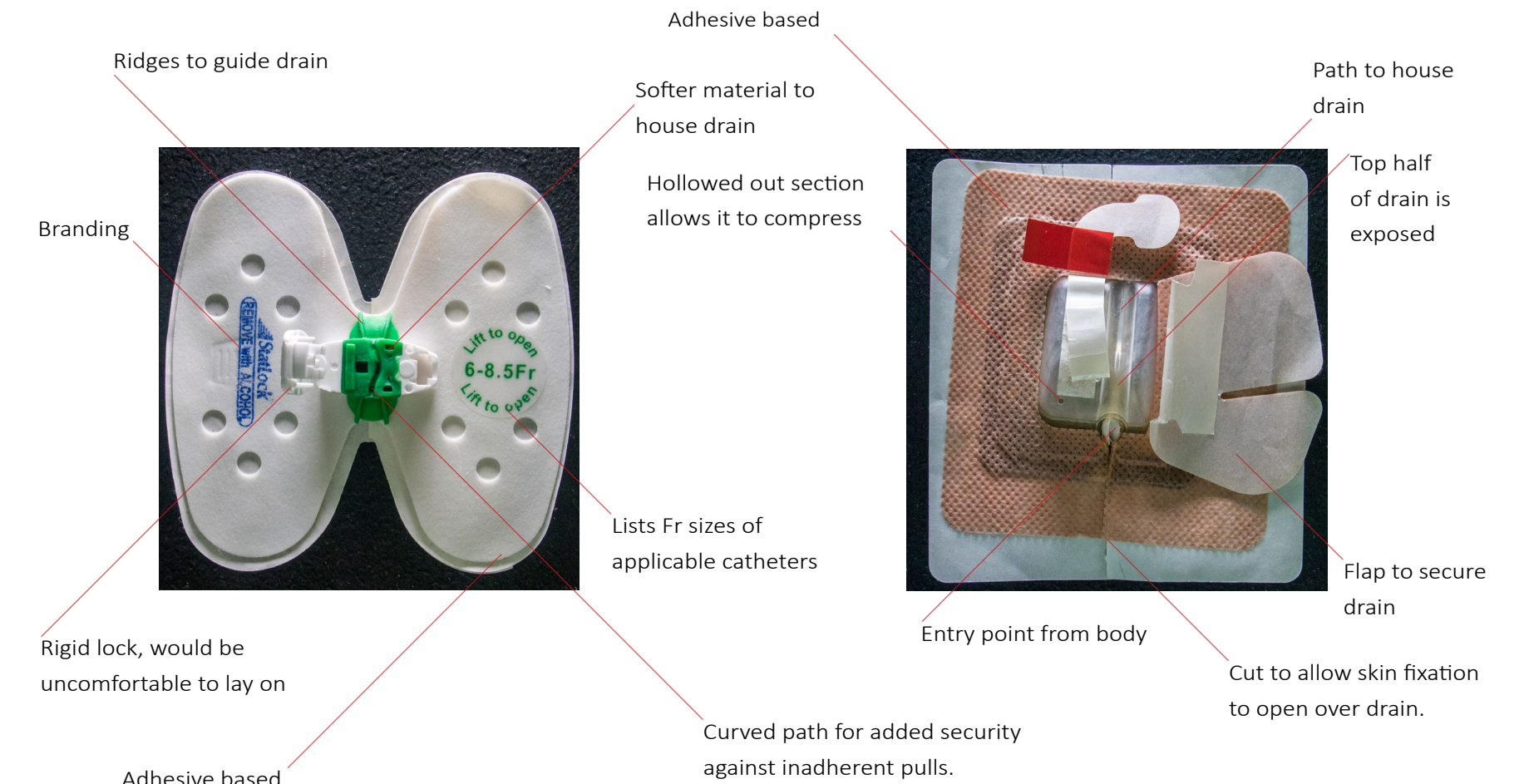


Figure 61. Analysis of current skin fixation devices.

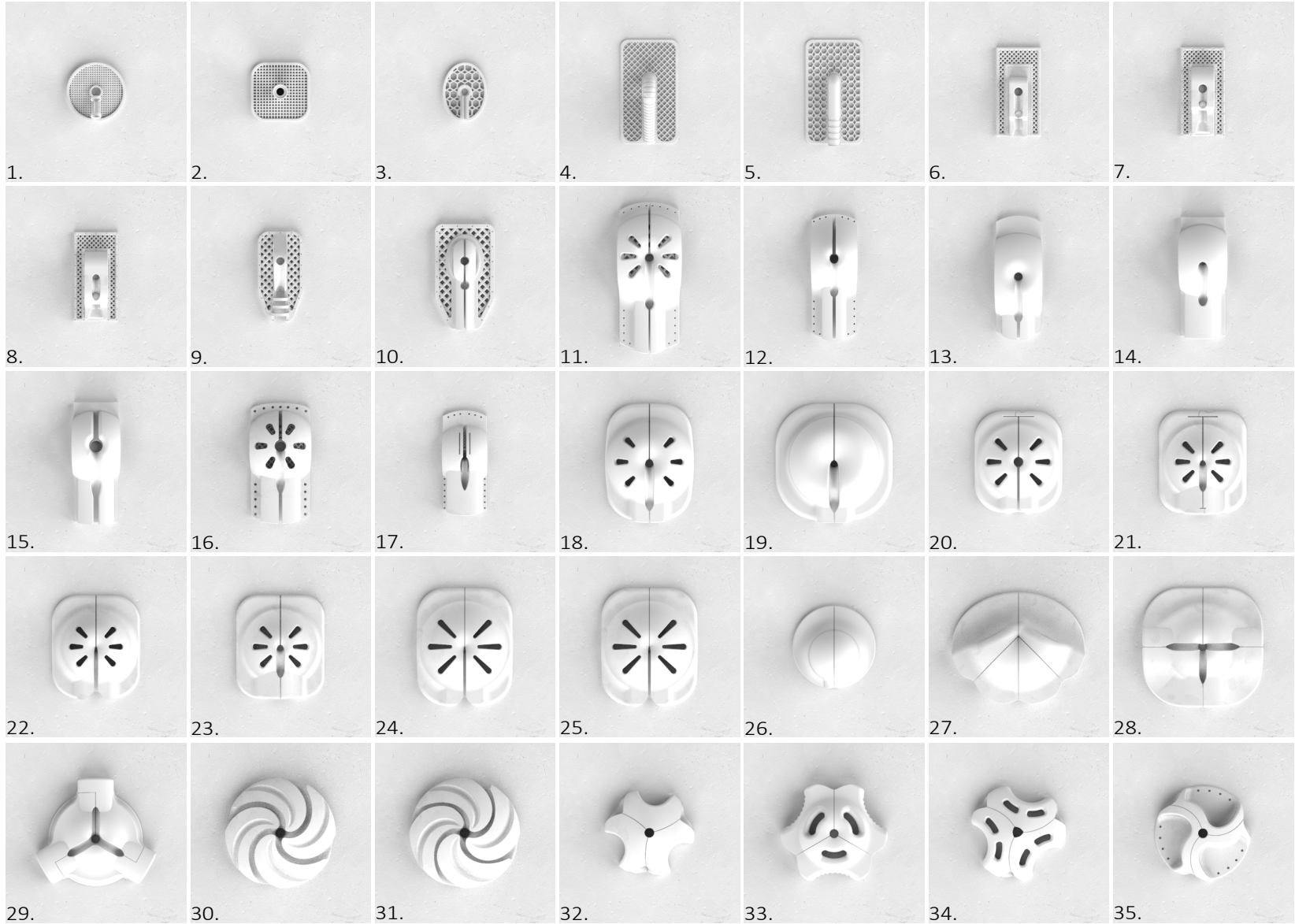
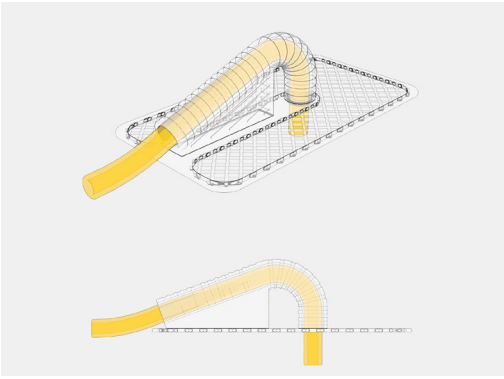
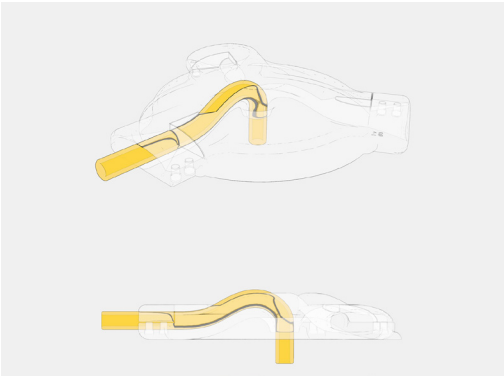


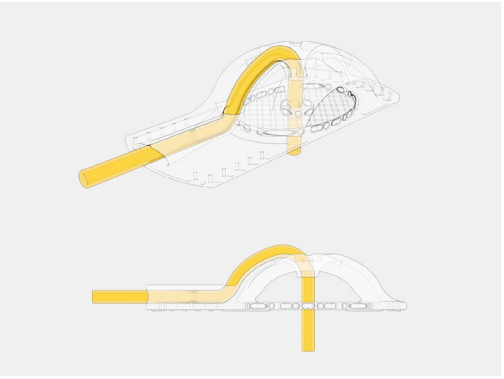
Figure 62. Form study of the various skin fixation devices explored.



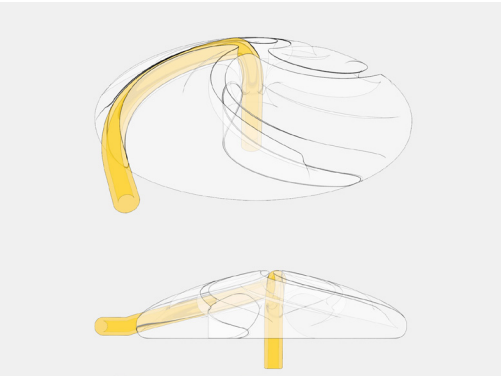
5. There is no access for the radiologist to change the drain without having to remove the device first.



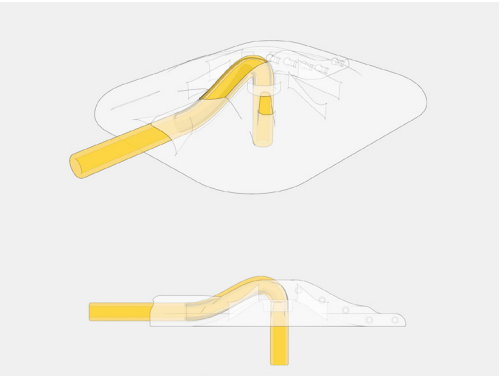
27. Additional paths allow the patient to adjust the drains security for comfort, depending on where the drainage bag is located.



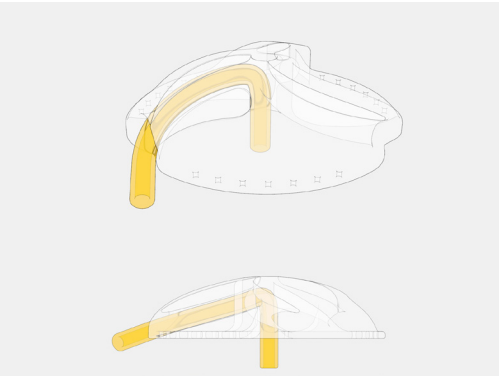
11. The drain is too exposed at the peak of the device. It could get caught and inadvertently dislodged. Redesign to reduce the height.



31. A curved path provides more friction between the drain and fixation device. Excess material needs to be removed, reducing weight and production cost.



23. The path to secure the drain is too low; it can easily be pulled out of the device.



35. Path secures the drain well however it pops out of the top slit. Needs a lid to lock it in place. Mesh needs incorporating into the base to improve wound breathability.

Figure 63. Analysis into the path of the drain from several skin fixation iterations.



Figure 64. Early low fidelity prototypes of the skin fixation device were generated with FDM 3D printing (Fused-Deposition-Modelling).



Figure 65. Support material proved to be an issue with FDM printing.



Figure 66. Detail view of a mesh form printed with FDM 3D printing.



Figure 67. Labelling of FDM prototypes.

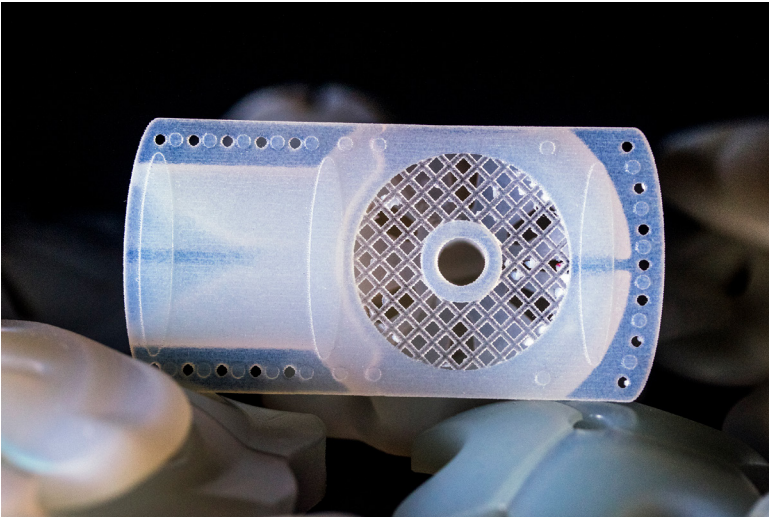


Figure 68. The project advanced to high-fidelity prototyping with the J750 when it was acquired.



Figure 69. Drains popping out of the slit was a frequent issue.



Figure 70. Sketching on prototypes signified changes. The red lines indicate the excess material to remove on the next iteration.



Figure 71. A curved path increased the friction on the drain, significantly improving the security.

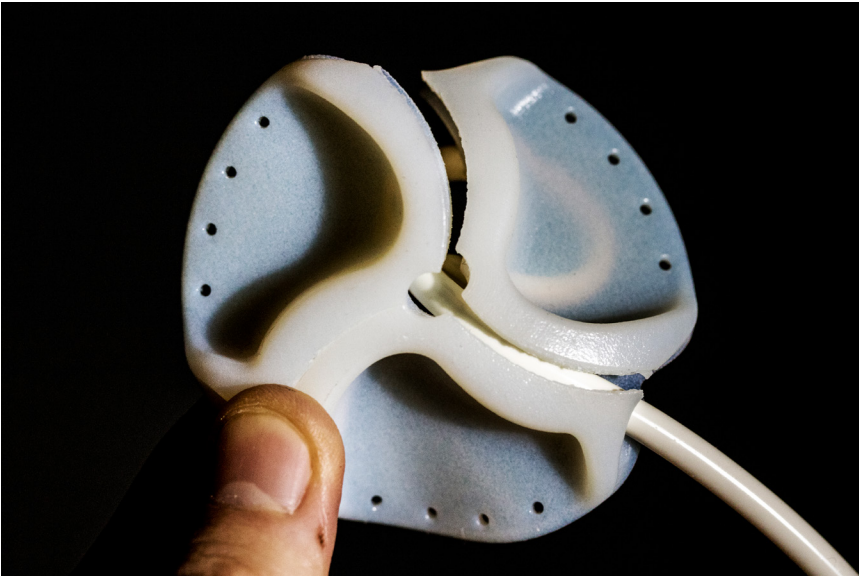


Figure 72. Refining the skin fixation form, the drain still pops out of the path.

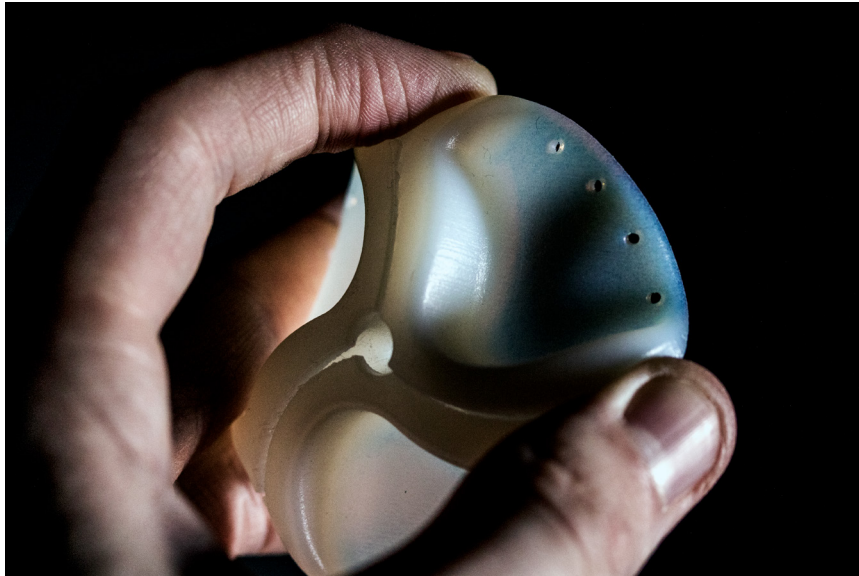


Figure 73. The base does not bend that well, it would not move well with the body.

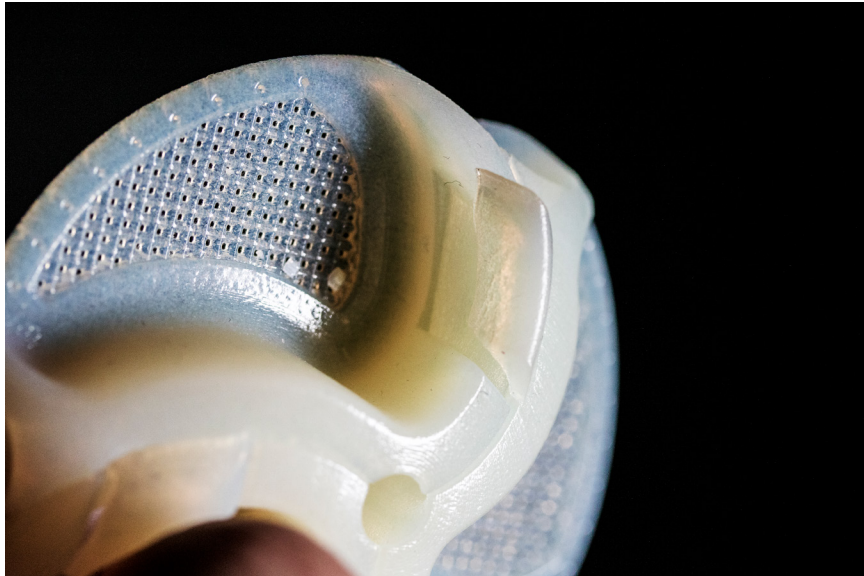


Figure 74. The folding lid is too weak to lock the drain. The mesh significantly increases the flexibility of the base.

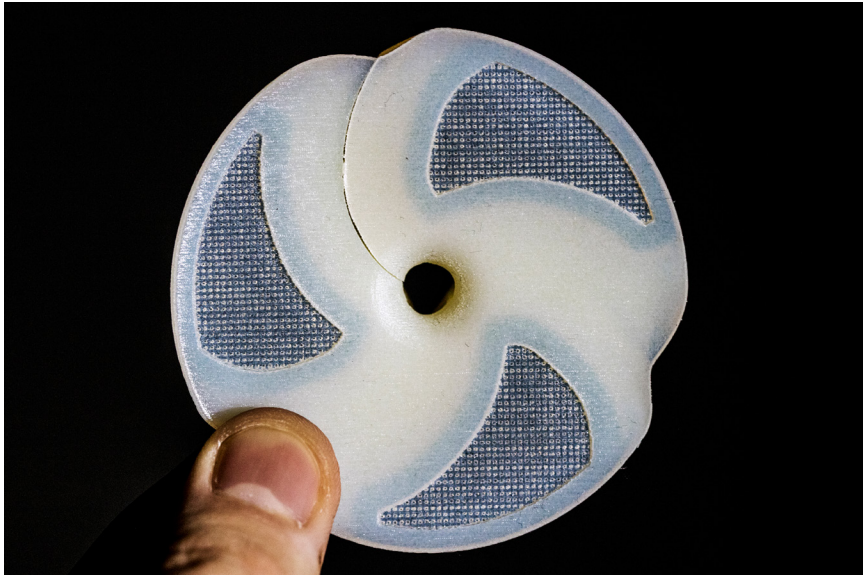
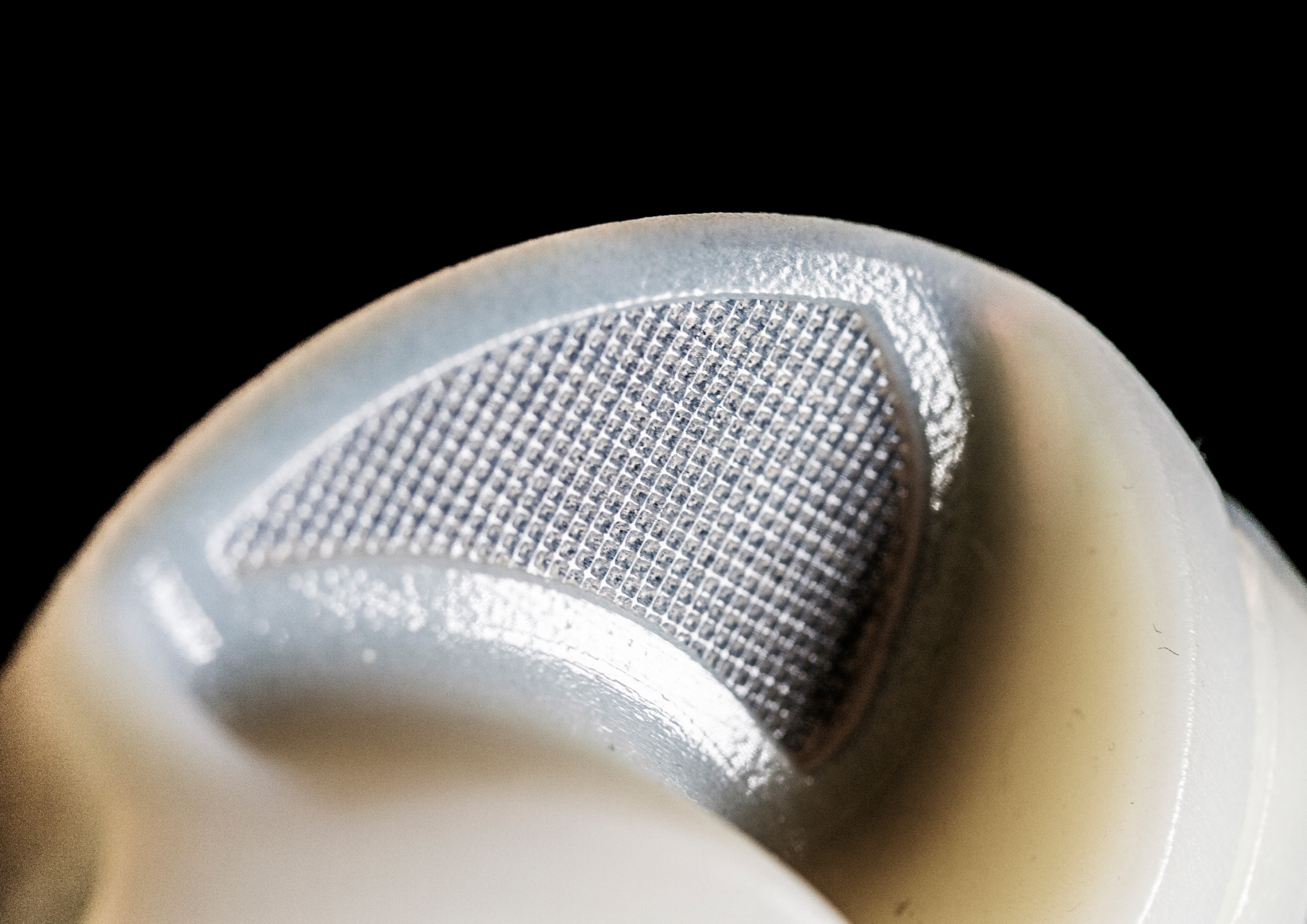


Figure 75. View of the base. The mesh is constructed with .6mm diameter thick rods.



SKIN FIXATION EXPERIMENTATION SUMMARY

The J750 provided the means to study the form and function of a skin fixation device to secure an indwelling drain (Figure 76). Numerous iterations explored the path of the catheter to restrict inadvertent dislodgment, allowing the end of the catheter to move with the patient, a thin mesh for wound breathability, and comfort when laid on. With 3D printing, a high fidelity prototype was able to be produced in a matter of hours, evaluated, then redesigned and printed again in a couple of days. Compared to tediously handcrafting prototypes, which could take several days or a week, additive manufacturing drastically speeds up the iterative process.

Common issues that arose during the development of the skin fixation were:

- Producing a secure path that did not kink the drain but also creates a secure fit so that the catheter cannot easily slide out.
- Providing methods for radiologists to change a drain without having to remove the device.
- Preventing the drain from popping out of the device.

Figure 76. Detail view of the mesh segment of the skin fixation device.

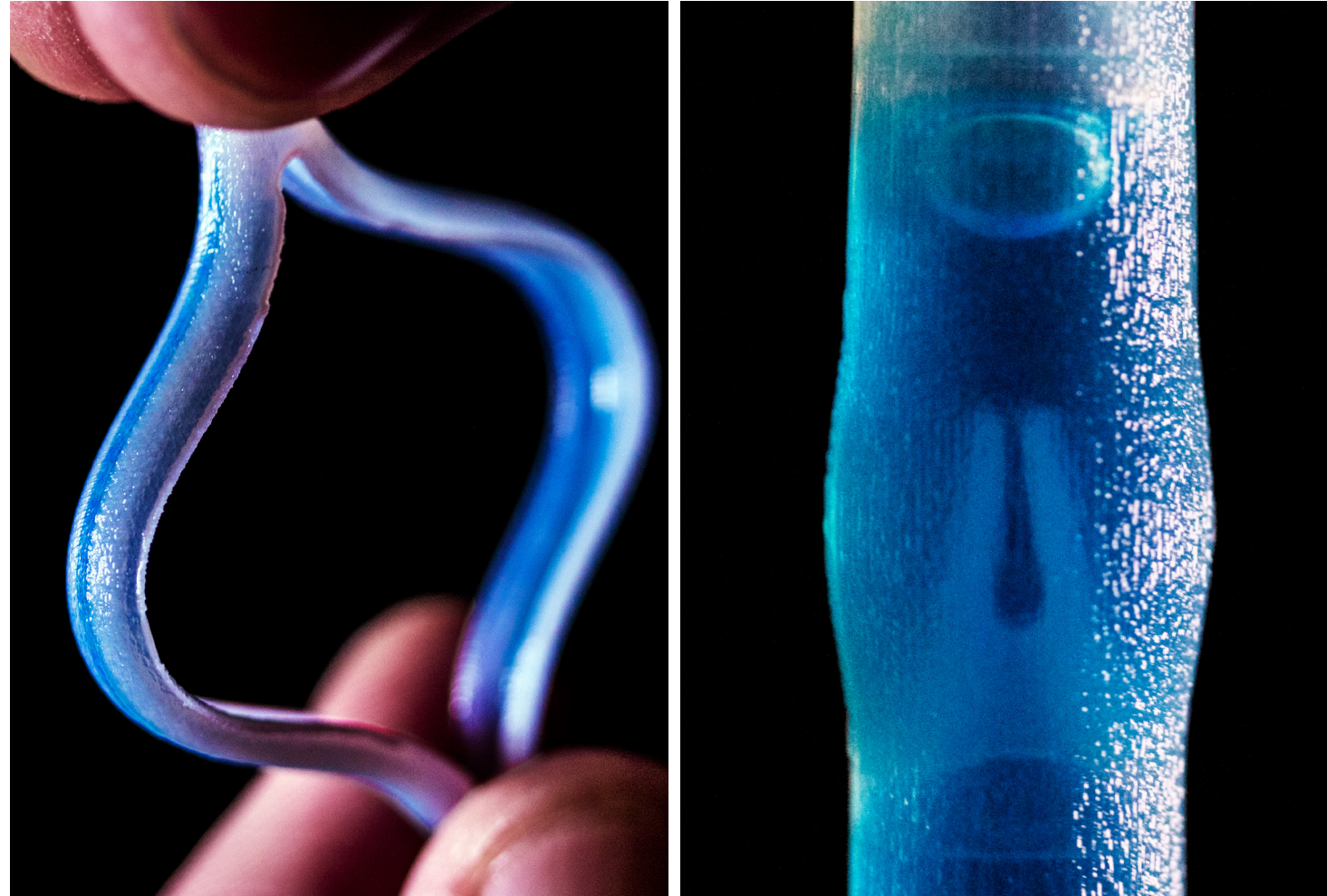


Figure 77. Speculative designs, Stimulus-responsive drain (left), Venous valve structure (right).

3.4 SPECULATIVE EXPERIMENTS

Perceiving how 3D printing can alter the production and function of medical devices, speculative ideas employ the J750's multi-properties to explore anatomical structures, dynamic forms and pneumatic/hydraulic activation methods (Figure 77). Incorporating multiple materials into a single print produces complex geometries with an increased physiological composition. With the J750, it is now possible to create and comprehend concepts thought unmakeable.

VENOUS VALVES*SPECULATIVE DESIGN*

Blockages within surgical drains are a common issue, extremely viscous matter can clog catheters hindering drainage speeds. Venous valves are bicuspid leaflets located in veins that open, propelling blood toward the heart, while closing to restrict it flowing back (Figures 78—79). Muscles surrounding the valves compress, helping to force the blood around the body. Simulating the anatomical properties of venous valves could produce a means for unblocking drains, while also promoting fluids out of the body.

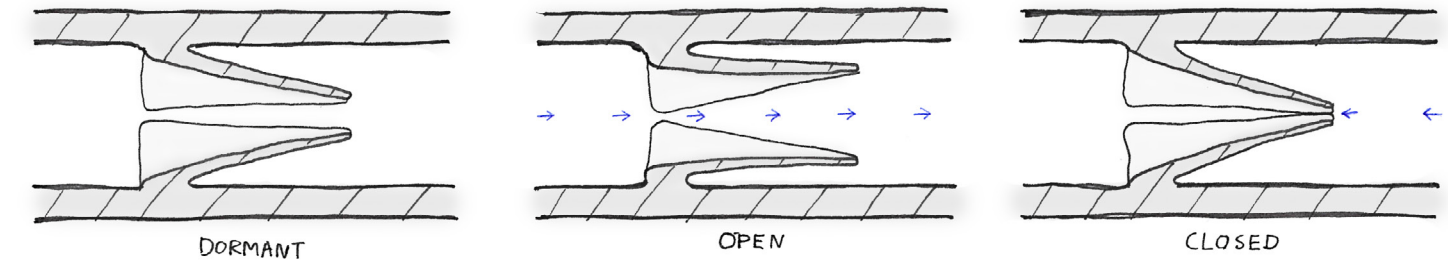


Figure 79. Diagram illustrating the function of a bicuspid venous valve.

Figure 78. Tangible interaction with a 3D printed venous valve.

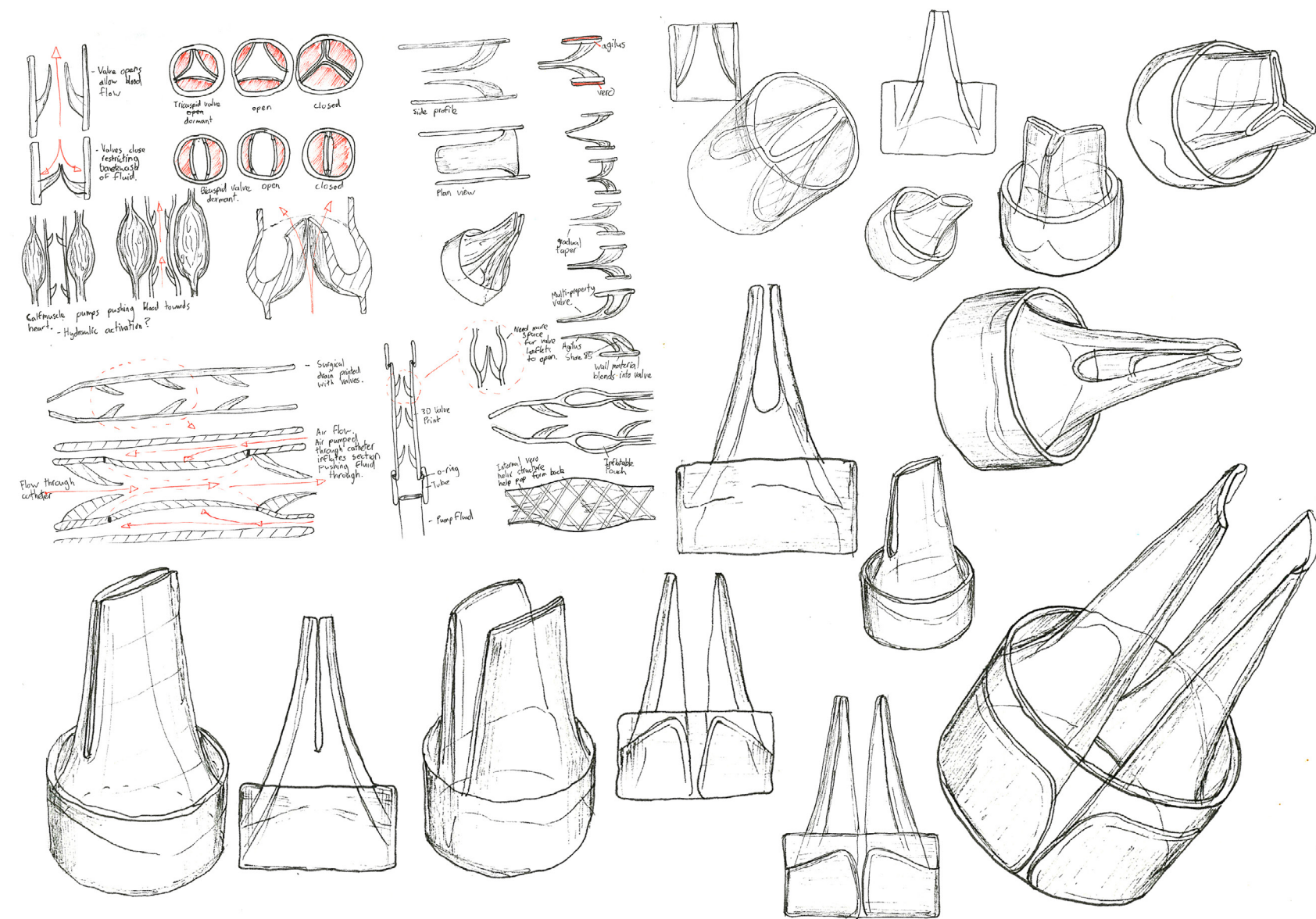


Figure 80. Venous valve ideation sketches.



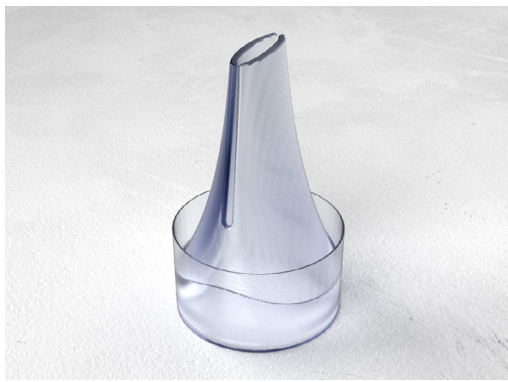
1. Bicuspid leaflets merged with wall, failed to open.



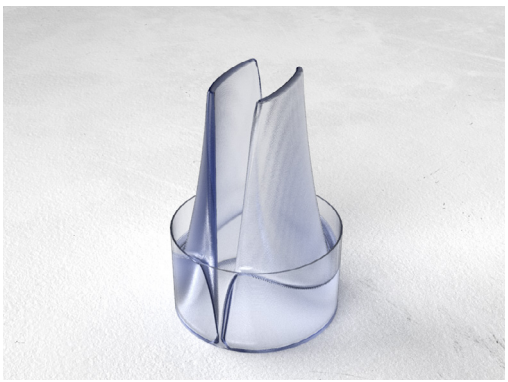
2. Tricuspid leaflets, failed to fully open and close.



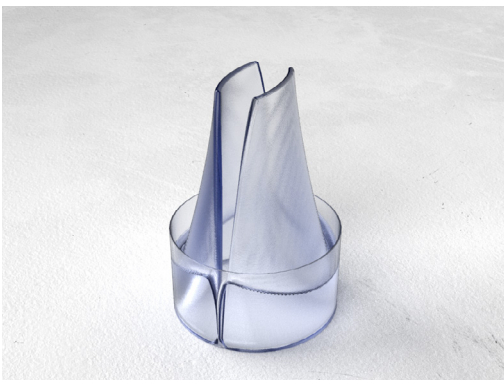
3. Extended leaflets open well, side cut prevents full closure.



4. Thinner side cuts restricts fluid flowing back but does not open allowing fluid to flow through well.



5. Leaflets have good movement, but are too far apart and bow out. Slight gap at the base allows fluid to pass.



6. Reduced gap at base prevents fluid flowing back while still opening to allow fluid to pass.

Figure 81. The iterative form development of the venous valve.

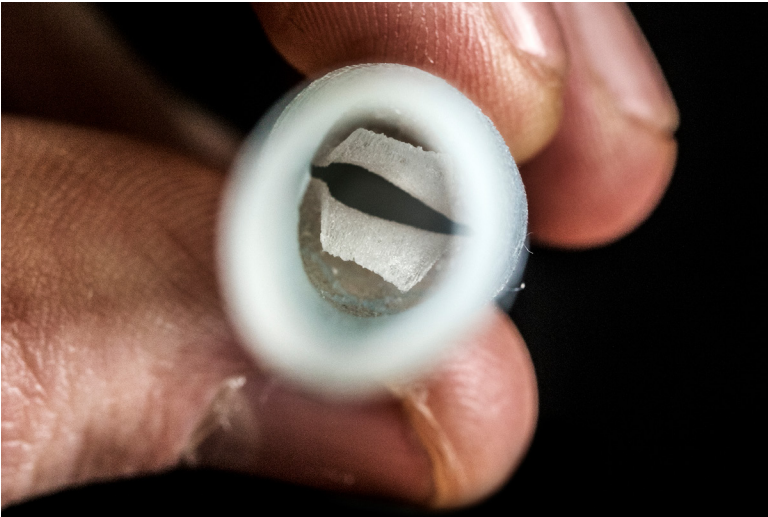


Figure 82. Valve leaflets bowing open due to being too thin and spaced apart.

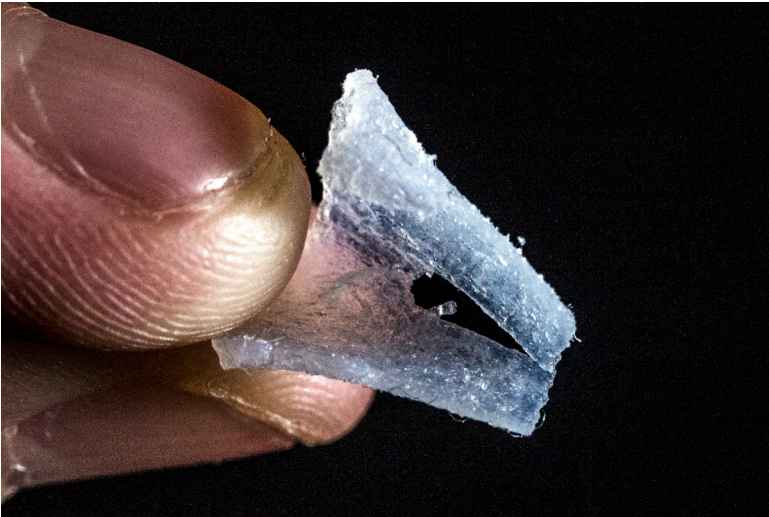


Figure 83. Valve leaflet that fell out of the tube during the removal of support material.



Figure 84. Exploring valve leaflets at a smaller scale to assess the J750's capabilities, the tubes inside diameter is 5mm.

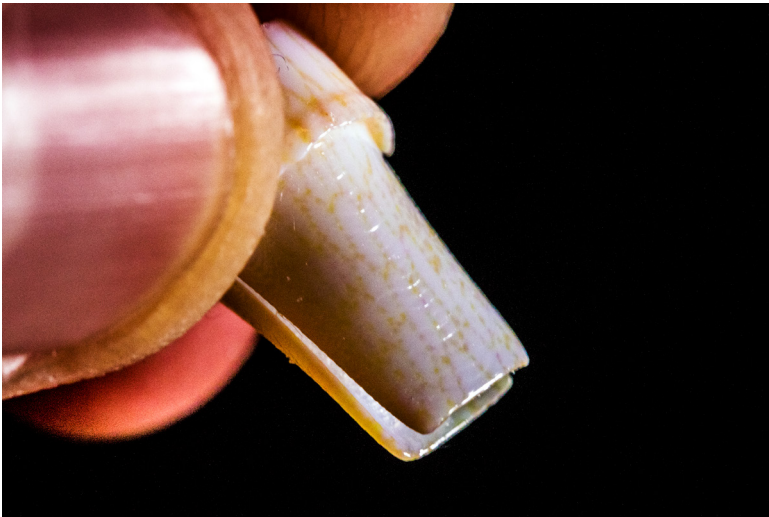


Figure 85. Detail image highlighting the Voronoi structure within the venous valves.

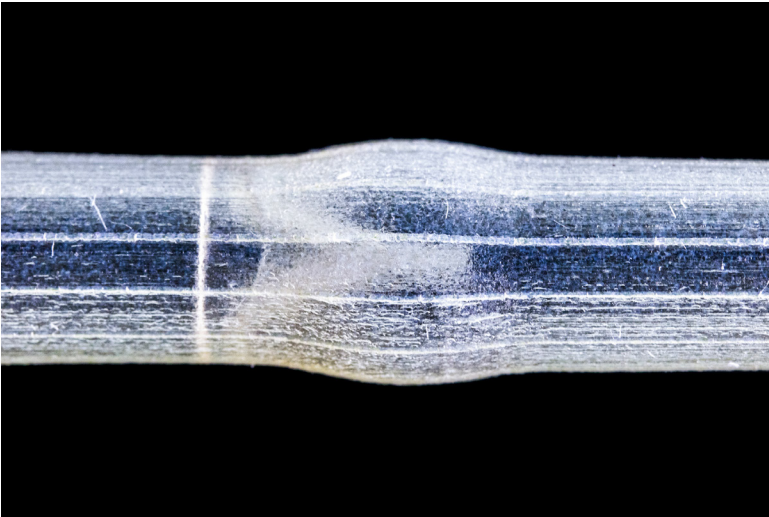


Figure 86. Vero ribs on the exterior surface of the tube to help the form return to its original state after being compressed.

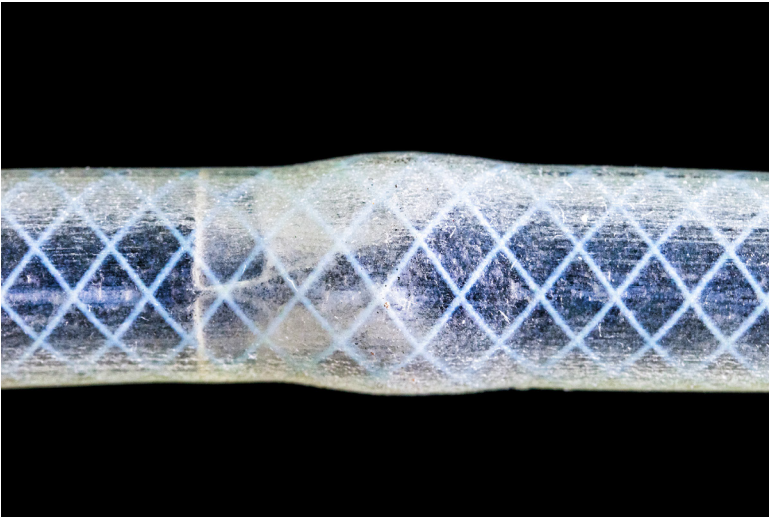


Figure 87. Vero helix structure within the tube to help the form return to its original state after being compressed.



Figure 88. Gills on the pneumatic valve to release air, in an attempt to prevent the material from splitting due to over inflation.

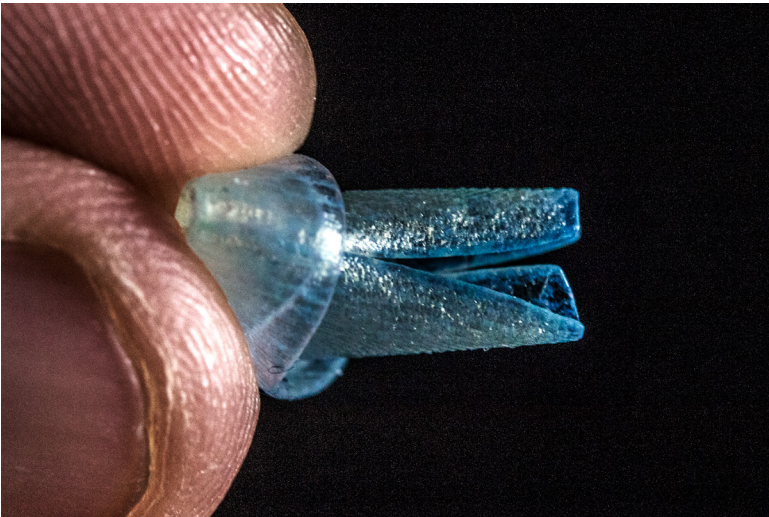


Figure 89. Detail image highlighting the Voronoi structure and tangible interaction of the venous valves.

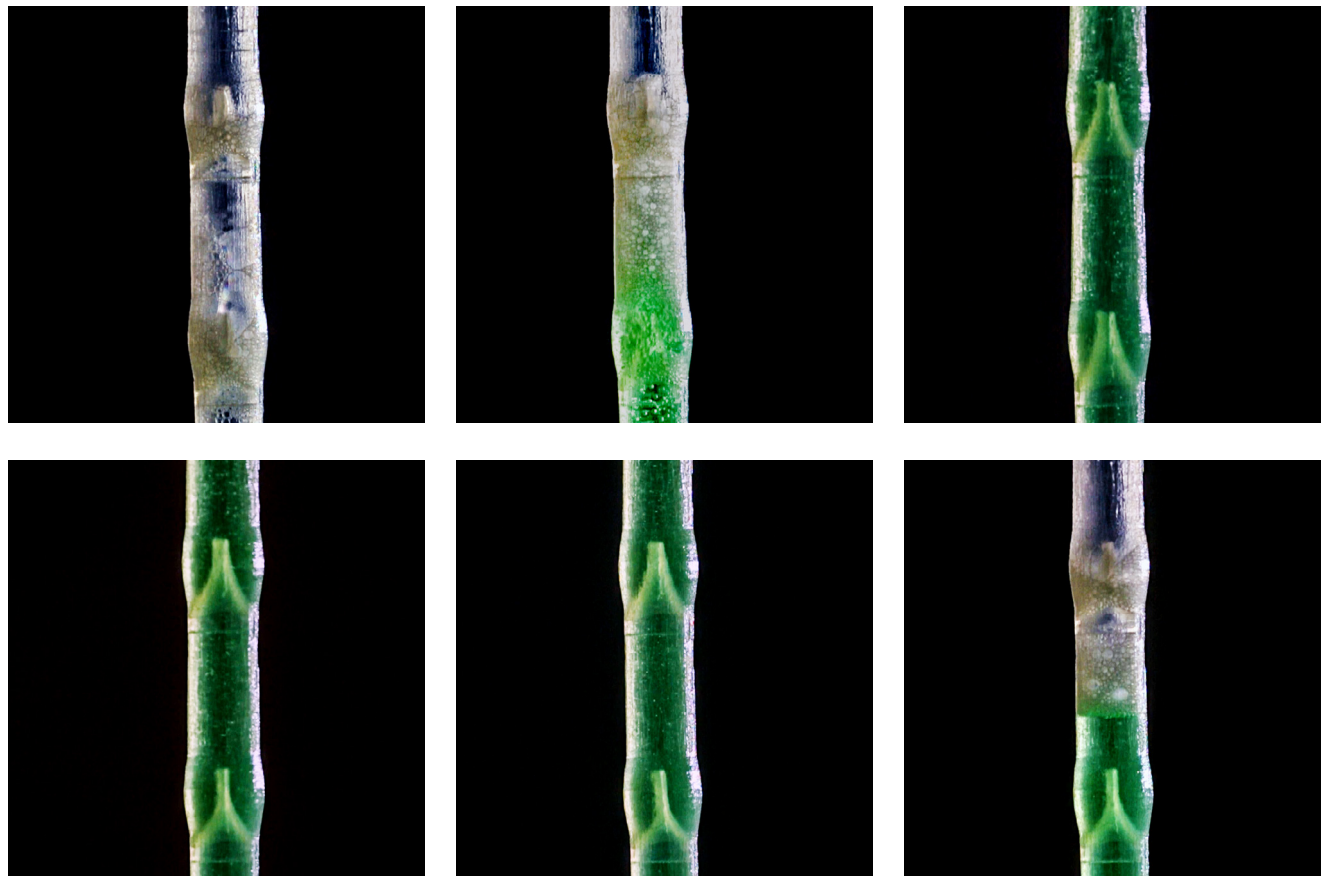
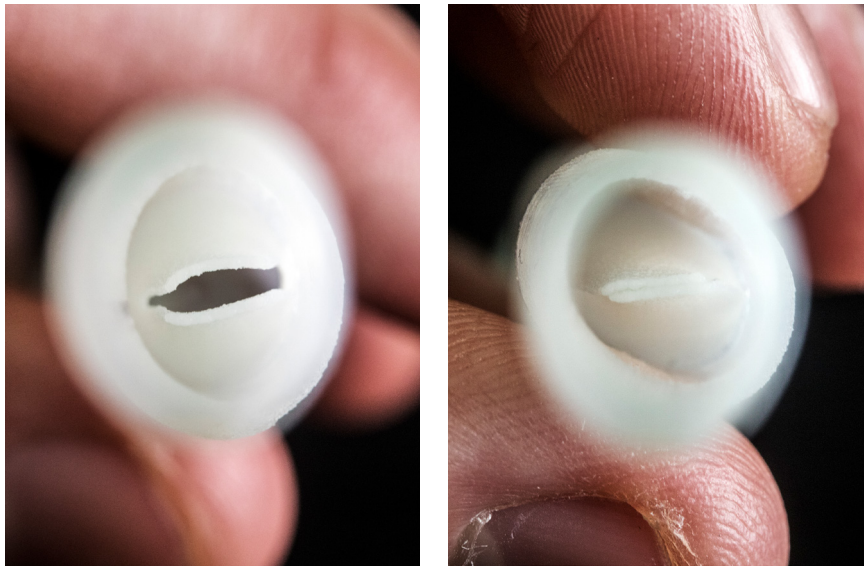


Figure 90. Movement sequence of the valve structure with a 50/50 solution of water and detergent flowing through the prototype.



BICUSPID VALVE

A series of four 3D printed bicuspid valves in a tube manages to emulate the function of biological venous valves (Figure 90). Placing the base of the prototype in a container of liquid and manually compressing the 3D print channels fluid through the tube and out of the end. As the liquid passes through the valves open, letting it progress, and when the pressure has released, they close, restricting it from backwashing.

The valve leaflets display an intriguing dynamic biological quality when interacting with the liquid. Over time the fluid slowly drains, but the valves do an outstanding job of limiting the flow back down the tube. Various solutions were used to test different viscosities, a 50/50 mix of water and detergent was used in figure #.

Figure 91. Left: Dormant valve, Right: Closed valve.

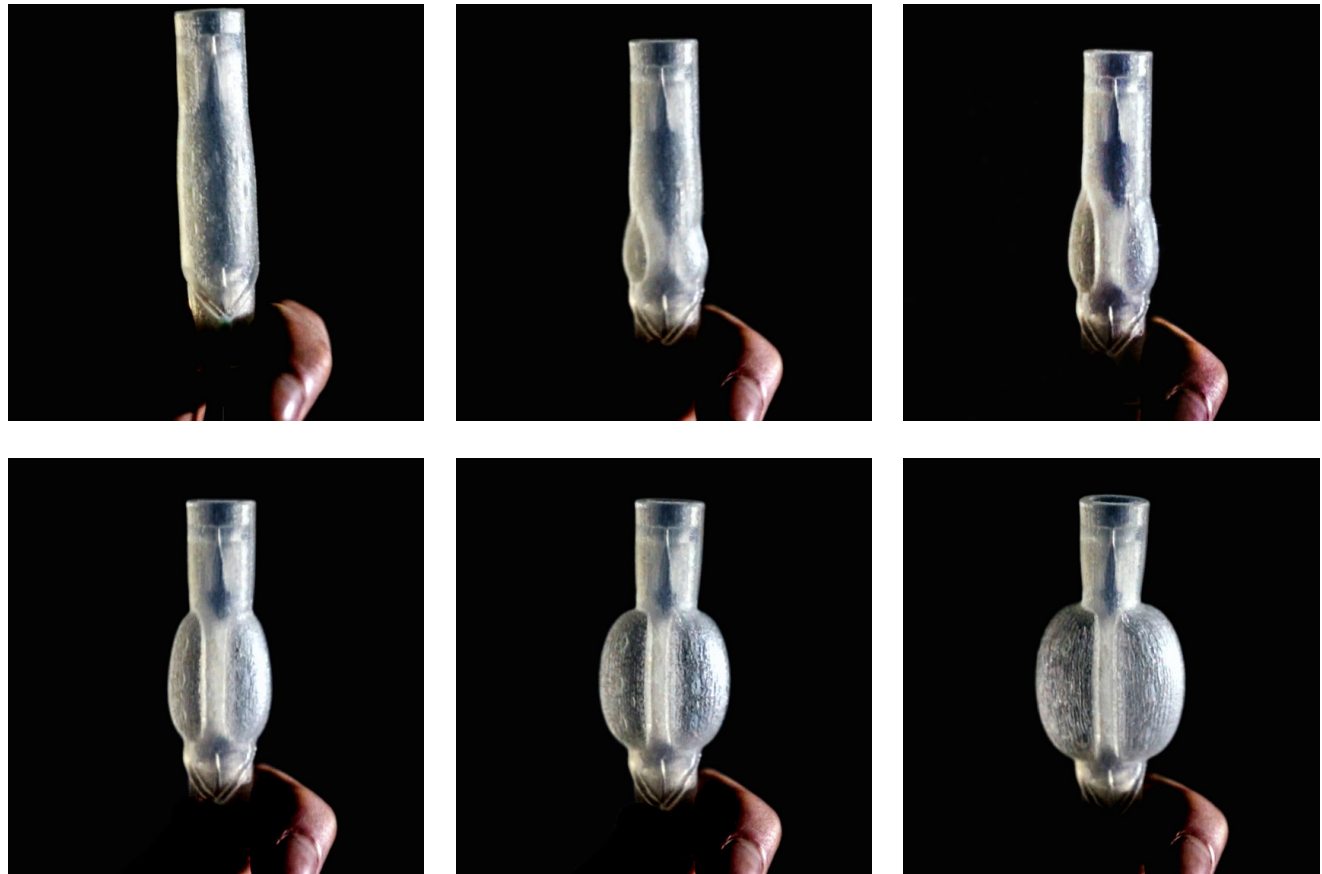


Figure 92. Movement sequence of the pneumatic valve structure, simulating muscles contracting to pump fluid towards the heart.



PNEUMATIC VALVE STRUCTURE

Incorporating pneumatic inflation acts as a method to compress sections of a drain propelling fluids through (Figures 92—93). This functionality emulates the effect of the muscles contracting veins to promote blood flow towards the heart, most notably the calf muscles. Small pockets in the material, no wider than .3mm, allowed air to channel through providing inflation. A minimal amount of support prints in the gap separating the two layers of material, which breaks up during expansion. However, material durability only allows several inflations before it splits due to overstress. The model has trouble deflating itself as the air gets trapped within the pockets — thin gill-like structures aid in releasing trapped air to self-deflate the structure (Figure 88).

Figure 93. Pneumatic valve structure.



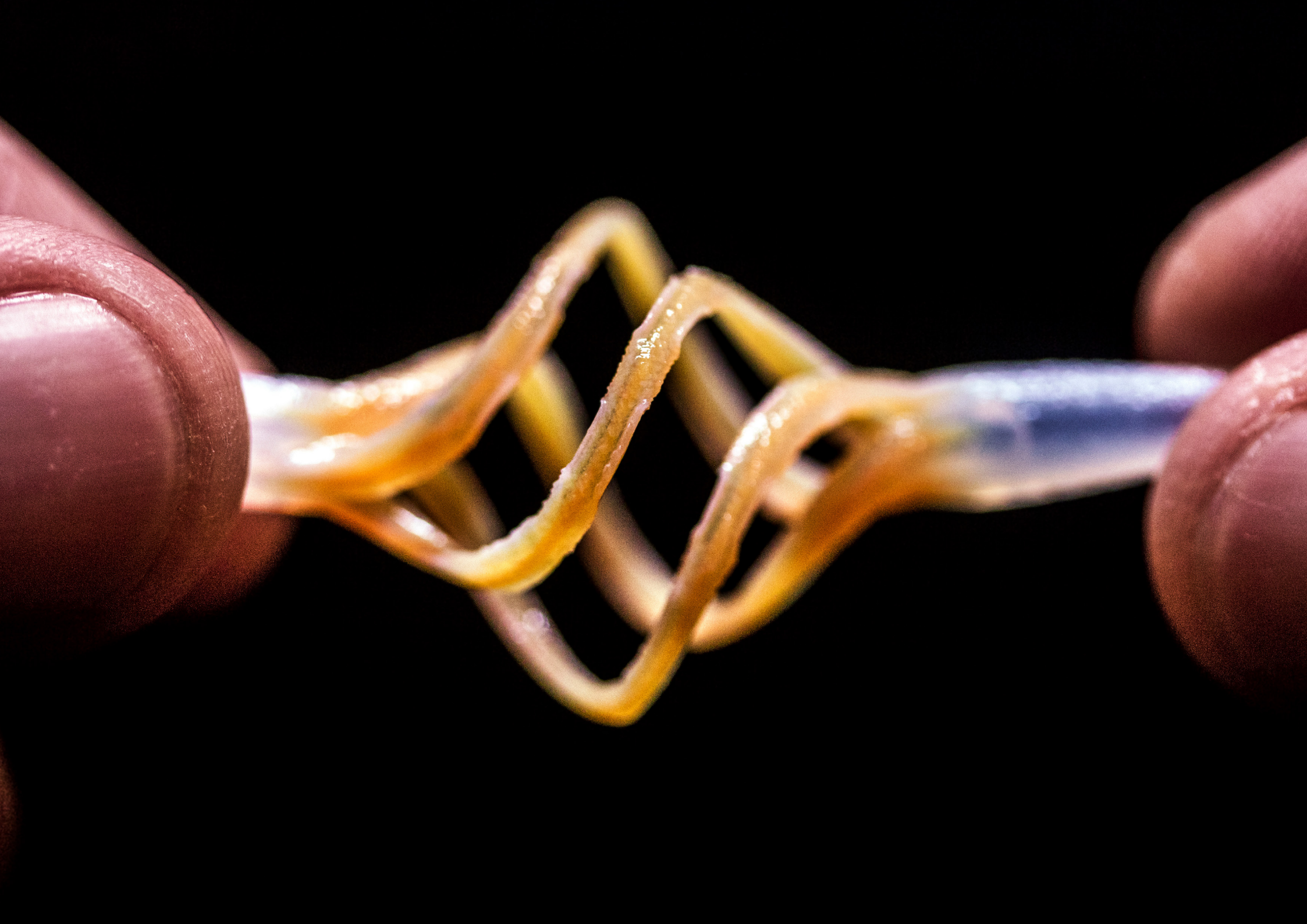
VENOUS VALVES EXPERIMENTATION SUMMARY

High-resolution 3D printing on the J750 allowed for an exploration into venous valve leaflets at a scale of .4mm. It was possible to produce several functioning bicuspid valves in a single tube that managed to pump fluid through while restricting it from flowing back down the prototype (Figure 94). Pneumatic activation was also explored through inflatable chambers to simulate the effect of contracting muscles that pump blood through veins.

As agilus absorbs water, at times this caused the thin leaflets to bow open naturally; also the strain from constantly forcing support material through the valves during cleaning affected this. The resolution of the J750 allowed for the incorporation of internal Voronoi forms no thicker than .15mm. These internal forms provided structural support to help leaflets maintain their shape while still allowing them to open.

Support material limited the thickness of the valves; when removing support if they are too thin, they would tear. Support within the prints had to be removed by continually compressing and pushing it through the tube. Tubes printed at higher shore values often split during removal of support material, even if there was an internal stent. Agilus proved capable of pneumatic expansion; however, it isn't robust enough to withstand multiple inflations and deflations. Continuous strain from stretching weakened it severally, causing it to split.

Figure 94. Dynamic 3D printed valves channelling fluids.



STIMULUS-RESPONSIVE DRAINS

Internal retention features of surgical drains aid in securing the catheter within the abscess, reducing the chance of dislodgment if inadvertently pulled. Radiologists noted that the string function of pigtail drains causes issues at times as it can get tangled with the catheter. With access to multi-property 3D printed SMP's an exploration into stimulus-responsive internal retention could eliminate the need for strings (Figure 95). This section investigates thermomechanically activated drains, assessing the potential for dynamic retention features.

Thermomechanical: Of or pertaining to the variation of the mechanical properties of a material with temperature.

Figure 95. Stimulus-responsive Helix drain under compression.

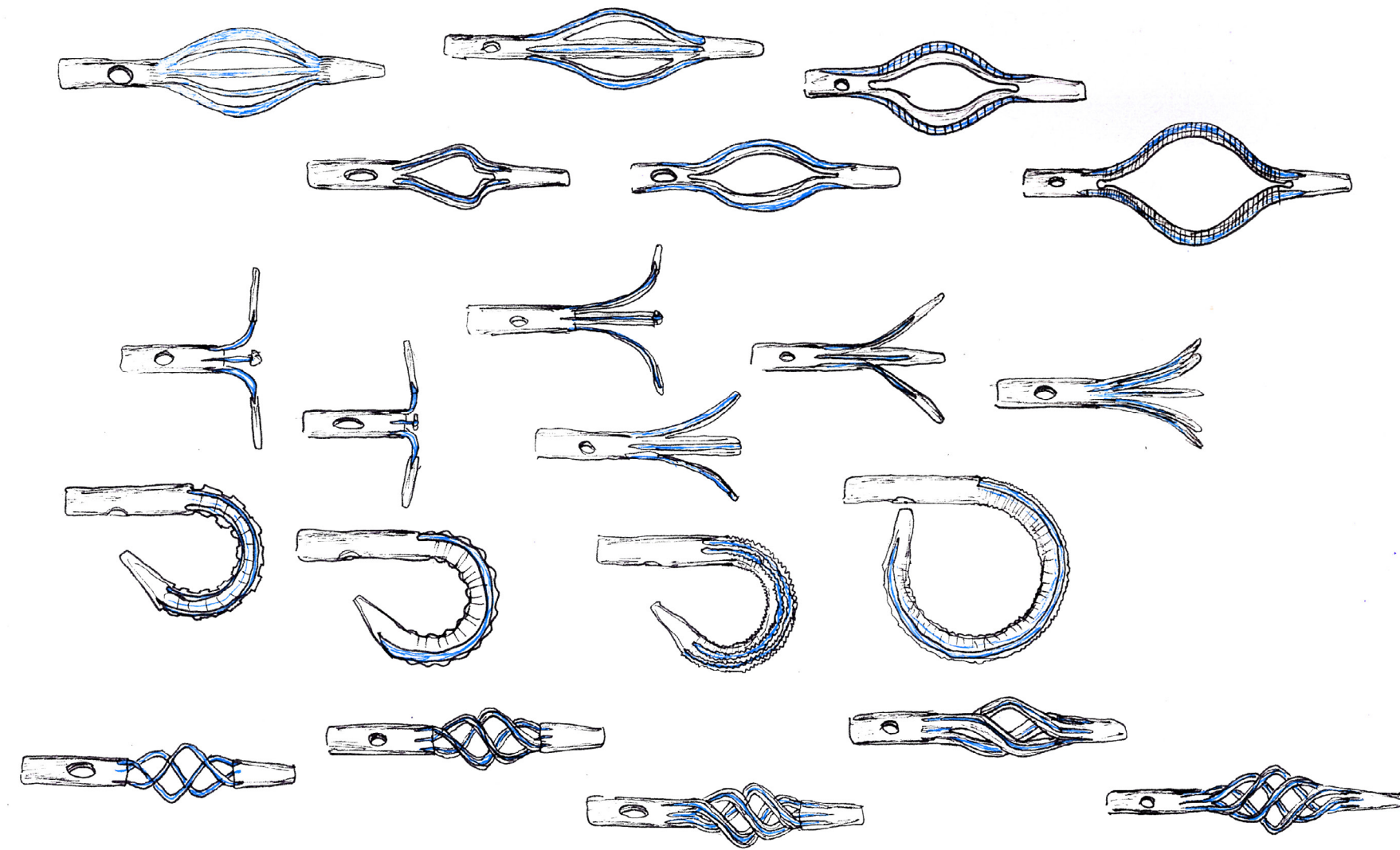


Figure 96. Stimulus-responsive drains ideation sketches.

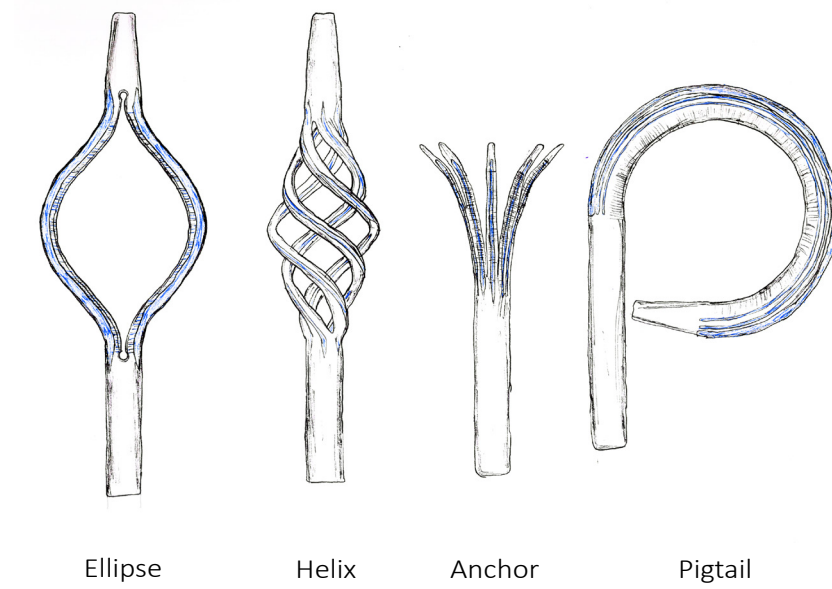


Figure 97. The various stimulus-responsive drain concepts.

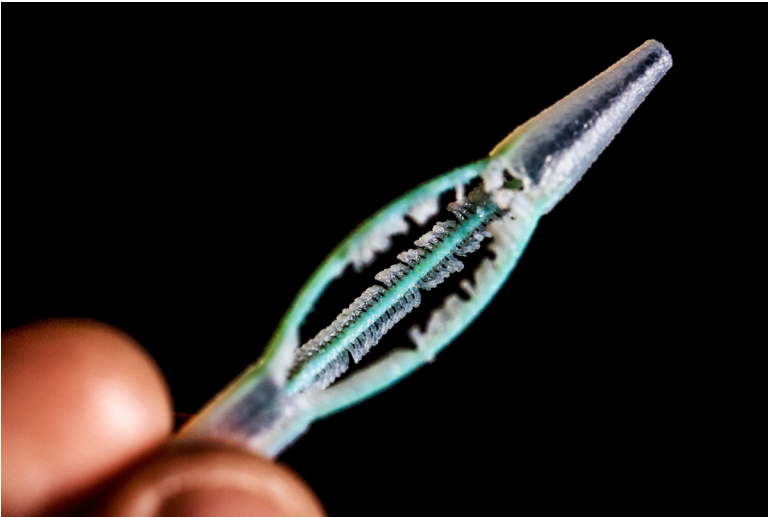


Figure 98. Exploring fins like structures protruding from the Vero rods, however, they were too weak and broke off when cleaning support.



Figure 99. Miniscule sized drain to test the capabilities of the J750.



Figure 100. An investigation into Vero Voronoi forms to increase the strength of the bands.



Figure 101. Thin strands of Vero were printed within the fins to provide more strength; however, some fins still broke off during cleaning.



Figure 102. Printing a thin strand of Vero piercing through all the fins provides enough strength to survive cleaning.

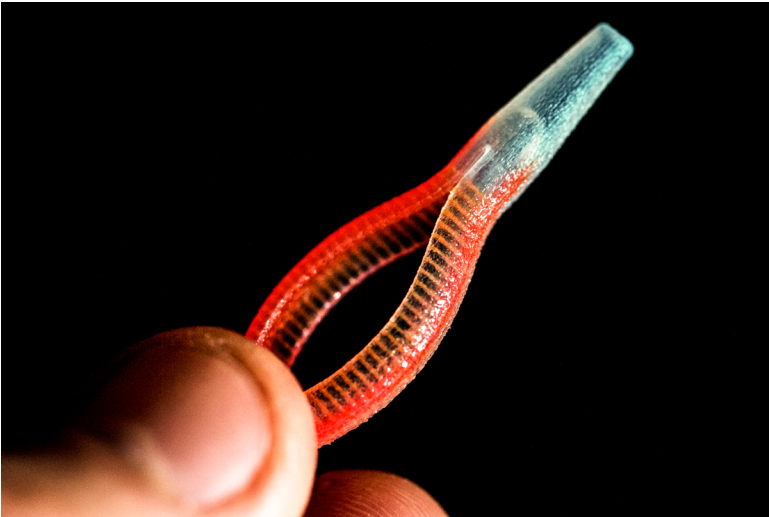


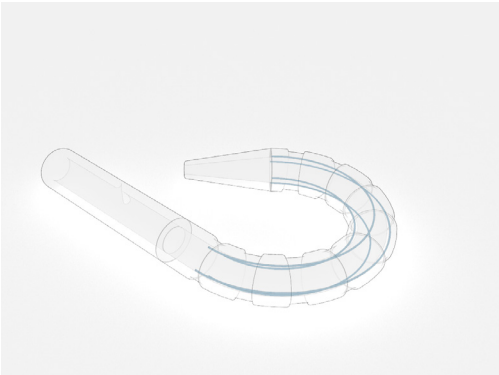
Figure 103. Exploration into internal skeletal forms for added strength, restricting the bands from being easily crushed by tissue or other body organs.



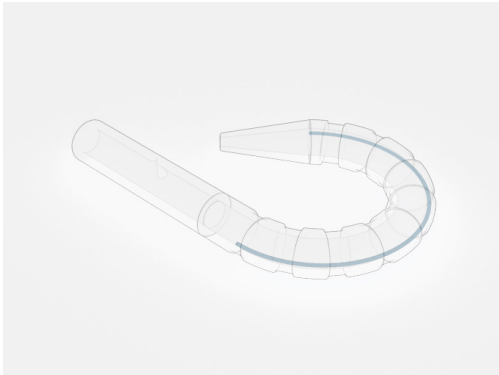
Figure 104. Thin strands of support started printing within the fins when the size of the bands increased. The support would not dissolve in the DT3 cleaning bath.



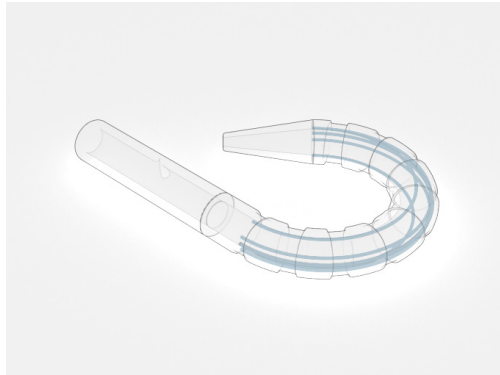
Figure 105. An investigation into internal lattice structures within the bands of a Helix drain.



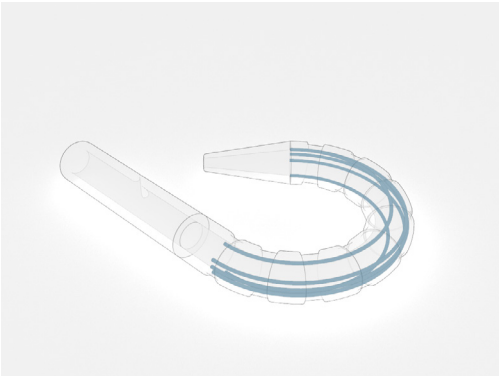
1. The internal vero strand restricts the form from unfurling without breaking.



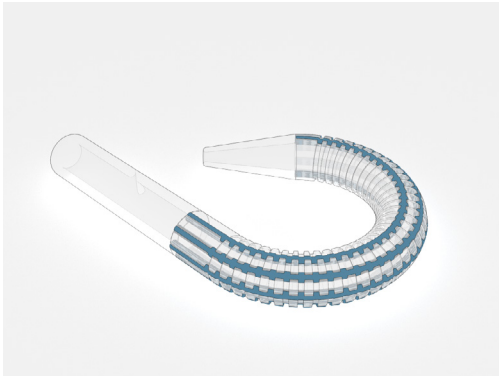
2. A single vero strand is not strong enough to maintain a straightened form.



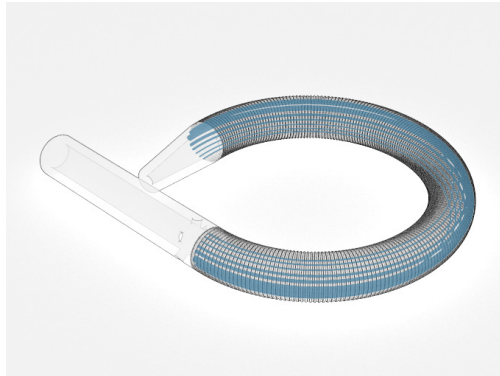
3. Three central strands on the outer curve and two on either side still is not enough to maintain a fully straightened form.



4. Tears when fully extended and does not hold its form. Thicker vero may be needed or thinner grooves on the pigtail curve.



5. Form splits at the joins of the vero and agilius. Internal vero worked better.



6. Lots of thin strands with a thicker central strand allows it to straighten. However, it doesn't hold its form for that long.

Figure 106. The iterative form development of the Pigtail stimulus-responsive drains.



PIGTAIL

Vero rods that gradient in size run through the outer curve of the pigtail, allowing it to straighten for entry on a guidewire. Stimulus-activated retention eliminates the need for string, which has been proven to cause issues at times (Figures 107—108).

Figure 107. Overview of the developed Pigtail drain.

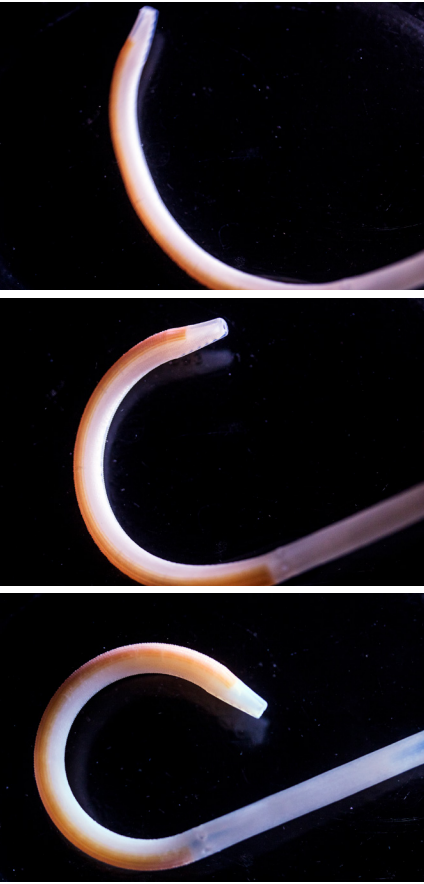
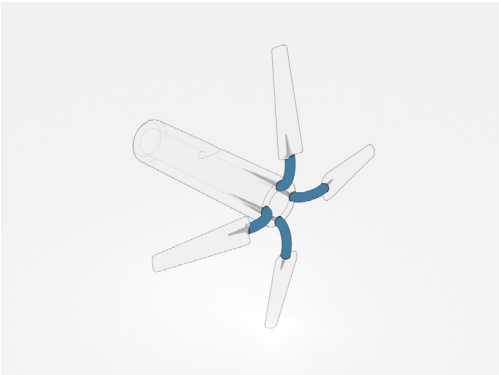
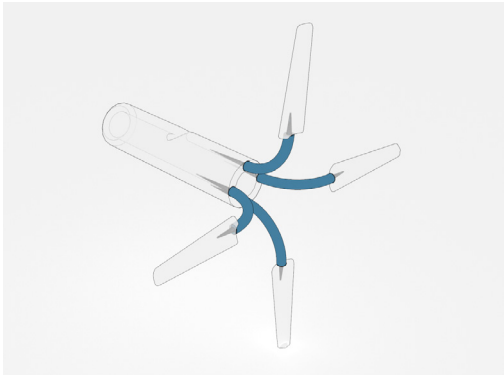


Figure 108. Movement sequence of the Pigtail drain.

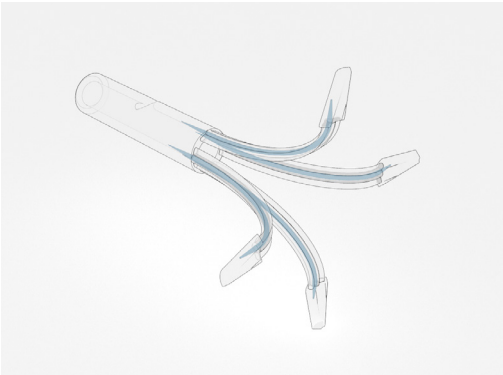
The pigtail can straighten fully but does not manage to hold this form. Continually applying heat and altering the structure reduces the shape memory causing the material to split.



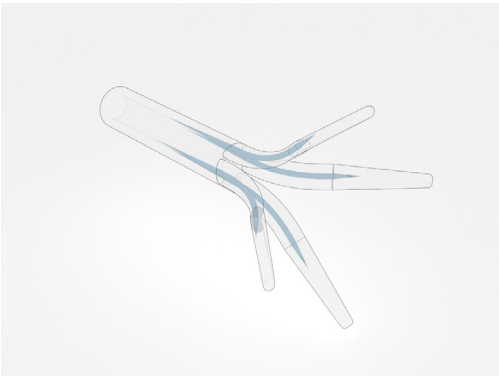
1. The path is too sharp preventing it from straightening as the vero breaks.



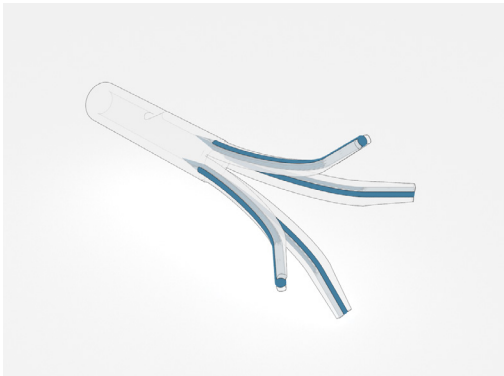
2. The longer path allows for more movement before breaking but still not a full straighten.



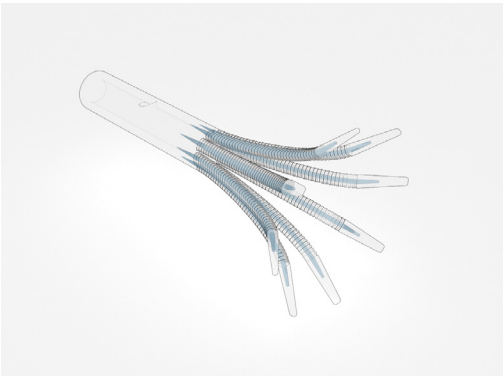
3. The end achieves a straighter form but still breaks well before being fully formed.



4. There is too much support material surrounding the vero, restricting its movement.

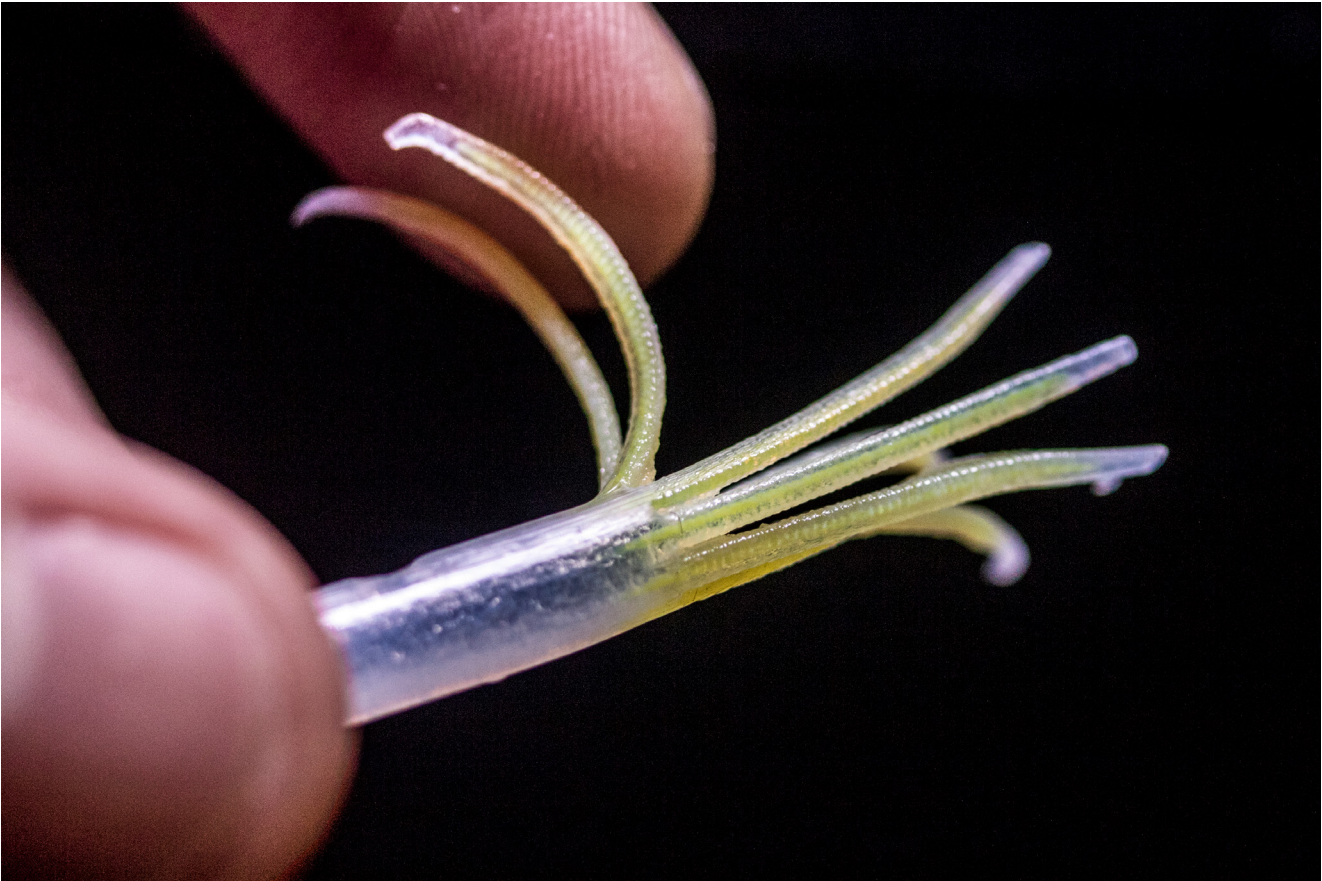


5. The rods appear too thick to straighten fully; thinner rods might elude this issue.



6. Thinner rods allow for a full straighten; however, aren't strong enough to produce a stable tip for guidewire entry.

Figure 109. The iterative form development of the Anchor stimulus-responsive drains.



ANCHOR

Several bands open at the tip of the catheter to form an anchor structure for internal retention. Upon activation, the bands reveal an opening used for drainage. During removal of the drain, the anchor bands would straighten for a painless extraction (Figures 110—111).

Figure 110. Overview of the developed Anchor drain.

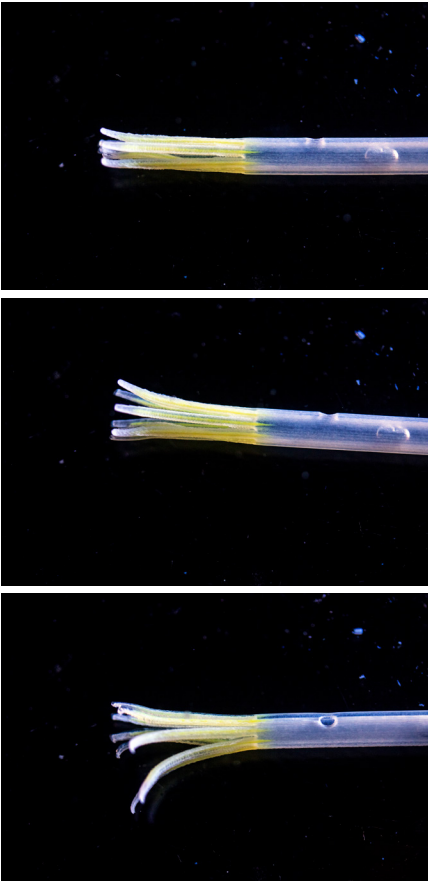
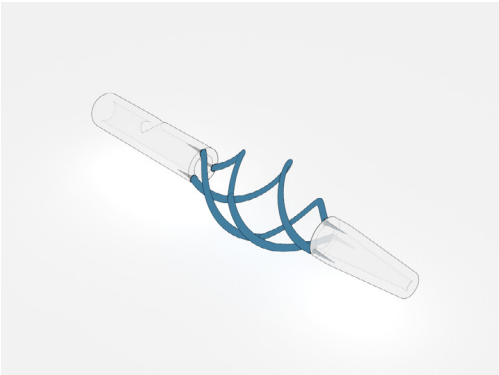
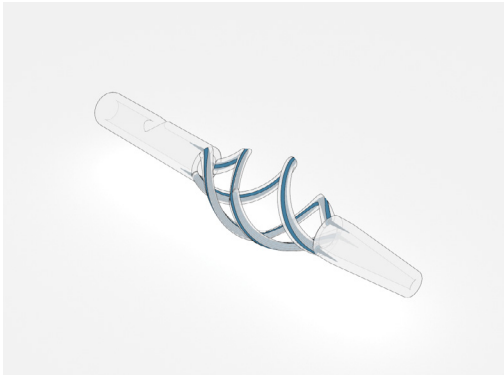


Figure 111. Movement sequence of the Anchor drain.

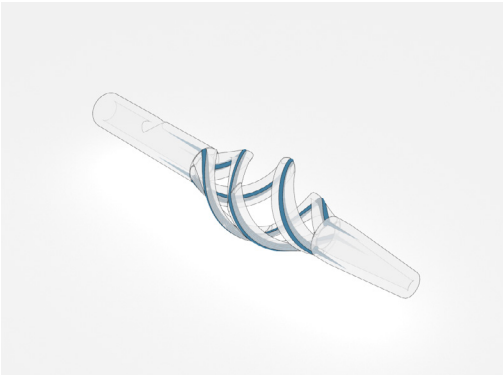
Achieving a balance in the vero to get the bands to straighten fully and maintain its form without breaking was challenging. The material loses its original shape memory properties after being altered as there is not enough vero, but applying more vero causes the anchor to snap during straightening.



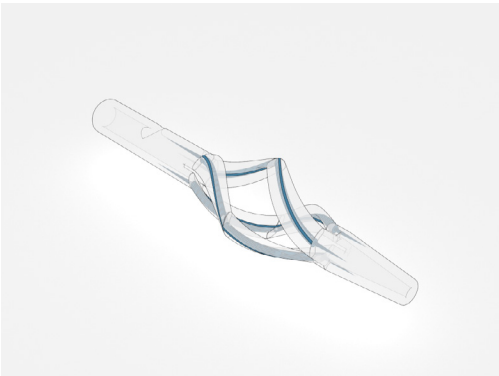
1. The internal vero strand restricts the form from unfurling without breaking.



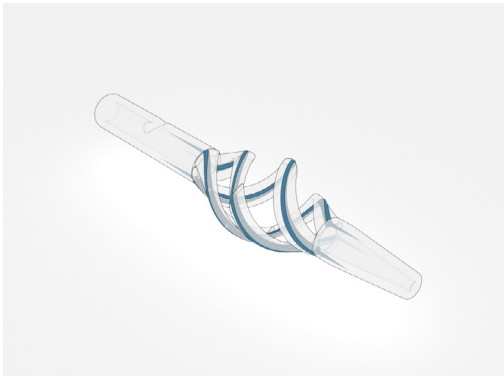
2. A single vero strand is not strong enough to maintain a straightened form.



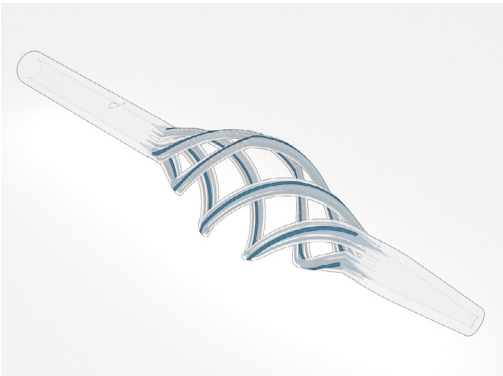
3. Three central strands on the outer curve and two on either side still is not enough to maintain a fully straightened form.



4. Tears when fully extended and does not hold its form. Thicker vero may be needed or thinner grooves on the pigtail curve.

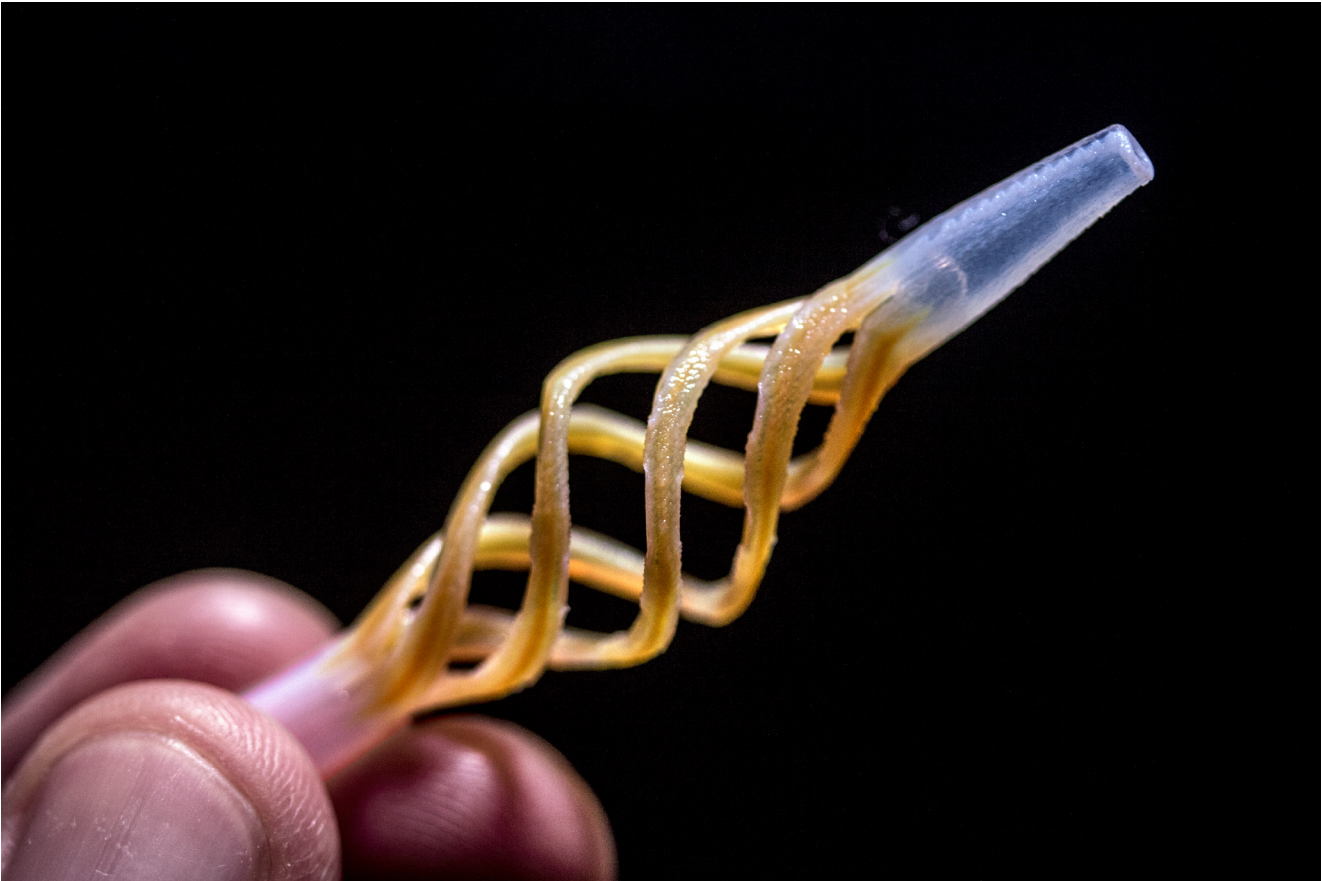


5. Form splits at the joins of the vero and agilius. Internal vero worked better.



6. Lots of thin strands with a thicker central strand allows it to straighten. However, it doesn't hold its form for that long.

Figure 112. The iterative form development of the Helix stimulus-responsive drains.



HELIX

Spiralling bands produce a twist activated retention. Once the helix form expands, it reveals a large opening used for drainage. The helix form can compress during removal, reducing the pain (Figures 113—114).

Figure 113. Overview of the developed Helix drain.

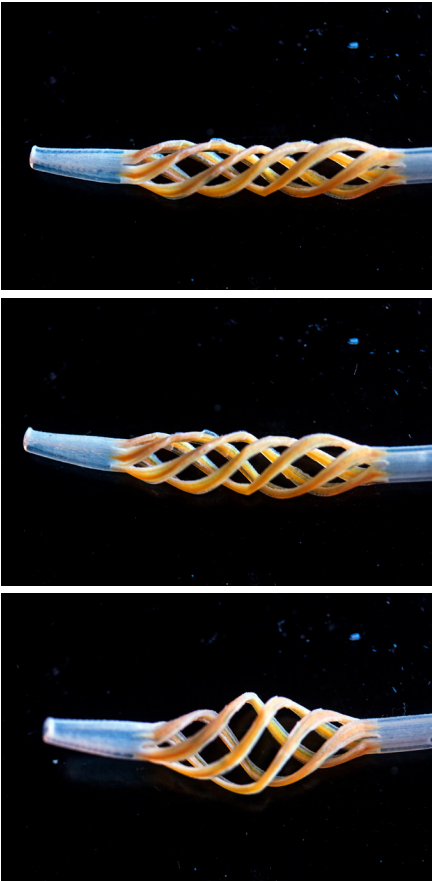
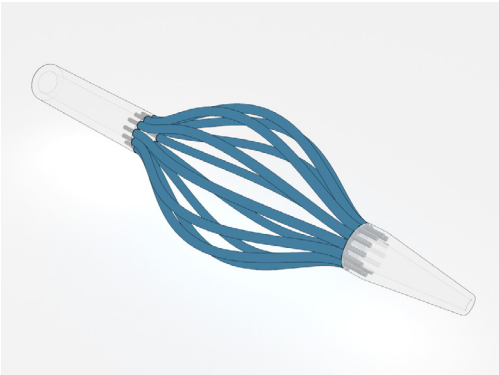
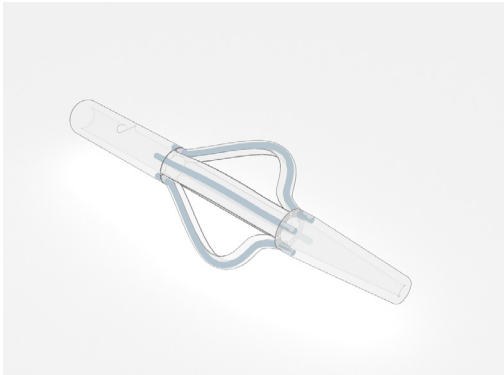


Figure 114. Movement sequence of the Helix drain.

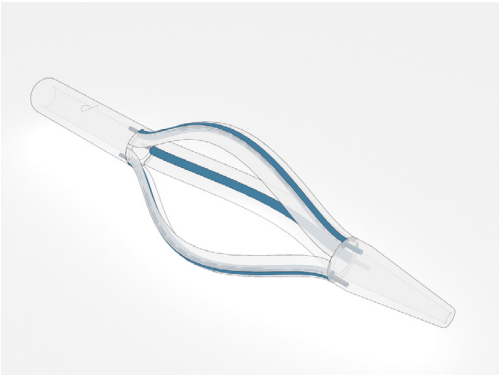
The twisting form allowed the drain to straighten well but results in too many open spaces for a guidewire to slip out of into the body. The helix form needs several bands to maintain its structural integrity, but this obstructs the entry into the large hole for drainage.



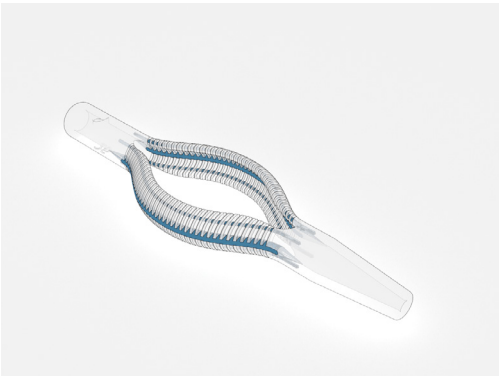
1. Too many vero rods, restricts larger and thicker matter from draining. Have soft material surrounding the vero to increase area of contact.



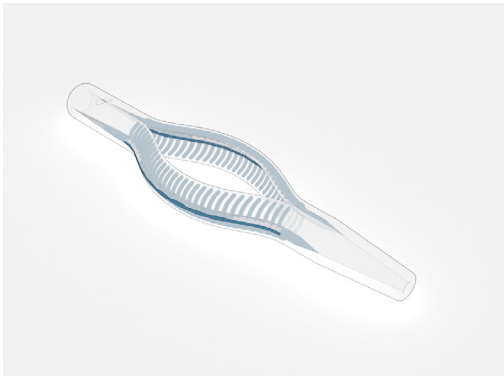
2. Shark fin style is too harsh, cannot fully straighten. Fully encasing the vero restrains it from holding its altered form.



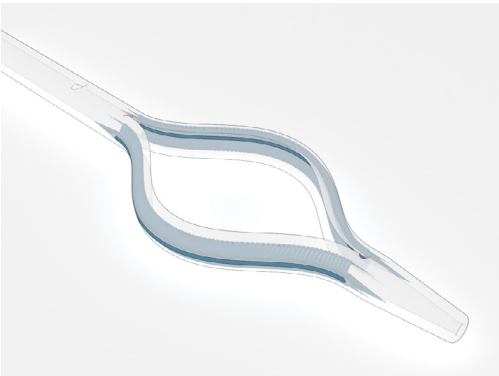
3. Smoother path straightens well. Rods are easily crushed with little pressure; having two larger rods would produce a more secure retention.



4. Spacing between the fins is too large, support prints in-between making it impossible to clean without ripping.



5. The Internal skeletal form provides increased strength. The bands need to be bigger for enhanced retention.



6. Increased size of the bands provides a wider area of retention. The form manages to almost fully straighten and hold its form for entry.

Figure 115. The iterative form development of the Ellipse stimulus-responsive drains.



ELLIPSE

Two lateral bands imbued with vero allows it to print in the active form then straightened for percutaneous entry. When the bands activate for retention, they present a large opening for drainage. Exploration of a Vero skeletal structure provides the bands with additional strength to resist being crushed by bodily organs (Figures 116—117).

Figure 116. Overview of the developed Ellipse drain.

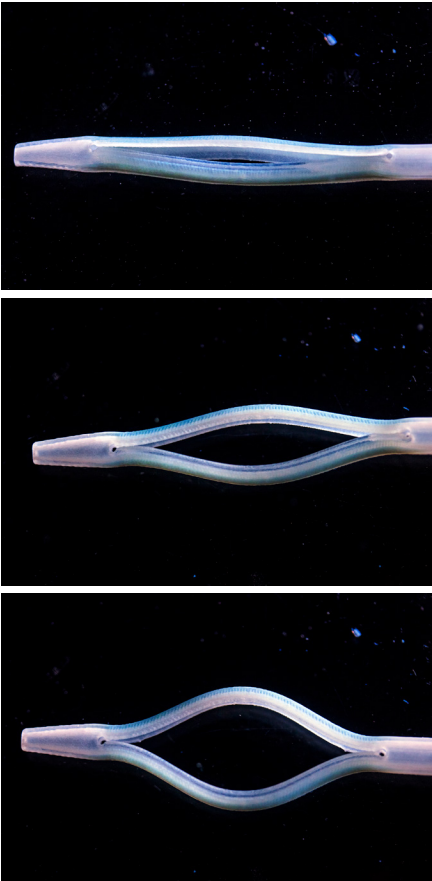


Figure 117. Movement sequence of the Ellipse drain.

The ellipse form manages almost to straighten fully, the middle bump in the vero path restricts this. The drain needs to fully straighten and close to allow it to be safely threaded over a guidewire and into the abscess.



STIMULUS-RESPONSIVE DRAINS SUMMARY

The access to Smart materials enabled exploration into stimulus activated internal retention (Figure 118). Couple that with the high-resolution multi-property capabilities of the J750, it was possible to fabricate forms imbued with strands of Vero down to .15mm, containing SMP's. The thin strands of SMP's allowed for thermomechanical programming. By applying heat, through submerging models in hot water, it transitions the vero from a rigid state into a rubbery state, allowing it to be shaped into a minimally-invasive form for insertion into the body. The print is then cooled down, maintaining its altered shape until heat is applied, reverting it to its original active state.

In theory, thermal activation is not the most suitable activation stimulus as the body temperature is not high enough to activate the T_g of the Vero material. Ph value or moisture might be a more appropriate stimulus as the fluid to drain from the abscess may have a significantly different ph value; however, more research is required to confirm this. Thermal activation was the most suitable means for exploring the idea of stimulus-activated drains, and with the J750, it was possible to visualise the performance tangibly.

Figure 118. Overview of various stimulus-responsive drain prototypes.

3.5 EXPERIMENTATION SUMMARY

This chapter examined various materials and additive manufacturing processes from commercial 3D printing services — Standard Resin produced through stereolithography (SLA) from i.Materialise possessed the highest quality. However, for Lab testing the 3Dsystems ProJet MJP 3600, utilising multi-jet printing technologies, provided high-resolution and was locally available, making it easy to produce large quantities of 3D prints regularly. The Lab tests proved 3D printings ability to generate micro-millimetre details consistently in large volumes for examination. Computational Fluid Dynamics was explored to analyse models digitally against physical testing. This set of software allowed for digital visualisations of the flow within drains to perceive how different sized or shapes of drain holes affect drainage, and to observe potential circulation issues. Viewing this information early in the design process allows designers to combat any circulation problems early in the development cycle.

It then explored the Stratasys J750's ability as a prototyping and visualisation method. As a prototyping method, the J750 managed to produce high-quality outputs that resembled finished products. It can also create numerous designs in one print run, making it extremely effective for a parallel prototyping design approach. It significantly sped up the iterative design process. Multiple CAD files could be submitted for production and received the next day. Compared to handcrafting, which could take several days for a single prototype, the J750 is capable of generating many high-fidelity models overnight. Post-processing models are relatively quick, removing support material and cleaning

is all that needs doing. The DT3 made cleaning large quantities of 3D prints very efficient, while the inclusion of removable internal stents significantly reduced the amount of support material within models.

As a visualisation method, it made it possible to manifest clinical ideas physically, and concepts thought unmakeable. Presenting tangible visualisations to clinicians allowed them to interact with, and learn the potential of multi-property additive manufacturing. In return, the enhanced understanding of the designs and 3D printing process heightened the clinical feedback received. During meetings, whenever 3D prints and digital media were presented, clinicians favoured the physical. Tangible interactions with 3D printed models also prompted the generation of new ideas (Figure 119). The J750 made it possible to communicate the concept of 4D printing. However, clinicians seemed wary of relying solely on stimuli for internal retention but were interested in the idea, encouraging further research. Lastly, the J750's ability to infuse a range of colours made it easier to visualise the material composition and various components of a prototype.

Although the J750 is excellent for prototyping and visualisation, some limitations were discovered during the design experimentations. Agilius and Vero are proficient 3D printing materials; however, the durability compared to contemporary materials used to produce surgical drains is lacking. Also, the support material limited the minimum size of design features. Fragile elements would print, but it was difficult to remove support material without breaking them. Finally, the sophistication with multi-property 3D prints made it hard to troubleshoot design issues. Material composition, thicknesses of parts, and the print orientation of models are just a few of the variables.

Figure 119. Iterative development in a documentation logbook, ideas generated from physically interacting with a multi-property 3D print.

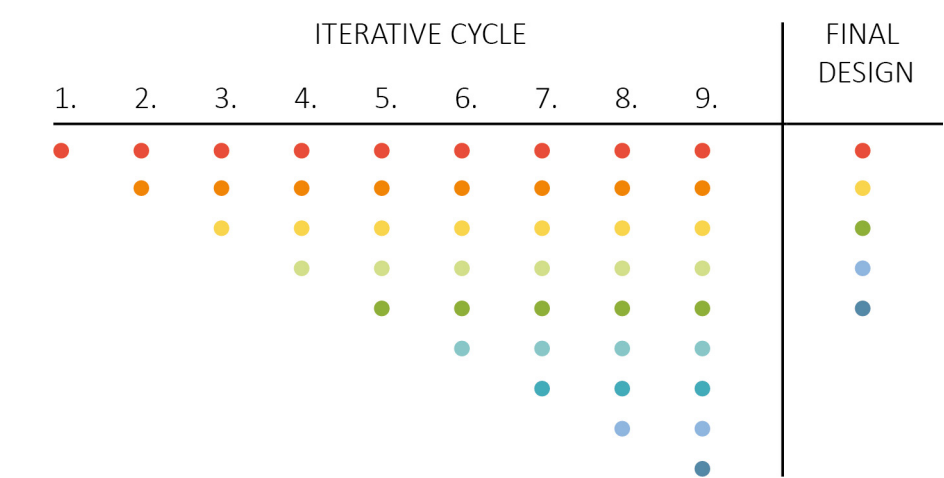


Figure 120. Diagram illustrating the accumulation of knowledge after each iterative cycle, represented by the dots.

RESULTS OF ITERATIVE DESIGNS

Resolved designs are the result of consolidating the most suitable findings from the previous chapter. After each iterative cycle, new knowledge is generated. From the amassed knowledge, the most appropriate findings are chosen while dismissing the less applicable ideas (Figure 120).



Figure 121. Overview of the 3D printed Contemporary pigtail drain.

4.1 CONTEMPORARY PIGTAIL DRAIN

Emulating the current pigtail drain allows for a direct comparison of contemporary and additive manufacturing. An assessment of the details and materials between the two production processes provides an understanding of the potential of 3D printing. Embedding branding, incorporating the string detail, and the locking mechanism at the full-scale provides the feel of a finished product (Figures 121—122).



Figure 122. Detail images of the 3D printed Contemporary pigtail drain.

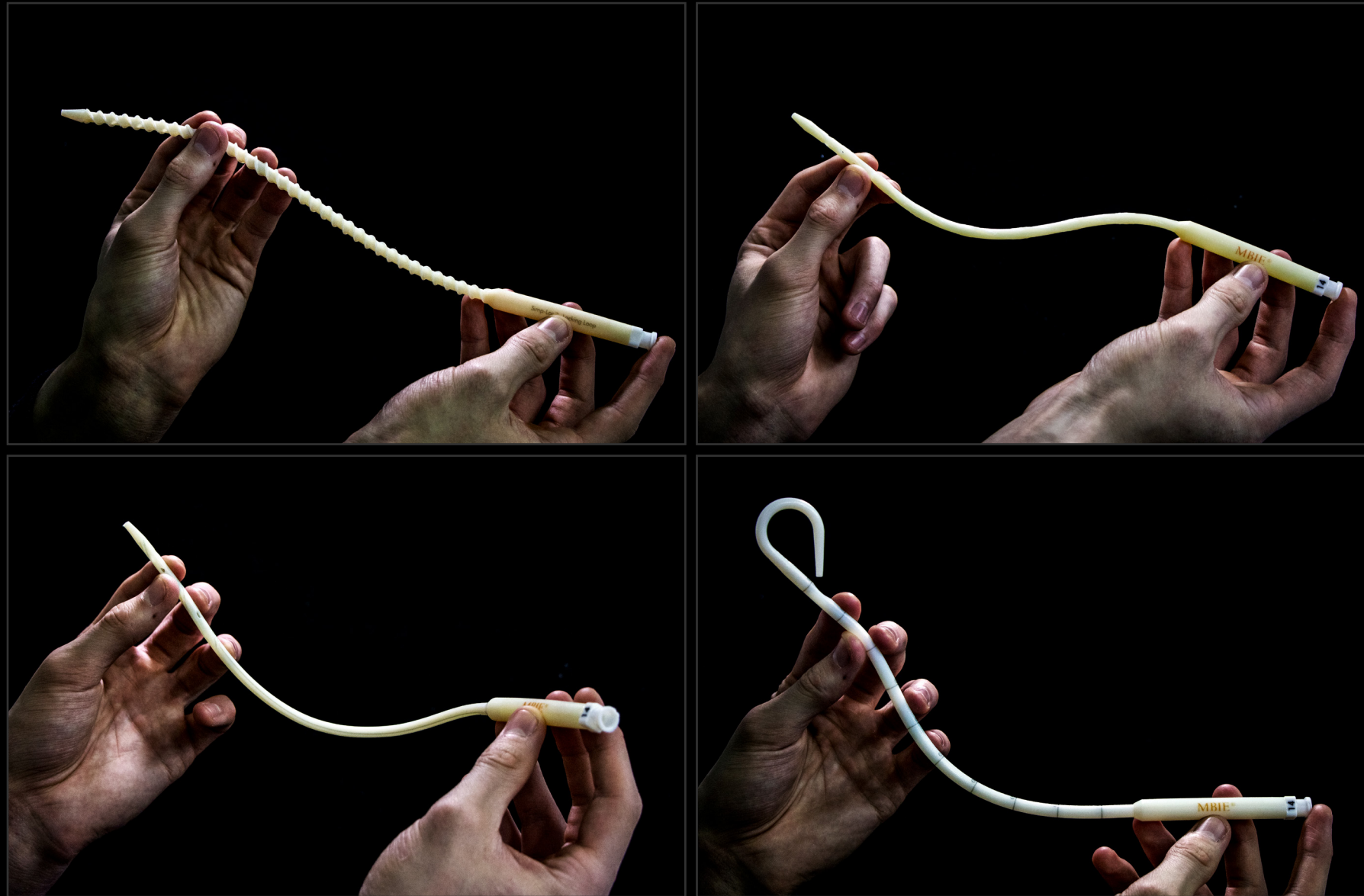


Figure 123. Overview of the various irrigation drains, Tight External Spiral (top left), Sparse External Spiral (top right), Internal Irrigation (bottom left), Irrigation Pigtail (bottom right).

4.2 IRRIGATION DRAINS

Additional lumens for irrigation introduce fluids, such as saline, into the cavity, reducing the viscosity of the infected fluids making it easier to drain. A series of irrigation designs explore various irrigation methods of the interior and exterior area of the catheter (Figures 123—128) .

The external spiral concepts offer continuous irrigation, while not impacting the primary drainage lumen by having the irrigation channels located in the spiral. Irrigation holes target the exterior and interior area of the drain. The protruding channels also push tissue off of the drainage holes to reduce obstructions.

The internal irrigation focusses on continuously irrigating the interior of the catheter. Directing the irrigation holes towards the drainage holes provides a means of unblocking. Markings along the exterior of the catheter indicate the internal channels to radiologists in case they want to make manual adjustments.

The pigtail concept offers dilutional irrigation to promote drainage. A small channel extends through to the tip of the catheter for irrigation. When the pigtail curls for retention, the tip aims towards the primary drainage hole injecting irrigation fluid back through the drain to promote drainage.



Figure 124. Detail images of the various irrigation drains, Tight External Spiral (left), Sparse External Spiral (middle left), Internal Irrigation (middle right), Irrigation Pigtail (right).

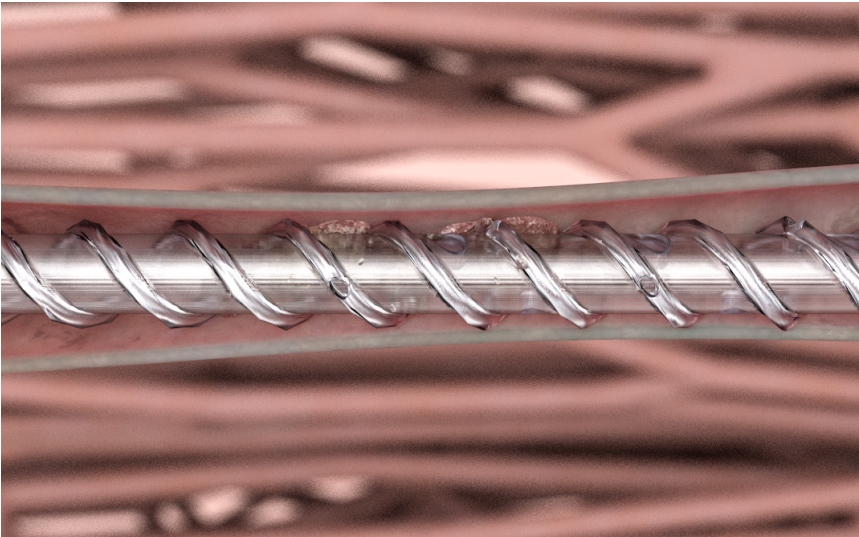


Figure 125. Context image of the Tight External Spiral irrigation drain within the human body.

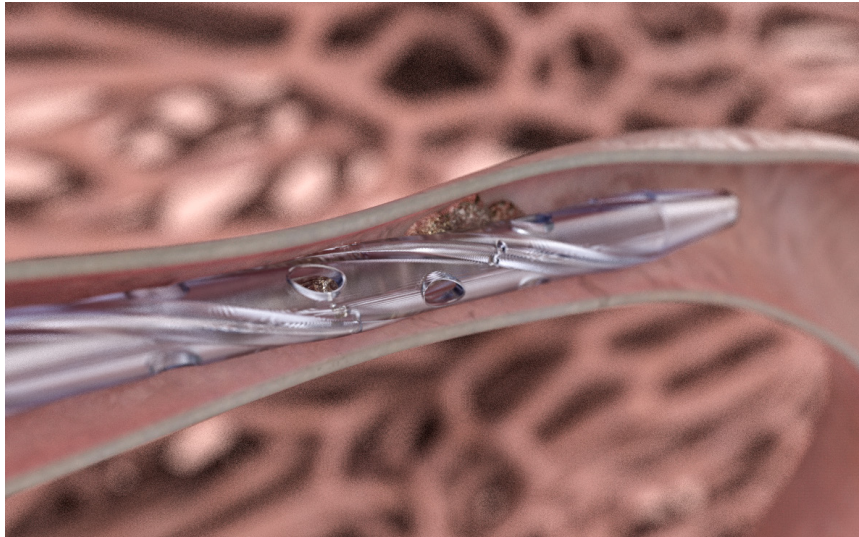


Figure 126. Context image of the Sparse External Spiral irrigation drain within the human body.

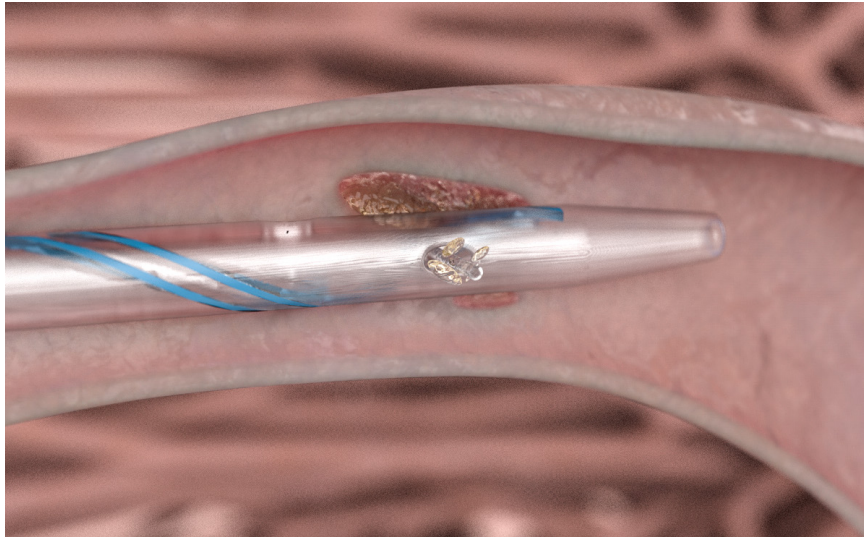


Figure 127. Context image of the Internal irrigation drain within the human body.

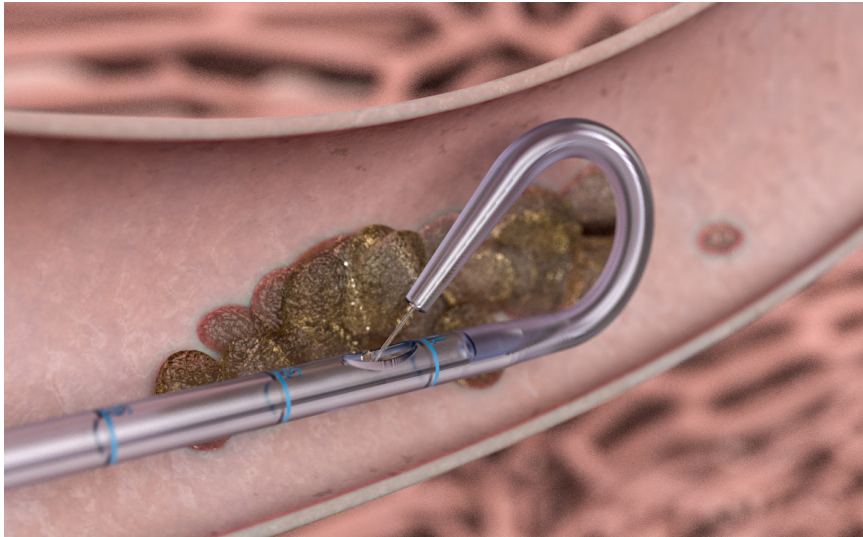


Figure 128. Context image of the Irrigation pigtail drain within the human body.



Figure 129. Context image of the skin fixation drain attached to the back of a patient.

4.3 EXTERNAL SKIN-FIXATION DEVICE

Providing external security of an indwelling surgical drain the skin-fixation device restricts dislodgement (Figures 129—132). The catheter sits in a slightly curved path, increasing the friction, enhancing retention. Offering three routes for the drain to sit in allows the patient to alter it, for comfort, if they want to move their drainage bag. The device can be either sutured or adhesively attached, giving the radiologist a couple of options. The mesh provides breathability around the wound while also making the device more flexible, allowing it to move more freely with the body. A rigid lid clips over the three paths to lock the drain in, but sits under the flexible section, so patients do not lay directly onto it.

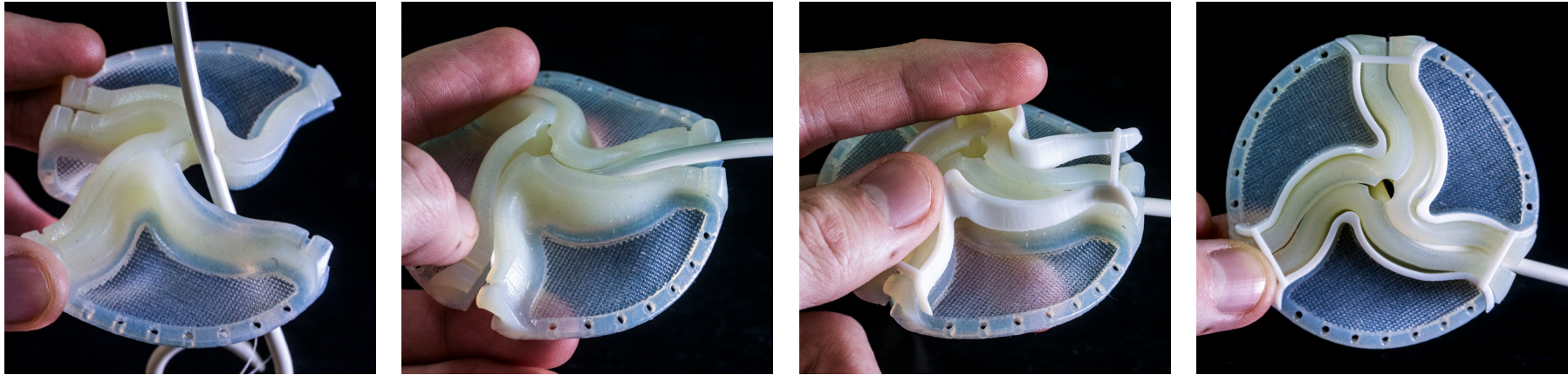


Figure 130. Step-by step process of attaching the skin fixation device over an indwelling surgical drain.

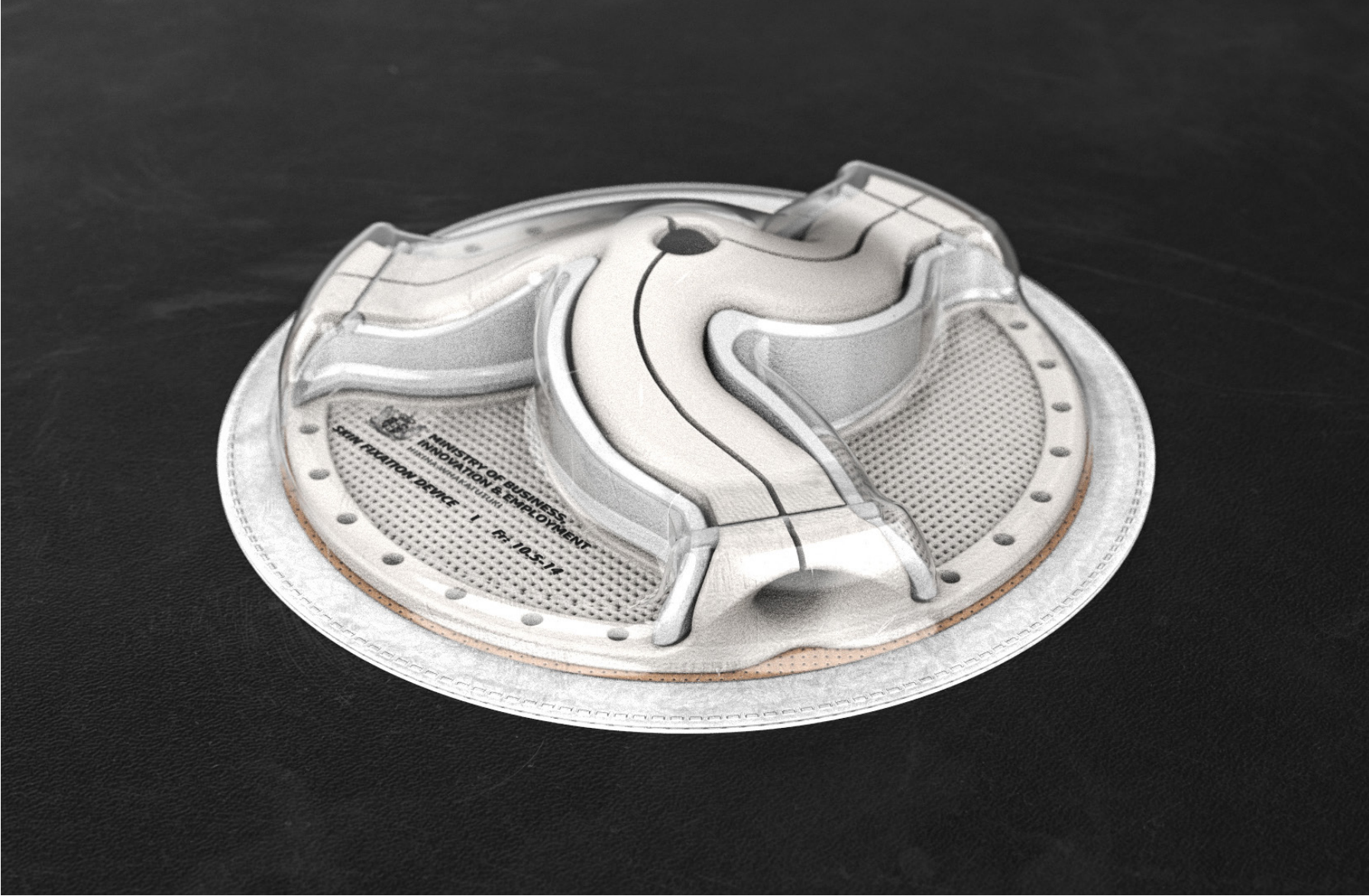


Figure 131. Packaging concept for the skin fixation device.

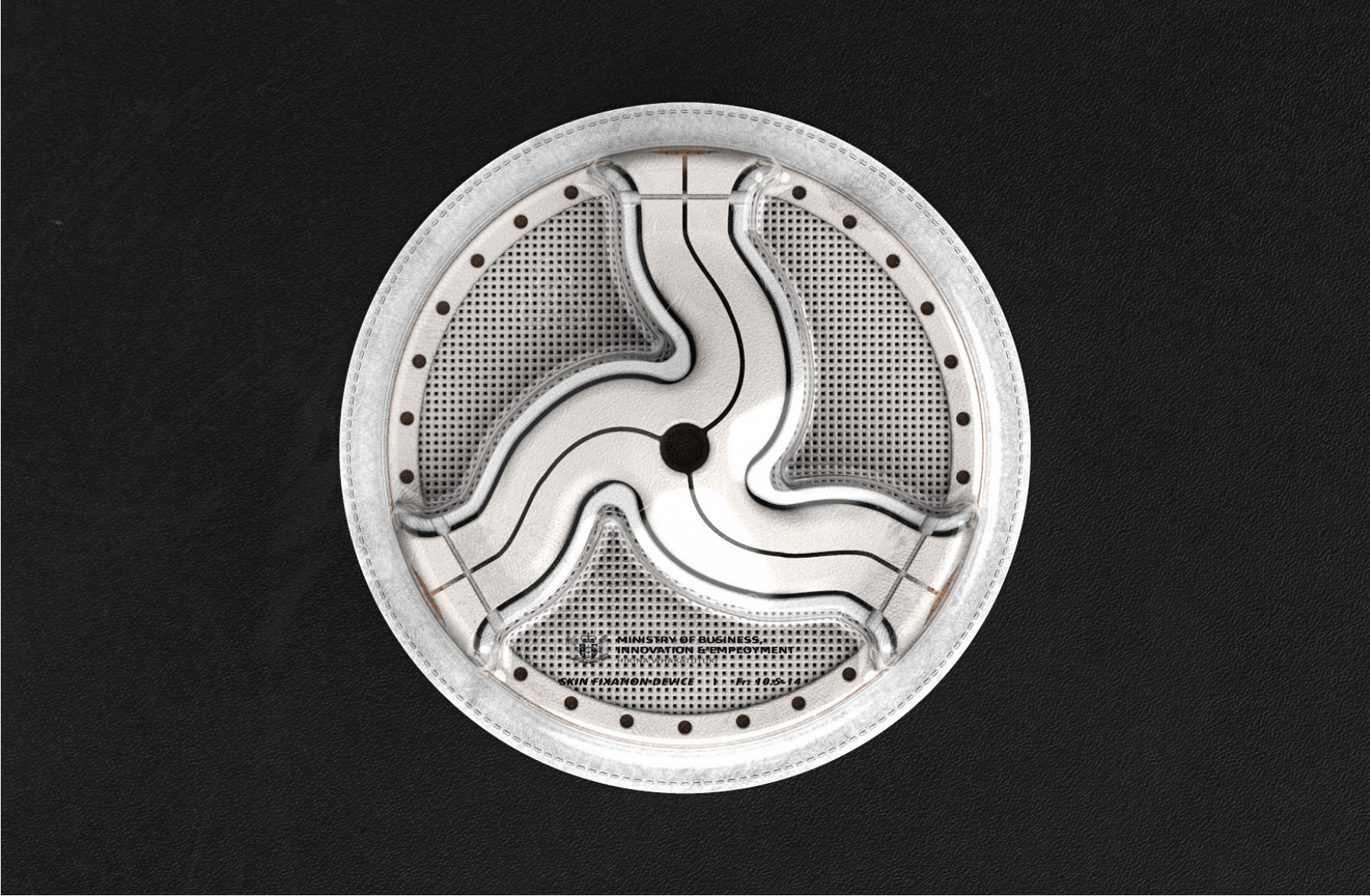


Figure 132. Packaging concept for the skin fixation device.

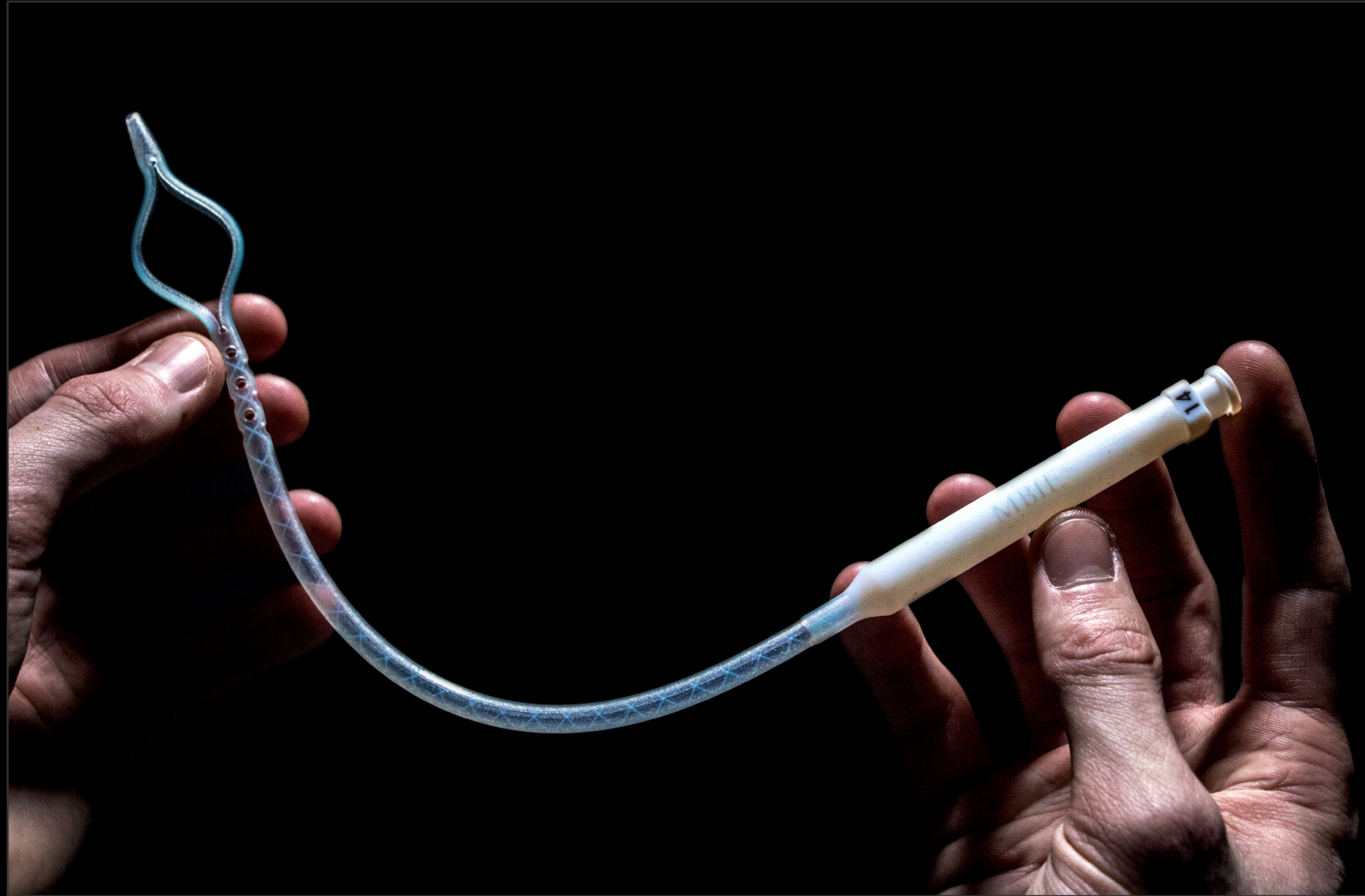


Figure 133. Interaction with the Ellipse stimulus-responsive drain.

4.4 ELLIPSE STIMULUS-RESPONSIVE DRAIN

Utilising the unique material properties and technical capabilities of the J750 enabled the production of a stimulus-responsive internal retention drain (Figures 133—136). When the tip of the catheter reaches the abscess, the change in environmental factors, temperature or ph-value, activates the shape memory properties of the material, opening the lateral bands, forming an ellipse form. When the two bands open, it presents a significant entry point for fluids to drain. The rigid skeletal structure permeated throughout the bands provides structural integrity, restricting it from being easily crushed by tissues or organs, which could lead to dislodgment.

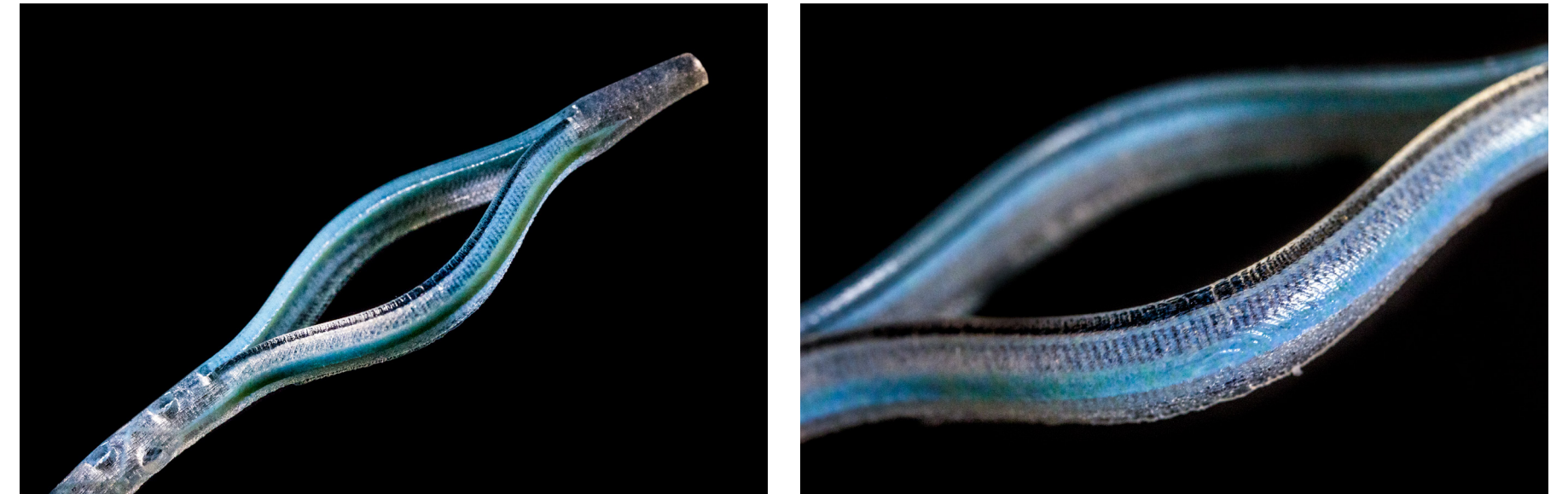


Figure 134. Detail images of the Ellipse stimulus-responsive drain.

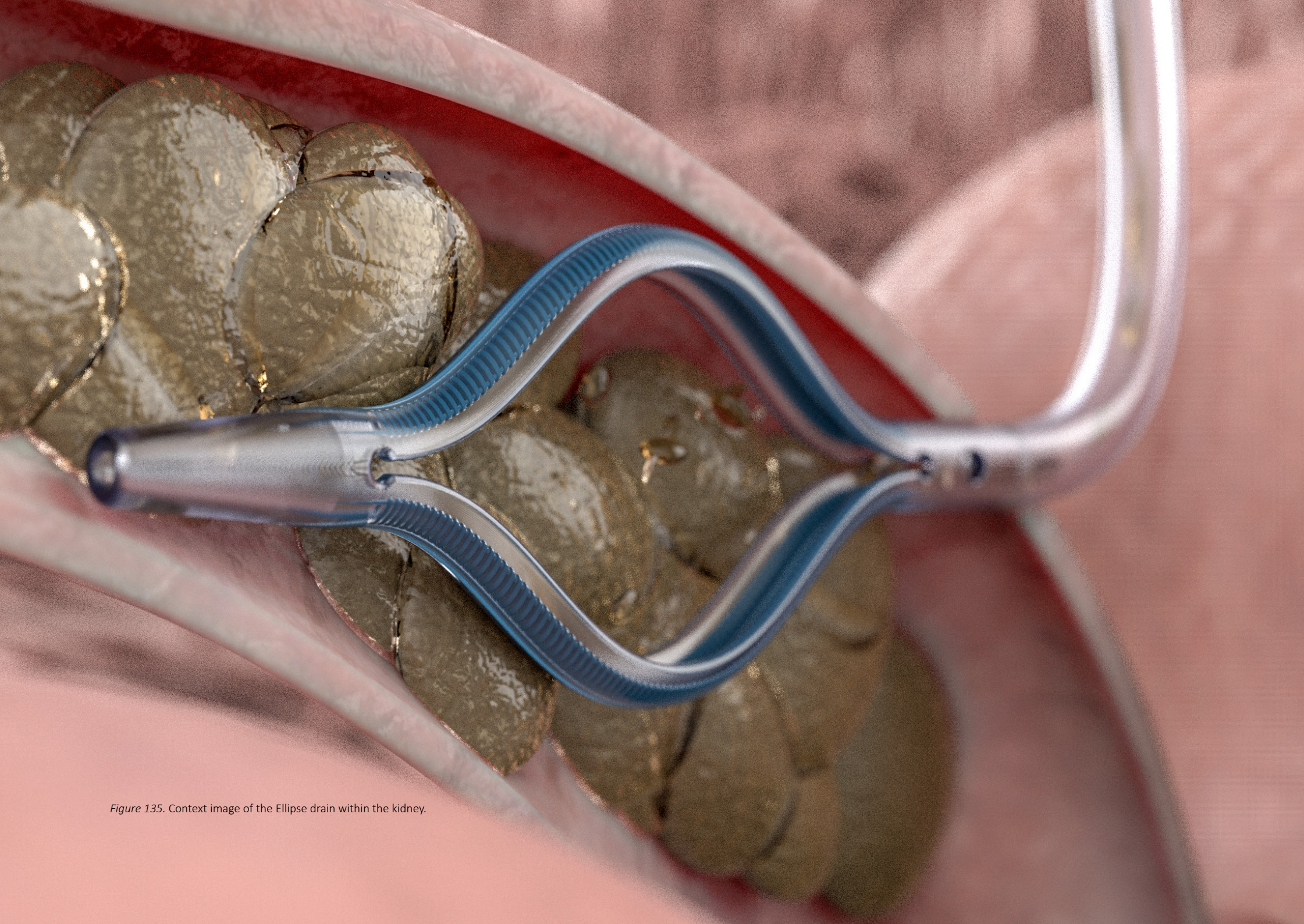


Figure 135. Context image of the Ellipse drain within the kidney.

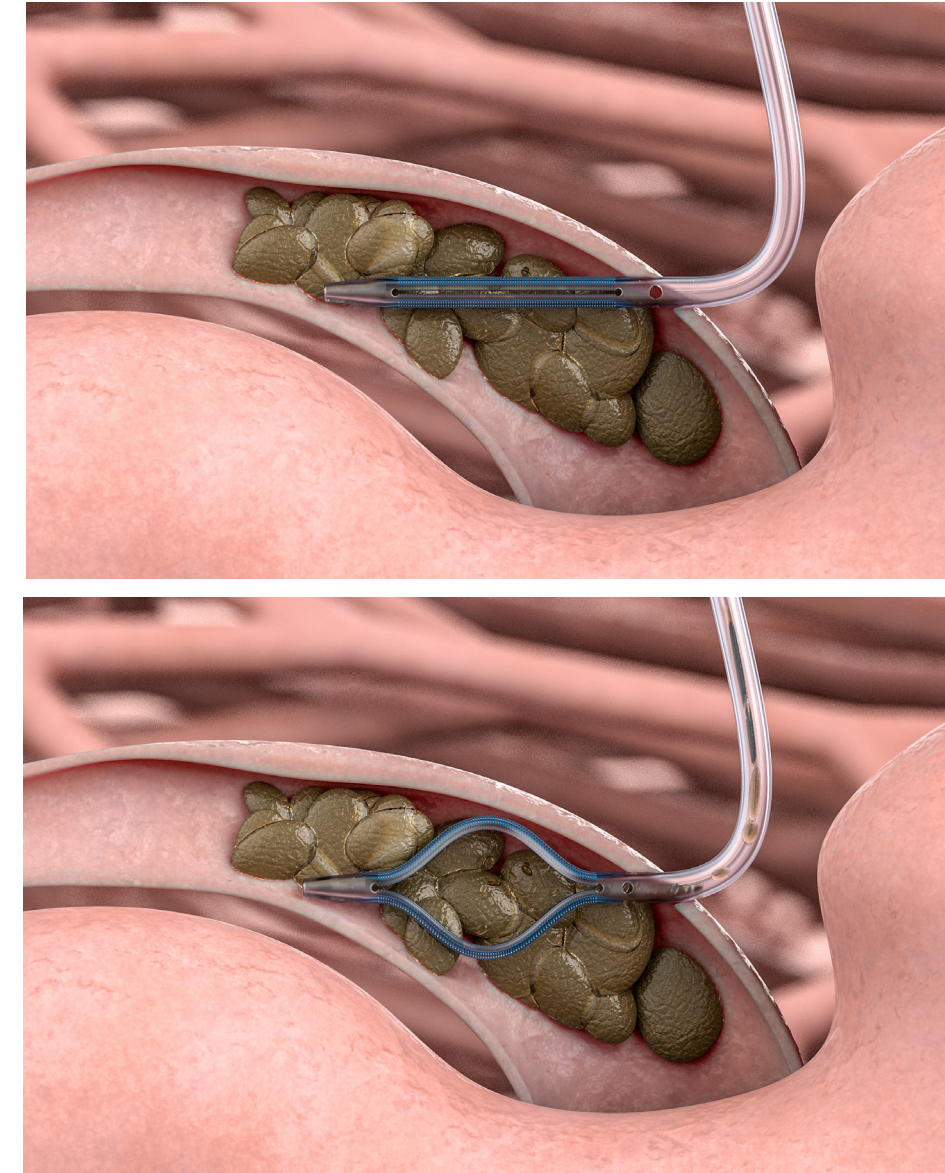


Figure 136. Context image of the Ellipse drain transitioning from the dormant state (top) for percutaneous entry into the active state (bottom) once it reaches the abscess area.

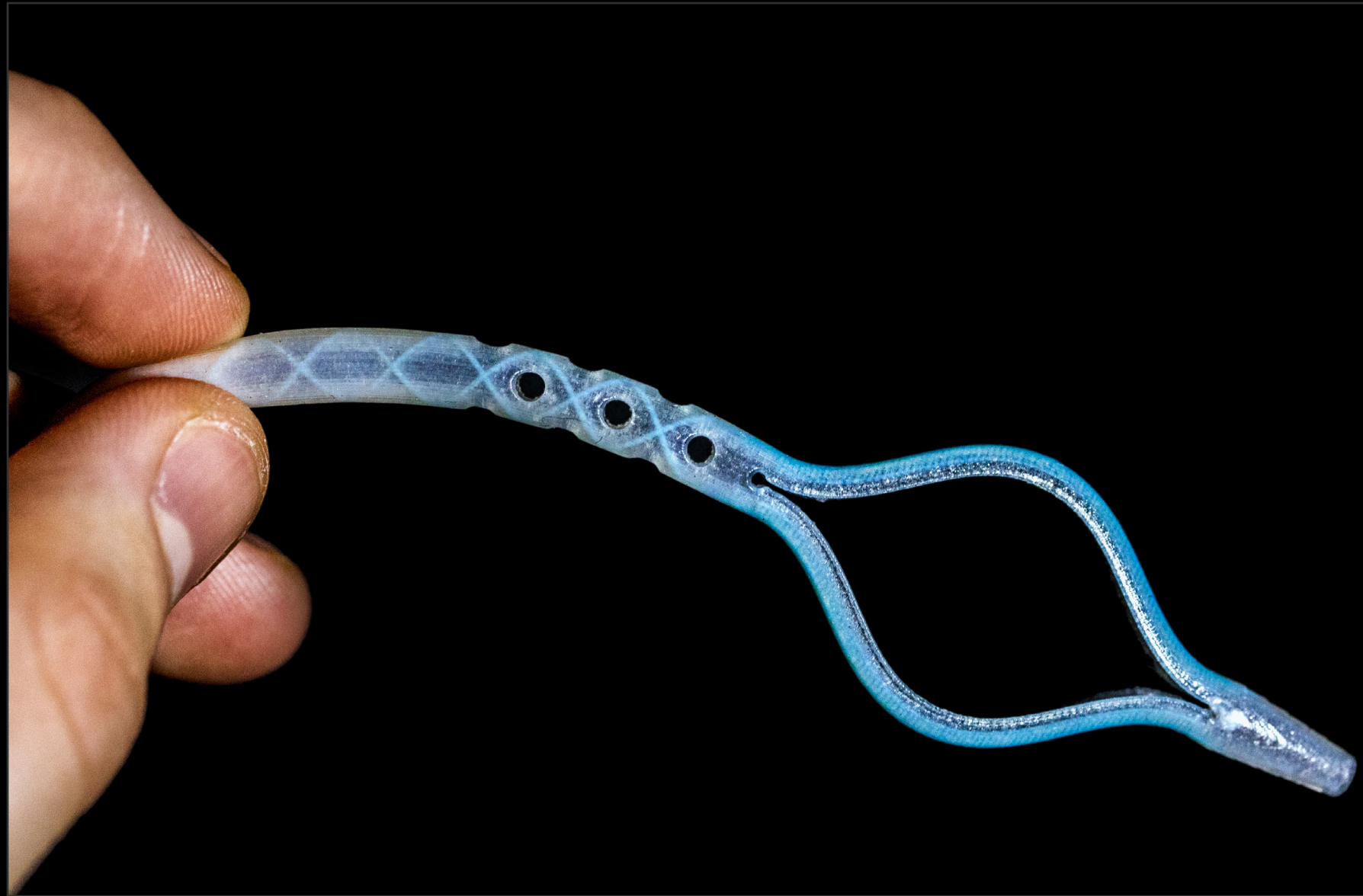


Figure 137. Internal helix structure supporting the tip of the drain.

4.5 INTERNAL STRUCTURES

Incorporating internal structures supports weaker segments of a drain with multiple drain holes (Figures 137—138). Numerous drain holes located in the same vicinity make the catheter susceptible to kinking. The structure can vary in rigidity, being more flexible in areas that need to move with the body. Depending on the drains path into the abscess, the internal structure could be tailored specifically to the unique patient-specific procedure.

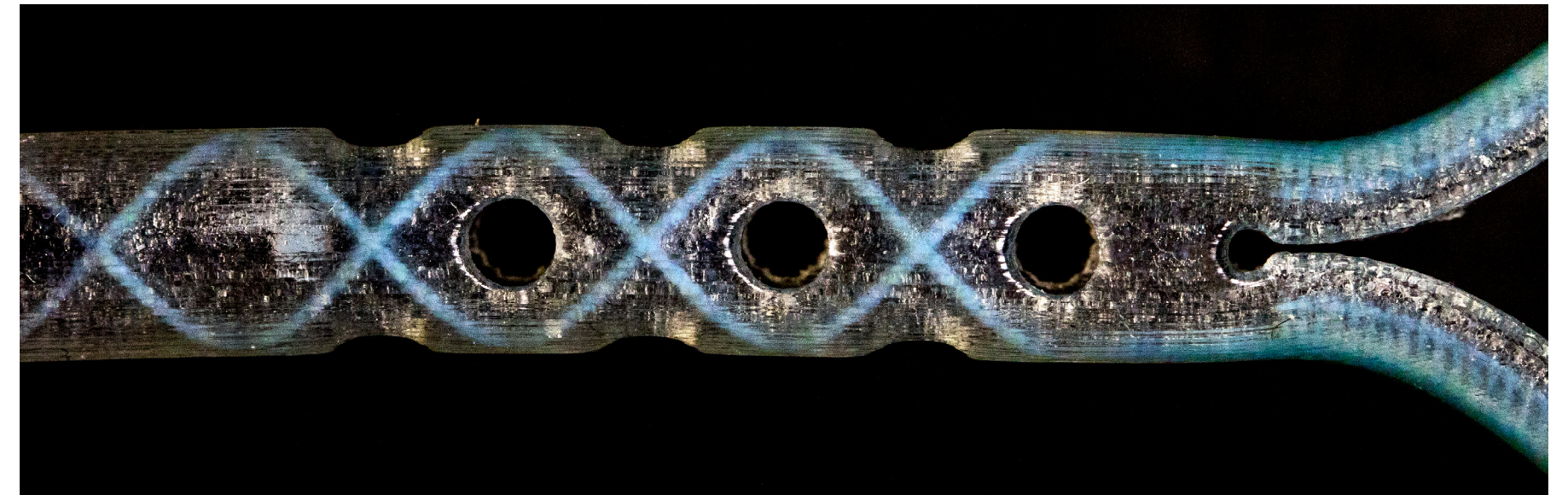


Figure 138. Internal helix structure weaved around the drainage holes.

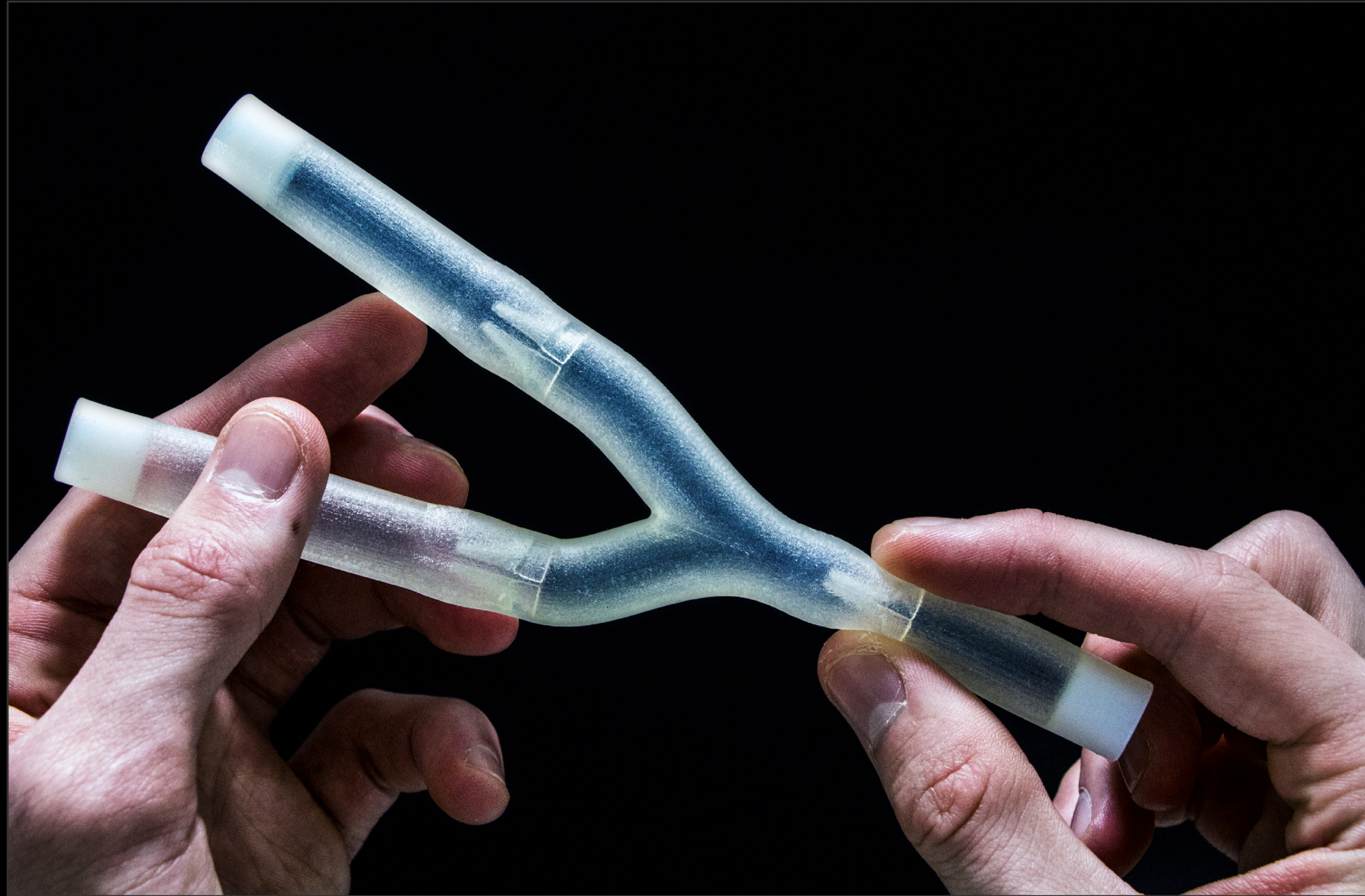


Figure 139. Interaction with a Y-path venous valve prototype.

4.6 VENOUS VALVES

Bicuspid valves inside a catheter could be used to promote fluid through a drain, while also closing to restrict it backwashing, potentially reducing blockages (Figures 139—142). The valve leaflets open with movements made by the patient, such as breathing or other contractions. Compressing the drain opens the valves, propelling fluids through, once the pressure is released the leaflets close.

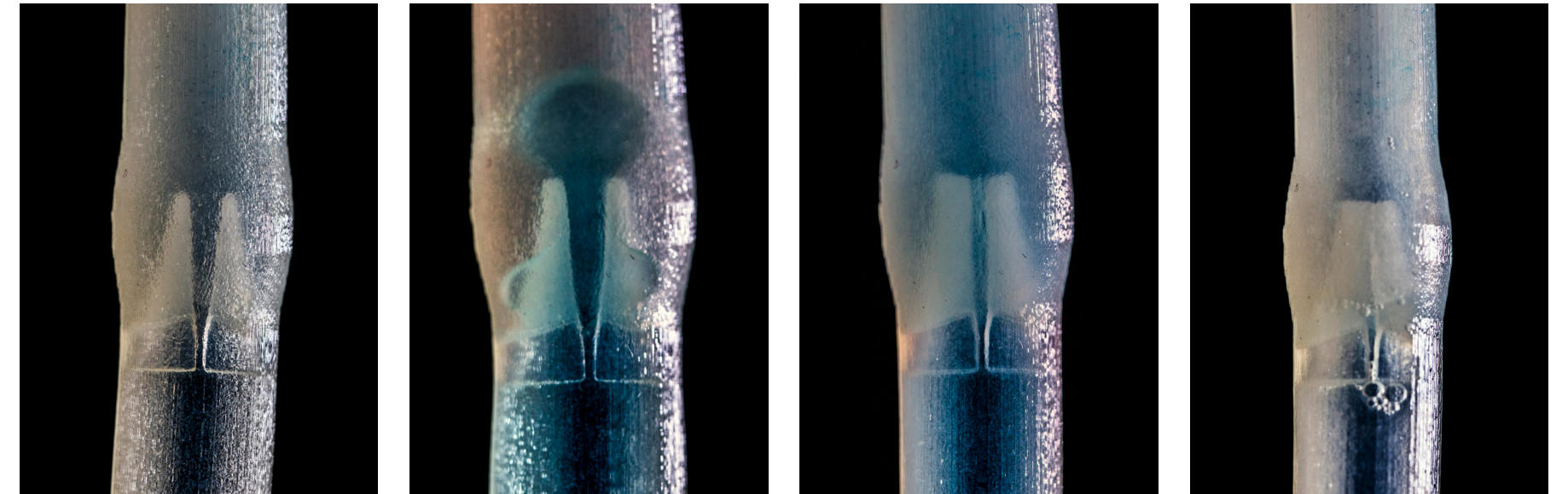


Figure 140. Movement sequence of fluids passing through a valve leaflet.



Figure 141. Fluid flowing through the Y-tube venous valve prototype.



Figure 142. One valve in the dormant state (left) while one valve is in the dormant state (right).

4.7 CONCLUDING CLINICAL EVALUATION

The concluding clinical evaluation consisted of a colorectal surgeon, who interacted with and evaluated 3D printed prototypes. The surgeon has experience with additive manufacturing, but no awareness about multi-property 3D printing. Also, the surgeon has experience in designing products, meaning the feedback received was from a clinician with expertise in the innovation of medical devices.

Projected images were presented along with the 3D printed models, although the surgeon seemed far more interested with the physical outputs as opposed to the digital. Throughout the presentation, he was interacting with the prototypes, somewhat dismissing the digital medium. The surgeon emphasised that there was a definite advantage to having physical prototypes that invoked tangible interactions. He said it allowed for an understanding of not only the constraints of the designs and multi-property 3D printing but also the opportunities. The generation of many more design ideas and applications for multi-property additive manufacturing then followed. Getting a hands-on perspective provides a sense of scale; it allowed the surgeon to assess if specific designs would meet the necessary design standard. The French (Fr) size of a catheter limits the maximum size of particular design features, such as the size of the ellipse drains lateral bands for internal retention. He also noted that there was a biological quality apparent with the material and how various elements could be blended. The organic feel was prevalent when interacting with the stimulus-responsive drains and the venous valves.

“Seeing and touching the (3D printed)examples was exciting. As part of the design process, it allowed the constraints to come out, but also the opportunities...”

(Colorectal surgeon interacting with 3D printed prototypes.)

SURGEONS CONSENSUS ON DESIGNS

Irrigation drains

Providing a method for introducing irrigation fluids into the cavity would positively help with draining abscess fluids. The protruding spirals to push tissue off of drainage holes was an intriguing idea; however, the more prominent spiral is too traumatic for insertion into the body. The surgeon much preferred the more minimally invasive sparse spiral concept.

Skin Fixation

The first impression of the skin fixation device is that it is aesthetically pleasing. The ability for it be either sutured or adhesively attached is appealing. The security of the drain seems reliable, and the form looks like it would move well with the body; however, it is hard to tell from the 3D printed material.

Stimulus-responsive drains

The full-scale ellipse prototype had the most product feel to it. The stimulus-responsive features were captivating and innovative, but there were too many limitations for it to be effective. Reliable activation of the retention, no indication that the retention is active and removal of the drain, were some of the main concerns.

Internal Structures

The surgeon was fond of the idea to introduce internal structures, strengthening particular areas of the drain. It would allow for more drain holes in specific locations, increasing drainage without the issue of the catheter kinking.

Venous valves

The valves had the most potential applications. The surgeon was impressed with how the valves functioned and the biological feel they had. The anatomical qualities allowed him to speculate on other applications, such as for vascular procedures or in the oesophagus.

5.1 DISCUSSION

Multi-property 3D printing on the Stratasys J750 proved to be an effective prototyping and visualisation method for the design and communication of surgical drain ideas. The ability to produce prototypes at a similar level to that of finished products in a matter of hours allowed for an unprecedented iterative design process, while the ability to generate tangible ideas deemed unmakeable demonstrated its potential as a communication method.

This research demonstrates how employing multi-property 3D printing can translate clinical ideas into physical prototypes for communication and critical reflection. Clinicians have the professional experience and awareness, knowing the products they use have issues, acknowledging that improvements can be made. However, for the most part, they do not have the expertise to turn their ideas into reality. The role of the designer is to visualise and communicate these concepts. Physically manifesting an idea allows for tactile interactions, providing the ability to perceive information that before was unavailable, such as material properties, texture, movement and mass.

Surgeons are hands-on individuals; their profession demands them to possess very skilled hand-eye coordination and manual dexterity for operating medical instruments. They understand the physiological composition of human anatomy through touch. The idea that surgeons are fundamentally tangible individuals may make them the perfect candidate for assessing high-quality 3D printed models. It would not be possible to convey the necessary information to understand these concepts through digital mediums alone; it is only possible through physical interaction. Multi-property 3D printing allows tangible visualisation to occur; it brings physicality to an idea that originated with a clinician or team, allowing clinical feedback to be received.

The J750 was used to explore the idea proposed by Wu (2010) about physically visualising digital information, how it should escape the constraints of screens allowing for tangible interactions. Whereas Wu’s study looked more at physically representing information visualisations, this research uses the J750 to create tangible visualisations of clinical ideas. During clinical evaluations, presentation slides and 3D printed prototypes were presented to surgeons. Throughout the presentation, the surgeons interacted continuously with the 3D printed models, almost disregarding the digital medium shown on the projected computer screen. Surgeons noted that interacting with the physical prototypes allowed them to understand the constraints but also the opportunities with the designs and the process of multi-property 3D printing, something the digital medium did not. The understanding of opportunities initiated the generation of even more potential applications. The scale of physical models also provided an assessment on whether or not they would achieve the safety standards required for medical devices, again, something not comprehensible by images alone.

Iteratively generating prototypes on the J750 provided an understanding of the constraints and capabilities. Initially, models created were fragile and susceptible to breaking, but as the project progressed and research through designing generated knowledge on the J750, outputs became robust, product like prototypes. Acquisition of the required tolerances for the design of internal stents was needed to achieve the maximum removal of support material without accidentally fusing the stent and the design. An understanding of material thicknesses, independent for each of the various shore values, and how different materials are blended, was required to prevent splitting and to allow for pneumatic inflation. Comprehension on how orienting models in line with the x-axis in GrabCad Print exploits the 14-micron resolution of the

J750 to produce diminutive features as small as 0.15mm. All of the iterative prototypes created during the design exploration chapter contributed to understanding the qualities the J750 can deliver.

VALUE OF THE RESEARCH

The value of this design research and its contribution to existing knowledge and practices is that multi-property 3D printing is a valid prototyping and visualisation method. As a prototyping method, it provided the technical abilities to produce high-quality models at a similar level to finished products. Generating concepts thought unmakeable, not only allowed for a hands-on clinical evaluation but also provided the notion that these speculative ideas could be incorporated into medical devices. The unique material qualities enabled an investigation into stimulus-responsive features, challenging the current functionality of surgical drains. It also provided the high-resolution needed to create operating anatomical features at a micromillimetre scale. Additive manufacturing drastically sped up the iterative design process, taking a matter of hours to produce prototypes as opposed to several days or weeks if handcrafted. Designs could also be generated in batch, during one print run, enabling an effective parallel prototyping approach.

As a visualisation method, multi-property 3D printing enabled the communication of complex ideas through tangible models. Visualising digital information should escape the constraints of screens and instead manifest in the real world, allowing for physical interactions and the ability to perceive information that before was unavailable. Multi-property 3D printing enables a heightened method of visualising. Clinical ideas translated into physical prototypes allows for expert advice and critical self-reflection to occur.

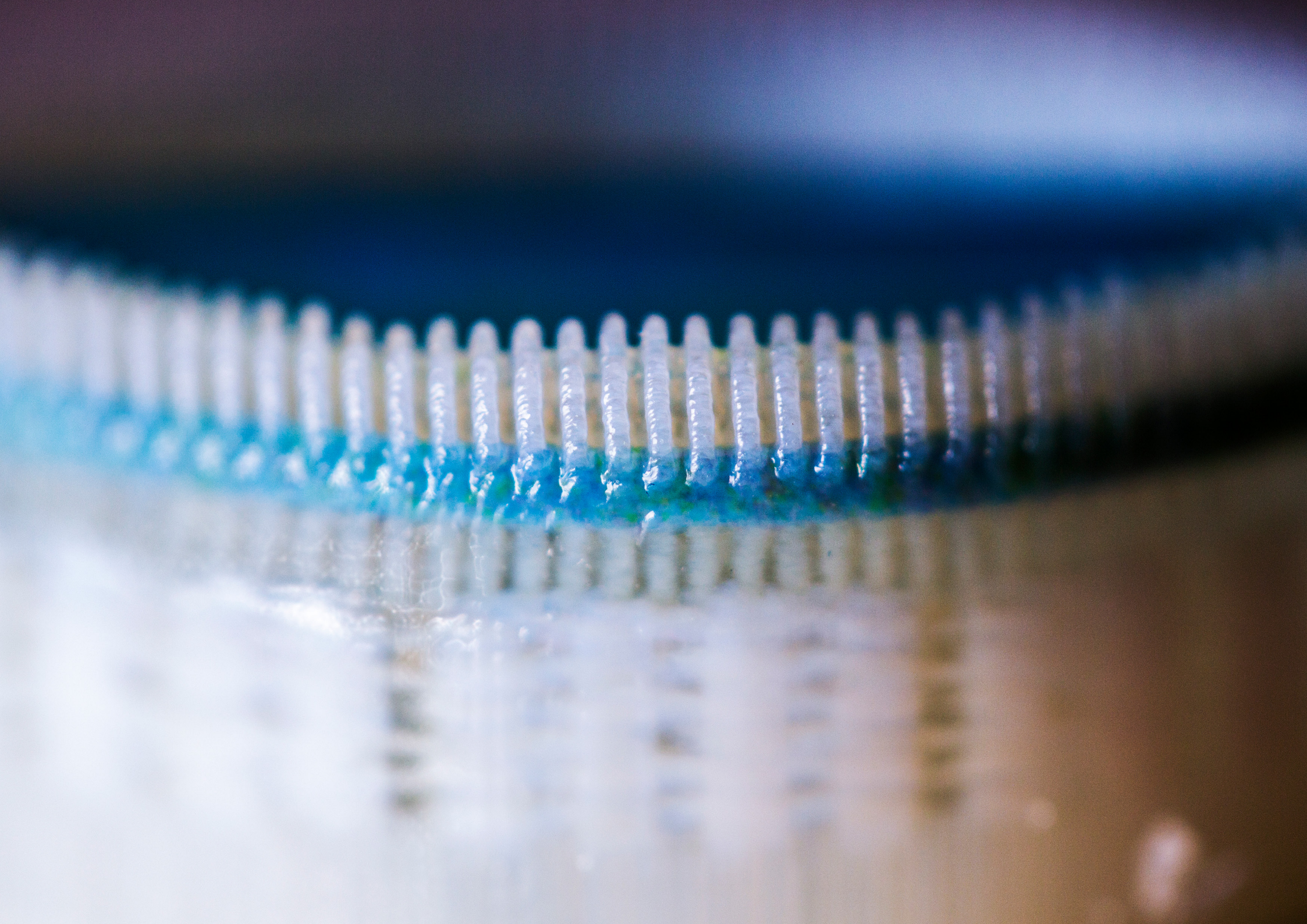
RESEARCH IMPLICATIONS

The implications of multi-property 3D printing discovered throughout this research advance on that learned from the initial background research.

The ability for clinicians to understand the constraints and opportunities from interacting with multi-property 3D printed models opens up many avenues for the future development of ideas. After interacting with models, clinical personal almost always generated new ideas. It allowed for speculation into how current designs and the additive manufacturing process could be applied to other applications. Producing scale prototypes that closely resemble finished products also enabled clinicians to asses if the concepts would satisfy strict medical standards early on in the products development.

The materials and additive manufacturing processes generated outputs with a unique biological quality to them. This quality not only made interacting with models an engaging experience but also enhanced the emulation of anatomical structures. The capability to blend sophisticated materials at almost a microscopic level, allow for the generation of dynamic models with increased physiological behaviour. All of this allows for accurate reproduction of organic models, further enhancing the communication of designs.

The implications discovered validate multi-property 3D printing as an exemplary communication method for medical ideas and anatomical structures. It can produce prototypes that no other manufacturing process is capable of rivalling. However, it does have its own unique set of constraints; more insight on the limitations is provided later in the discussion.



POTENTIAL FUTURE APPLICATIONS OF MULTI-PROPERTY 3D/4D PRINTING

The rapid rise of 3D printed models from 2D scans for tangible comprehension demonstrates that given a need additive manufacturing can be applied for the production of healthcare products. The potential impact multi-property 3D printing may have on the medical industry is immense. The introduction of FDA approved, radiopaque or doping materials and on-site production of medical devices in hospitals are just a few. The development of FDA authorised materials for the J750 is clearly a requirement before using 3D printing for the production of functioning medical device. There is a promising trend with 3D printed materials as companies are starting to prioritise material development, as this factor separates them from other businesses providing similar 3D printers. If there is enough demand for the development of FDA approved materials for medical products, companies such as Stratasys could start investing in it. Adding a radiopaque element, such as barium or iodineare into the J750 material library would allow models to absorb x-rays, improving the radiological image obtained.

Additionally, if there was a dopant material, such as silver, loaded into the J750, then materials could be doped during the printing process. This process could apply silver coatings to 3D prints, which could help prevent infections on medical devices. Doping would also allow for the production of multi-property 3D printed semi-conductors with unique electrical, optical, and structural properties. This process could provide an activation method for certain features, such as an alternative to the thermal stimulus-responsive internal retention. Fitting a hospital with a multi-property 3D printer, such as the J750, would provide the means for in-house production of medical instruments. An online archive of CAD files could be available for hospital

technicians to access, download files, and produce on-site. Updating the online archive would seamlessly give hospitals access to the latest designs at the click of a few buttons.

The distribution of medical products would also change. Instead of producing and packaging individual products in a factory and having to ship them around the world, they could generate them in a hospital room. In-house production would reduce the time and money spent on shipping, while also drastically reducing the waste produced individually packaging products. On-site additive manufacturing would also reduce the time patients spend waiting for customised medical tools to arrive for operations. Rather than waiting several weeks for custom devices to be designed, manufactured, packaged, and shipped, as soon as the designer finishes the CAD file it could be sent online and printed in a matter of hours.

Figure 143. Ellipse drain in support material printed with the gloss setting.



Figure 144. Tight External Spiral irrigation drain splitting during the removal of the internal stent.

LIMITATIONS

Material durability

Although Agilius is a much more durable material compared to the previous flexible option, Tango+, it is still considerably weaker than the materials used to manufacture current surgical drains. Specific design features split (Figure 144) due to the layer-by-layer manufacturing process and material properties of additive manufacturing, so they were trouble-shooted to amend production issues. Some of these design features may have worked through traditional materials and production processes, impacting design intentions. Constantly compressing the higher shore values to remove support material resulted in a lot of split prints, which was apparent printing long tubes containing venous valve structures. Durability was also an issue for the pneumatic valve structures. Continually inflating and deflating the pneumatic chambers weakened the material, causing it to split. Considerable time throughout this research was spent altering designs to ensure they did not split, affecting the desired outcome.

Support material

The soluble support made cleaning large batches of prints much more efficient and removing material from delicate features easier, but it limited the minimum size of details and internal channels for additional lumens. Removing the bulk of the support material needs to be done before placing prints in the DT3 cleaning bath. Extremely fragile elements encased in the support material would still break during the initial removal of the support. Considerable time was spent gaining an understanding of the print tolerances to generate delicate details that would survive the punctilious cleaning

process. Some of the additional irrigation lumens and pneumatic channels were no bigger then .5mm in diameter. The technical capabilities of the J750 managed to produce these details without any problems, but the issues arose trying to clean the internal support. Typically, removable stents were used to reduce the amount of support; however, for the tiny channels, it was not possible to print stents as they would snap. Trying to remove the support by compressing and squeezing it out would lead to the small channels splitting.

Sophisticated variables

The complexity with multi-property 3D printings process of blending materials made trouble-shooting design issues difficult. Due to variations in material properties, part thicknesses, and orientations, to name a few, generated so many variables that impacted the performance of prototypes. At times it was difficult deciphering the variable that needed altering to improve the performance of models.

OPPORTUNITIES

Voxel printing

Volumetric pixel, or Voxels, 3D printing allows control over materials and colours at a particle level scale. Utilising voxel 3D printing opens up potential avenues to generate models with even more prominent organic qualities and sophisticated details — another exclusive design feature for multi-property 3D printing on the Stratasys J750 that sets it apart from other manufacturing technologies.

4D printing

The discovery of 4D printing allowed for an exploration into stimulus-responsive features; however, even with physical models, these ideas were challenging for clinicians to grasp. Relying solely upon external stimulus to activate features of medical devices seemed too risky. Nevertheless, surgeons found the concept of 4D printing intriguing. Continuation of this research was encouraged by several clinical personnel to uncover other potential applications and develop the current performance.

Excess of clinical ideas.

The abundance of clinical ideas generated during meetings was surprising. On top of that, as ideas developed during this research and the capabilities of the J750 discovered, ideas continuously formulated from group discussions. There was such an excess of ideas that it was not possible to fully explore them during the timeframe. Concepts such as hydraulic activated internal retention, mucociliary escalator structures, capillary drains, are just a few. There is further research available once this project concludes to explore the remaining clinical ideas.



Figure 145. Tangible Visualisation.

5.2 CONCLUSION

This research explores how multi-material 3D/4D printing can be an effective prototyping and visualisation method for the design and communication of novel percutaneous surgical drains. It investigates the method of Tangible Visualisation, which results in the physical manifestation of an idea, designs rendered visible, capable of being touched and experienced for development, reflection, and communication. The translation of clinical ideas into physical prototypes through multi-property 3D printing allows for the comprehension and exploration of sophisticated concepts. A colorectal surgeon analysed designs, gauging the potential of the generated ideas and the multi-material additive manufacturing process. This study identifies that interacting with tangible models provides an understanding of the constraints, but more importantly, the opportunities of an idea.

A practice-based iterative design process is employed throughout this research to develop designs and to attain new knowledge on the capabilities of the Stratasys J750. The J750, along with the materials agilus and vero, allows for the production of pragmatic prototypes at a similar quality to

finished products, and speculative dynamic anatomical models. The material attributes provided the means for an investigation into 4D printed stimulus-responsive structures, that prototypes to life.

Multi-material 3D printing has immense potential to benefit the medical industry through, on-site production of products in hospitals, and the introduction of radiopaque or dopant materials. However, the lack of FDA approved materials, the durability, and need for support material limits the practical implementation of this technology. Voxel 3D/4D printing offers future research opportunities to explore more prominent organic qualities. Also, an excess of clinical ideas provides additional research possibilities to investigate after the completion of the project.

Multi-material 3D/4D printing proves to be an effective prototyping and visualisation method through the production of high-quality models that endows tangible interactions, elevating the design and communication of novel percutaneous surgical drain ideas.

5.3 REFERENCES

Banks, J. (2013). Adding Value in Additive Manufacturing : Researchers in the United Kingdom and Europe Look to 3D Printing for Customization. *IEEE Pulse*, 4(6), 22–26. <https://doi.org/10.1109/MPUL.2013.2279617>

Bodaghi, M., Damanpack, A. R., & Liao, W. H. (2016). Self-expanding/ shrinking structures by 4D printing. *Smart Materials and Structures*, 25(10), 105034. <https://doi.org/10.1088/0964-1726/25/10/105034>

Business Dictionary. (2019). What is iterative process? definition and meaning. Retrieved from <http://www.businessdictionary.com/definition/iterative-process.html>

Candy, L. (2006). Practice Based Research: A Guide. *Report from Creativity and Cognition Studios, University of Technology, Sydney.*, 19. Retrieved from <https://www.creativityandcognition.com/resources/PBR%20Guide-1.1-2006.pdf>

Cinat, M. E., Wilson, S. E., & Din, A. M. (2002). Determinants for Successful Percutaneous Image-Guided Drainage of Intra-abdominal Abscess. *Archives of Surgery*, 137(7), 845–849. <https://doi.org/10.1001/archsurg.137.7.845>

C. M. Editors. 2015. The Future Is Now: Christ Hospital Creates 3D-Printed Knee Implants. Cincinnati Magazine. <https://www.cincinnati-magazine.com/top-doctors-archive/future-now-christ-hospital-creates-3d-printed-knee-implants/> (April 29, 2019).

Cook Medical. (2018). Retrieved November 8, 2018, from <https://www.cookmedical.com/>

Chua, C. K., & Leong, K. F. (2014). *3D Printing and Additive Manufacturing: Principles and Applications (with Companion Media Pack) Fourth Edition of Rapid Prototyping Fourth Edition*. World Scientific Publishing Company.

Dix, A. (2013). Introduction to Information Visualisation. In M. Agosti, N. Ferro, P. Forner, H. Müller, & G. Santucci (Eds.), *Information Retrieval Meets Information Visualization: PROMISE Winter School 2012, Zinal, Switzerland, January 23-27, 2012, Revised Tutorial Lectures*(pp. 1–27). Berlin, Heidelberg: Springer Berlin Heidelberg. https://doi.org/10.1007/978-3-642-36415-0_1

Dow, S. P., Glassco, A., Kass, J., Schwarz, M., Schwartz, D. L., & Klemmer, S. R. (2010). Parallel prototyping leads to better design results, more divergence, and increased self-efficacy. *ACM Transactions on Computer-Human Interaction (TOCHI)*, 17(4), 18. <https://doi.org/10.1145/1879831.1879836>

Durai, R., & Ng, P. C. H. (2010). Surgical vacuum drains: types, uses, and complications. *AORN Journal*, 91(2), 266–271; quiz 272–274. <https://doi.org/10.1016/j.aorn.2009.09.024>

Frankel, L., & Racine, M. (2010). The Complex Field of Research: for Design, through Design, and about Design. *In Design & Complexity: International Conference of the Design Research Society*. Retrieved from <http://www.drs2010.umontreal.ca/data/PDF/043.pdf>

Fredieu, J. R., Kerbo, J., Herron, M., Klatte, R., & Cooke, M. (2015). Anatomical Models: a Digital Revolution. *Medical Science Educator*, 25(2), 183–194. <https://doi.org/10.1007/s40670-015-0115-9>

Ge, Q., Qi, H. J., & Dunn, M. L. (2013). Active materials by four-dimension printing. *Applied Physics Letters*, 103(13), 131901. <https://doi.org/10.1063/1.4819837>

Ge, Q., Sakhaei, A. H., Lee, H., Dunn, C. K., Fang, N. X., & Dunn, M. L. (2016). Multimaterial 4D Printing with Tailorable Shape Memory Polymers. *Scientific Reports*, 6, 31110. <https://doi.org/10.1038/srep31110>

Ghosh, P., & Mitchell, M. (2006). Segmentation of Medical Images Using a Genetic Algorithm. *In Proceedings of the 8th Annual Conference on Genetic and Evolutionary Computation* (pp. 1171–1178). New York, NY, USA: ACM. <https://doi.org/10.1145/1143997.1144183>

Gul, J. Z., Sajid, M., Rehman, M. M., Siddiqui, G. U., Shah, I., Kim, K.-H., ... Choi, K. H. (2018). 3D printing for soft robotics – a review. *Science and Technology of Advanced Materials*, 19(1), 243–262. <https://doi.org/10.1080/14686996.2018.1431862>

Hanington, B., & Martin, B. (2012). *Universal Methods of Design: 100 Ways to Research Complex Problems, Develop Innovative Ideas, and Design Effective Solutions*. Osceola, UNITED STATES: Quayside Publishing Group. Retrieved from <http://ebookcentral.proquest.com/lib/vuw/detail.action?docID=3399583>

Heider, R., Meyer, A. A., Galanko, J. A., & Behrns, K. E. (1999). Percutaneous Drainage of Pancreatic Pseudocysts Is Associated With a Higher Failure Rate Than Surgical Treatment in Unselected Patients. *Annals of Surgery*, 229(6), 781. Retrieved from <https://www.ncbi.nlm.nih.gov/pmc/articles/PMC1420824/>

Hone, N. (2018). Hydrophytes. Retrieved April 26, 2019, from <https://www.nicolehone.com/hydrophytes>

Khoo, Z. X., Teoh, J. E. M., Liu, Y., Chua, C. K., Yang, S., An, J., ... Yeong, W. Y. (2015). 3D printing of smart materials: A review on recent progresses in 4D printing. *Virtual and Physical Prototyping*, 10(3), 103–122. <https://doi.org/10.1080/17452759.2015.1097054>

Lawson, B. (2006). *How Designers Think: Demystifying the Design Process*. Jordan Hill, UNITED STATES: Routledge. Retrieved from <http://ebookcentral.proquest.com/lib/vuw/detail.action?docID=269907>

Li, C., Cheung, T. F., Fan, V. C., Sin, K. M., Wong, C. W. Y., & Leung, G. K. K. (2017). Applications of Three-Dimensional Printing in Surgery. *Surgical Innovation*, 24(1), 82–88. <https://doi.org/10.1177/1553350616681889>

Makama, J., & Ameh, E. (2008). Surgical Drains: What the resident needs to know, 17(3). <https://doi.org/10.4314/njm.v17i3.37389>

Malinauskas, R. A., Hariharan, P., Day, S. W., Herbertson, L. H., Buesen, M., Steinseifer, U., ... Craven, B. A. (2017). FDA Benchmark Medical Device Flow Models for CFD Validation. *ASAIO Journal*, 63(2), 150. <https://doi.org/10.1097/MAT.0000000000000499>

Martelli, N., Serrano, C., van den Brink, H., Pineau, J., Prognon, P., Borget, I., & El Batti, S. (2016). Advantages and disadvantages of 3-dimensional printing in surgery: A systematic review. *Surgery, 159*(6), 1485–1500. <https://doi.org/10.1016/j.surg.2015.12.017>

Mitsouras, D., Liacouras, P., Imanzadeh, A., Giannopoulos, A. A., Cai, T., Kumamaru, K. K., ... Rybicki, F. J. (2015). Medical 3D Printing for the Radiologist. *RadioGraphics, 35*(7), 1965–1988. <https://doi.org/10.1148/rg.2015140320>

Mogali, S. R., Yeong, W. Y., Tan, H. K. J., Tan, G. J. S., Abrahams, P. H., Zary, N., ... Ferenczi, M. A. (2018). Evaluation by medical students of the educational value of multi-material and multi-colored three-dimensional printed models of the upper limb for anatomical education. *Anatomical Sciences Education, 11*(1), 54–64. <https://doi.org/10.1002/ase.1703>

Momeni, F., M.Mehdi Hassani.N, S., Liu, X., & Ni, J. (2017). A review of 4D printing. *Materials & Design, 122*, 42–79. <https://doi.org/10.1016/j.matdes.2017.02.068>

Morrison, R. J., Kashlan, K. N., Flanagan, C. L., Wright, J. K., Green, G. E., Hollister, S. J., & Weatherwax, K. J. (2015). Regulatory Considerations in the Design and Manufacturing of Implantable 3D-Printed Medical Devices. *Clinical and Translational Science, 8*(5), 594–600. <https://doi.org/10.1111/cts.12315>

Mueller, P., van Sonnenberg, E., & Ferrucci, J. (1982). Percutaneous biliary drainage: technical and catheter-related problems in 200 procedures. *American Journal of Roentgenology, 138*(1), 17–23. <https://doi.org/10.2214/ajr.138.1.17>

Newell, R. (1992). Anxiety, accuracy and reflection: the limits of professional development. *Journal of Advanced Nursing, 17*(11), 1326–1333.

O’Donnell, J., Ahmadkhanlou, F., Yoon, H.-S., & Washington, G. (2014). All-printed smart structures: a viable option? In *Active and Passive Smart Structures and Integrated Systems 2014* (Vol. 9057, p. 905729). International Society for Optics and Photonics. <https://doi.org/10.1117/12.2045284>

Oxman, N. (2014). Mushtari. Retrieved from <http://neri.media.mit.edu/projects/details/mushtari>

Peck, J., & Childers, T. L. (2003a). To have and to Hold: The Influence of Haptic Information on Product Judgments. *Journal of Marketing, 67*(2), 35–48. <https://doi.org/10.1509/jmkg.67.2.35.18612>

Peck, J., & Childers, T. L. (2003b). Individual Differences in Haptic Information Processing: The “Need for Touch” Scale. *Journal of Consumer Research, 30*(3), 430–442. <https://doi.org/10.1086/378619>

Phillips. (2017). Philips teams with 3D printing industry leaders 3D Systems and Stratasys. Retrieved April 25, 2019, from <https://www.usa.philips.com/a-w/about/news/archive/standard/news/press/2017/20171127-philips-teams-with-3d-printing-industry-leaders-3d-systems-and-stratasys.html>

Redwood, B. (2019). Additive Manufacturing technologies: An overview. Retrieved January 7, 2019, from <https://www.3dhubs.com/knowledge-base/additive-manufacturing-technologies-overview>

Rengier, F., Mehndiratta, A., von Tengg-Kobligh, H., Zechmann, C. M., Unterhinninghofen, R., Kauczor, H.-U., & Giesel, F. L. (2010). 3D printing based on imaging data: review of medical applications. *International Journal of Computer Assisted Radiology and Surgery, 5*(4), 335–341. <https://doi.org/10.1007/s11548-010-0476-x>

Sachs, E., Allen, S., Guo, H., Banos, J., Cima, M., Serdy, J., & Brancazio, D. (1997). Progress on Tooling by 3D Printing; Conformal Cooling, Dimensional Control, Surface Finish and Hardness. <https://doi.org/10.15781/T29P2WR9G>

Schneider, B. (2007). Design as Practice, Science and Research. In R. Michel (Ed.), *Design Research Now: Essays and Selected Projects* (pp. 207–218). Basel: Birkhäuser Basel. https://doi.org/10.1007/978-3-7643-8472-2_12

Slagmolen, P. (2017). 5 Essential Tips on Getting the Best 3D-Printed Results for Your Anatomical Models. Retrieved April 29, 2019, from <https://www.materialise.com/en/node/4089>

Stevens, R., & Guy, B. (2015). Lissom. Retrieved April 26, 2019, from <http://made.ac.nz/project/computer-generated-objects-lissom/>

Stratasys. (2015). Polyjet multi-material 3D printing. Retrieved from http://usglobalimages.stratasys.com/Main/Files/Technical%20Application%20Guides_TAG/TAG_PJ_MultiMaterial_EN_1015.pdf?v=635969150902140765

Stratasys. (2017). The Jacobs Institute. Retrieved from <http://www.stratasys.com/polyjet-technology>

Stratasys. (2018). Stratasys J750 3D printer. Retrieved from <http://www.stratasys.com/3d-printers/j735-j750>

Tack, P., Victor, J., Gemmel, P., & Annemans, L. (2016). 3D-printing techniques in a medical setting: a systematic literature review. *BioMedical Engineering OnLine, 15*(1), 115. <https://doi.org/10.1186/s12938-016-0236-4>

Tangible. (n.d.). The Free Dictionary. Retrieved from <https://www.dictionary.com/browse/tangible>

Tibbits, S. (2014). 4D Printing: Multi-Material Shape Change. *Architectural Design, 84*(1), 116–121. <https://doi.org/10.1002/ad.1710>

Trivedi, D., Rahn, C. D., Kier, W. M., & Walker, I. D. (2008). Soft robotics: Biological inspiration, state of the art, and future research. *Applied Bionics and Biomechanics, 5*(3), 99-117 [doi:10.1080/11762320802557865](https://doi.org/10.1080/11762320802557865)

Trounson, A. (2017). Five ways 3D printing is changing medicine. Retrieved July 5, 2019, from <https://pursuit.unimelb.edu.au/articles/five-ways-3d-printing-is-changing-medicine>

UWTSD (CBM). (2018). Bespoke Medical Devices. Retrieved May 2, 2019, from <http://www.cbmwales.co.uk/our-services/medical-services/>

Ventola, C. L. (2014). Medical Applications for 3D Printing: Current and Projected Uses. *Pharmacy and Therapeutics*, 39(10), 704–711. Retrieved from <https://www.ncbi.nlm.nih.gov/pmc/articles/PMC4189697/>

Visualising. (n.d.). The Free Dictionary. Retrieved from <https://www.thefreedictionary.com/visualising>

Waran, V., Narayanan, V., Karuppiah, R., Owen, S. L. F., & Aziz, T. (2013). Utility of multimaterial 3D printers in creating models with pathological entities to enhance the training experience of neurosurgeons. *Journal of Neurosurgery*, 120(2), 489–492. <https://doi.org/10.3171/2013.11.JNS131066>

Wohlers Associates. (2010). What is Additive Manufacturing? Retrieved January 7, 2019, from <https:// Wohlersassociates.com/additive-manufacturing.html>

Wu, A. (2010). Tangible visualization. In *Proc. Conf. Tangible Embedded Interaction*, 317–318. Retrieved from <http://people.ischool.berkeley.edu/~daniela/tei2010/gsc10a.pdf>

Wu, J., Yuan, C., Ding, Z., Isakov, M., Mao, Y., Wang, T., ... Qi, H. J. (2016). Multi-shape active composites by 3D printing of digital shape memory polymers. *Scientific Reports*, 6, 24224. <https://doi.org/10.1038/srep24224>

Xiong, J., Mines, R., Ghosh, R., Vaziri, A., Ma, L., Ohrndorf, A., ... Wu, L. (2015). Advanced Micro-Lattice Materials. *Advanced Engineering Materials*, 17(9), 1253–1264. <https://doi.org/10.1002/adem.201400471>

Yan, Q., Dong, H., Su, J., Han, J., Song, B., Wei, Q., & Shi, Y. (2018). A Review of 3D Printing Technology for Medical Applications. *Engineering*, 4(5), 729–742. <https://doi.org/10.1016/j.eng.2018.07.021>

Yu, K., Ritchie, A., Mao, Y., Dunn, M. L., & Qi, H. J. (2015). Controlled Sequential Shape Changing Components by 3D Printing of Shape Memory Polymer Multimaterials. *Procedia IUTAM*, 12, 193–203. <https://doi.org/10.1016/j.piutam.2014.12.021>

Zimmerman, J., Stolterman, E., & Forlizzi, J. (2010). An Analysis and Critique of Research Through Design: Towards a Formalization of a Research Approach. In *Proceedings of the 8th ACM Conference on Designing Interactive Systems* (pp. 310–319). New York, NY, USA: ACM. <https://doi.org/10.1145/1858171.1858228>

5.4 APPENDIX

An overview of the various designs explored during the Lab testing section.

Project Ethics: Professional perspective, gaining an expert opinion from industry / 0000024294





















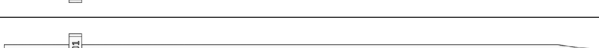

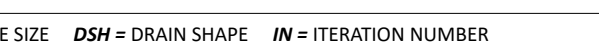

CODE	DOCUMENTATION	
<i>C/L</i> : SSC001, <i>CS</i> : S = Small, <i>DS</i> : S = Small, <i>DSH</i> : C = Circle, <i>IN</i> : 1		
<i>C/L</i> : SMC001, <i>CS</i> : S = Small, <i>DS</i> : M = Medium, <i>DSH</i> : C = Circle, <i>IN</i> : 1		
<i>C/L</i> : SLC001, <i>CS</i> : S = Small, <i>DS</i> : L = Large, <i>DSH</i> : C = Circle, <i>IN</i> : 1		
<i>C/L</i> : SSO001, <i>CS</i> : S = Small, <i>DS</i> : S = Small, <i>DSH</i> : O = Oval, <i>IN</i> : 1		
<i>C/L</i> : SMO001, <i>CS</i> : S = Small, <i>DS</i> : M = Medium, <i>DSH</i> : O = Oval, <i>IN</i> : 1		
<i>C/L</i> : SLO001, <i>CS</i> : S = Small, <i>DS</i> : L = Large, <i>DSH</i> : O = Oval, <i>IN</i> : 1		
<i>C/L</i> : SSS001, <i>CS</i> : S = Small, <i>DS</i> : S = Small, <i>DSH</i> : S = Slot, <i>IN</i> : 1		
<i>C/L</i> : SMS001, <i>CS</i> : S = Small, <i>DS</i> : M = Medium, <i>DSH</i> : S = Slot, <i>IN</i> : 1		
<i>C/L</i> : SLS001, <i>CS</i> : S = Small, <i>DS</i> : L = Large, <i>DSH</i> : S = Slot, <i>IN</i> : 1		
<i>C/L</i> : SST001, <i>CS</i> : S = Small, <i>DS</i> : S = Small, <i>DSH</i> : T = Teardrop, <i>IN</i> : 1		
<i>C/L</i> : SMT001, <i>CS</i> : S = Small, <i>DS</i> : M = Medium, <i>DSH</i> : T = Teardrop, <i>IN</i> : 1		
<i>C/L</i> : SLT001, <i>CS</i> : S = Small, <i>DS</i> : L = Large, <i>DSH</i> : T = Teardrop, <i>IN</i> : 1		
KEY: <i>C/L</i> = CODE/LABEL <i>CS</i> = CATHETER SIZE <i>DS</i> = DRAIN HOLE SIZE <i>DSH</i> = DRAIN SHAPE <i>IN</i> = ITERATION NUMBER		

Figure 146. Lab testing drains, Series of small drains exploring various sizes and shapes of drain holes.



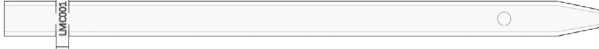

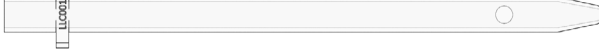



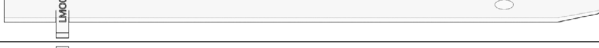
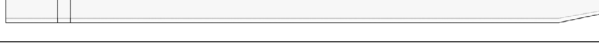












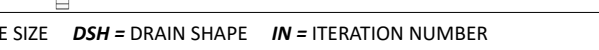

CODE	DOCUMENTATION	
<i>C/L</i> : LSC001, <i>CS</i> : L = Large, <i>DS</i> : S = Small, <i>DSH</i> : C = Circle, <i>IN</i> : 1		
<i>C/L</i> : LMC001, <i>CS</i> : L = Large, <i>DS</i> : M = Medium, <i>DSH</i> : C = Circle, <i>IN</i> : 1		
<i>C/L</i> : LLC001, <i>CS</i> : L = Large, <i>DS</i> : L = Large, <i>DSH</i> : C = Circle, <i>IN</i> : 1		
<i>C/L</i> : LSO001, <i>CS</i> : L = Large, <i>DS</i> : S = Small, <i>DSH</i> : O = Oval, <i>IN</i> : 1		
<i>C/L</i> : LMO001, <i>CS</i> : L = Large, <i>DS</i> : M = Medium, <i>DSH</i> : O = Oval, <i>IN</i> : 1		
<i>C/L</i> : LLO001, <i>CS</i> : L = Large, <i>DS</i> : L = Large, <i>DSH</i> : O = Oval, <i>IN</i> : 1		
<i>C/L</i> : LSS001, <i>CS</i> : L = Large, <i>DS</i> : S = Small, <i>DSH</i> : S = Slot, <i>IN</i> : 1		
<i>C/L</i> : LMS001, <i>CS</i> : L = Large, <i>DS</i> : M = Medium, <i>DSH</i> : S = Slot, <i>IN</i> : 1		
<i>C/L</i> : LLS001, <i>CS</i> : L = Large, <i>DS</i> : L = Large, <i>DSH</i> : S = Slot, <i>IN</i> : 1		
<i>C/L</i> : LST001, <i>CS</i> : L = Large, <i>DS</i> : S = Small, <i>DSH</i> : T = Teardrop, <i>IN</i> : 1		
<i>C/L</i> : LMT001, <i>CS</i> : L = Large, <i>DS</i> : M = Medium, <i>DSH</i> : T = Teardrop, <i>IN</i> : 1		
<i>C/L</i> : LLT001, <i>CS</i> : L = Large, <i>DS</i> : L = Large, <i>DSH</i> : T = Teardrop, <i>IN</i> : 1		
KEY: <i>C/L</i> = CODE/LABEL <i>CS</i> = CATHETER SIZE <i>DS</i> = DRAIN HOLE SIZE <i>DSH</i> = DRAIN SHAPE <i>IN</i> = ITERATION NUMBER		

Figure 147. Lab testing drains, Series of large drains exploring various sizes and shapes of drain holes.













CODE	DOCUMENTATION	
C/L: LLC002, CS: L = Large, DS: L = Large, DSH: C = Circle, IN: 2		
Design 1 from 13/04/2018, Total surface area of all drain holes = 47.8mm ²		
C/L: LLO002, CS: L = Large, DS: L = Large, DSH: O = Oval, IN: 2		
Design 2 from 13/04/2018, Total surface area of all drain holes = 47.8mm ²		
C/L: LLS002, CS: L = Large, DS: L = Large, DSH: S = Slot, IN: 2		
Design 3 from 13/04/2018, Total surface area of all drain holes = 47.8mm ²		
C/L: LLT002, CS: L = Large, DS: L = Large, DSH: T = Teardrop, IN: 2		
Design 4 from 13/04/2018, Total surface area of all drain holes = 47.8mm ²		
C/L: LRC001, CS: L = Large, DO: R = Ring, DSH: C = Circle, IN: 1		
Design 1 from 08/08/2018, Total surface area of all drain holes = 30mm ²		
C/L: LRC002, CS: L = Large, DO: R = Ring, DSH: C = Circle, IN: 2		
Design 2 from 08/08/2018, Total surface area of all drain holes = 30mm ²		
C/L: LRC003, CS: L = Large, DO: R = Ring, DSH: C = Circle, IN: 3		
Design 3 from 08/08/2018, Total surface area of all drain holes = 30mm ²		
C/L: LRS001, CS: L = Large, DO: R = Ring, DSH: S = Slot, IN: 1		
Design 4 from 08/08/2018, Total surface area of all drain holes = 378mm ²		
C/L: LRS002, CS: L = Large, DO: R = Ring, DSH: S = Slot, IN: 2		
Design 5 from 08/08/2018, Total surface area of all drain holes = 378mm ²		
C/L: LSTC001, CS: L = Large, DO: ST = Straight, DSH: C = Circle, IN: 1		
Design 1 from 28/08/2018, Total surface area of all drain holes = 15mm ²		
C/L: LSTC002, CS: L = Large, DO: ST = Straight, DSH: C = Circle, IN: 2		
Design 2 from 28/08/2018, Total surface area of all drain holes = 15mm ²		
C/L: LSTC003, CS: L = Large, DO: ST = Straight, DSH: C = Circle, IN: 3		
Design 3 from 28/08/2018, Total surface area of all drain holes = 15mm ²		
KEY: C/L = CODE/LABEL CS = CATHETER SIZE DS = DRAIN HOLE SIZE DO = DRAIN ORIENTATION DSH = DRAIN SHAPE IN = ITERATION NUMBER		

Figure 148. Lab testing drains, Series of large drains exploring various orientations of multiple drain holes.















CODE	DOCUMENTATION	
C/L: LRC004, CS: L = Large, DO: R = Ring, DSH: C = Circle, IN: 4		
Design 1 from 25/10/2018, Total surface area of all drain holes = 30mm ²		
C/L: LRC005, CS: L = Large, DO: R = Ring, DSH: C = Circle, IN: 5		
Design 2 from 25/10/2018, Total surface area of all drain holes = 30mm ²		
C/L: LRC006, CS: L = Large, DO: R = Ring, DSH: C = Circle, IN: 6		
Design 3 from 25/10/2018, Total surface area of all drain holes = 30mm ²		
C/L: LSTC004, CS: L = Large, DO: ST = Straight, DSH: C = Circle, IN: 4		
Design 4 from 25/10/2018, Total surface area of all drain holes = 30mm ²		
C/L: LGC001, CS: L = Large, DO: G = Gradient, DSH: C = Circle, IN: 1		
Design 1 from 07/11/2018, Total surface area of all drain holes = 30mm ²		
C/L: LGC002, CS: L = Large, DO: G = Gradient, DSH: C = Circle, IN: 2		
Design 2 from 07/11/2018, Total surface area of all drain holes = 30mm ²		
C/L: LGC003, CS: L = Large, DO: G = Gradient, DSH: C = Circle, IN: 3		
Design 1 from 06/12/2018, Total surface area of all drain holes = 30mm ²		
C/L: LGC004, CS: L = Large, DO: G = Gradient, DSH: C = Circle, IN: 4		
Design 2 from 06/12/2018, Total surface area of all drain holes = 30mm ²		
C/L: LRC007, CS: L = Large, DO: R = Ring, DSH: C = Circle, IN: 7		
Design 1 from 11/04/2019, Total surface area of all drain holes = 30mm ²		
C/L: LRC008, CS: L = Large, DO: R = Ring, DSH: C = Circle, IN: 8		
Design 2 from 11/04/2019, Total surface area of all drain holes = 30mm ²		
C/L: LRC009, CS: L = Large, DO: R = Ring, DSH: C = Circle, IN: 9		
Design 3 from 11/04/2019, Total surface area of all drain holes = 30mm ²		
C/L: LRC010, CS: L = Large, DO: R = Ring, DSH: C = Circle, IN: 10		
Design 4 from 11/04/2019, Total surface area of all drain holes = 30mm ²		
C/L: LRC011, CS: L = Large, DO: R = Ring, DSH: C = Circle, IN: 11		
Design 5 from 11/04/2019, Exploring how small 3D printing can produce drainage holes.		
C/L: LRS003, CS: L = Large, DO: R = Ring, DSH: S = Slot, IN: 3		
Design 6 from 11/04/2019, Total surface area of all drain holes = 30mm ²		
KEY: C/L = CODE/LABEL CS = CATHETER SIZE DO = DRAIN ORIENTATION DSH = DRAIN SHAPE IN = ITERATION NUMBER		

Figure 149. Lab testing drains, Series of large drains exploring various orientations of multiple drain holes.

TANGIBLE VISUALISATION

Multi-property 3D/4D printing for the design exploration of percutaneous surgical drains.